# LGMD-1C: ROLE OF CAVEOLIN-3 IN NEUROMUSCULAR JUNCTION STRUCTURE AND FUNCTION

by

**Michael P. Hezel**

B. S. in Biological Sciences, Fordham University, 2001

Submitted to the Graduate Faculty of

the School of Medicine in partial fulfillment

of the requirements for the degree of

Doctor in Philosophy

UNIVERSITY OF PITTSBURGH

School of Medicine

This dissertation was presented

by

Michael P. Hezel

It was defended on

November 25, 2009

and approved by

Chairperson: Yu Jiang Ph.D., Associate Professor, Pharmacology and Chemical Biology

William C. de Groat Ph.D., Distinguished Professor, Pharmacology and Chemical Biology

Michael J. Palladino Ph.D., Associate Professor, Pharmacology and Chemical Biology

Paula R. Clemens M.D., Associate Professor, Microbiology and Molecular Genetics

Dissertation Advisor: Ferruccio Galbiati Ph.D., Associate Professor, Pharmacology and Chemical Biology

**LGMD-1C: ROLE OF CAVEOLIN-3 IN NEUROMUSCULAR JUNCTION STRUCTURE AND FUNCTION**

Michael P. Hezel, Ph.D.

University of Pittsburgh, 2009

Caveolin-3 is a muscle specific scaffolding protein with both structural and signaling roles. Lack of caveolin-3 expression has been implicated in limb-girdle muscular dystrophy, along with distal myopathy and rippling muscle disease. These diseases are characterized by progressive muscle weakness and muscle wasting. Nicotinic acetylcholine receptor (nAChR) clustering and localization are important for efficient nerve to muscle contractile signal transmission. It is hypothesized that muscle weakness could originate through disrupted nAChR clustering, disrupting the efficiency of signaling from the motorneuron to the muscle. While the molecular mechanisms involved in nAChR clustering remain to be fully defined, we hypothesize caveolin-3 is important for nAChR clustering and overall neuromuscular junction function.

Caveolin-3 and the nAChR co-localize and associate evidenced by immunofluorescence and immunoprecipitation. These results were replicated in differentiated wildtype myotubes treated with the nAChR clustering agent, neural agrin. In differentiated caveolin-3 null myotubes, agrin treatment yields a 60% reduction in nAChR clusters as compared to agrin treated wildtype myotubes. Agrin induces nAChR clustering, through activation of muscle specific kinase (MuSK) and downstream through Rac-1 activation. In differentiated wildtype myotubes, Rac-1 activation peaks at 1 hour of agrin treatment, while in differentiated caveolin-3 null myotubes there is dramatically reduced Rac-1 activation upon agrin treatment. Immunoprecipitation of MuSK shows that caveolin-3 and MuSK association peaks at 1 hour of

agrin treatment in wildtype cells. This corresponds to the peak of MuSK phosphorylation which also occurs at 1 hour. Agrin induced MuSK phosphorylation was decreased more significantly than the overall decrease in MuSK expression in the caveolin-3 null cells as compared to the wildtype results. These results indicate a role for caveolin-3 in efficient nAChR clustering.

Electromyography studies in anesthetized mice indicated lengthened latencies of the muscle action potential in the caveolin-3 null mice as compared to wildtype mice. There were also decreased overall electromyography (EMG) amplitude and EMG area under the curve in caveolin-3 null mice. Comparison of contractile strength in wildtype and caveolin-3 null animals indicated tetanic contractions to be less stable in the caveolin-3 null animals, though there was late potentiation in actual contractile strength.

Lack of caveolin-3 affects the neuromuscular junction formation and transmission without affecting overall contractile strength. This research opens a novel view, that correct neuromuscular junction formation and neuromuscular transmission is important in the development of muscular dystrophies.

## TABLE OF CONTENTS

## LIST OF TABLES

## LIST OF FIGURES

## PREFACE

I dedicate my thesis to my wonderful wife, Ashley.

My eventual interest in science was fostered at an early age in elementary school though a gifted program called project apple and an annual event called the invention convention organized by Mrs. Jan Wright. These events exposed me to critical thinking, involved with identifying problems and exploring different solutions. It was in these first formative experiences that I was first exposed to many of the basics of scientific research. This was further supported by excellent science teachers throughout primary and secondary school including Mr. Art Choffin, Mrs. Marie Fullagar and Mr. Theodore Mullen.

These excellent learning experiences, inspired me to study Biology in college, and to find interesting summer research experiences with Greg Loeb at Cornell University and Hans-Peter Knopf at Novartis in Basel, Switzerland. In college and afterwards I received excellent guidance and support from Moses Kaloustian.

To gain further experience in research, I was fortunate to work as a research technician with Dr. William Jarnagin and Dr. Yuman Fong at Memorial Sloan-Kettering Cancer Center after college. Here, while working with a number of excellent surgical research fellows, I realized I wanted to direct research and decided to pursue my doctoral degree.

Since I entered the interdisciplinary program at the University of Pittsburgh, I have been exposed to a number of excellent professors, all of whom have been dedicated to seeing students succeed. This includes my advisor Ferruccio Galbiati, who worked closely with me to iron out kinks that arose in my project. My thesis committee of: Yu Jiang, Michael Palladino, Paula Clemens and Chet de Groat, who gave me good advice in pursuing and strengthening the science of my thesis project. Chet de Groat was essential in providing me the tools and assistance for examining whether our molecular findings were physiologically relevant.

Special thanks go out to all the people in charge of both the School of Medicine Interdisciplinary Graduate Program and Pharmacology and Chemical Biology, for their support and making sure all the milestones and correct paperwork was filled out and processed accordingly. This includes but is not limited, Stephen Phillips, John Horn, Sandra Honick, Cindy Duffy, Veronica Cardamone, Bruce Freeman, Jim Kaczynski, Jen Wong, Patricia Smith, Holly Gergely, Lisa McGreal and Jeanette McDew. It is through the hard work of all the support staff that the graduate students are able to focus on their research and courses.

I would like to thank everyone I worked with in the lab. Daniela Volonte and Janine Bartholomew, were always around to bounce ideas and vent about the few experiments that didn't work out. They made lab fun to go to everyday. I would also like to thank summer students Bradley Morneweck and Paul Musille, for making my summers working in the lab more interesting.

To all the many friends both in and outside of graduate school who were supportive of my studies, but also in enticing me to leave work and go play. Again there are too many people to list but the main list includes, Dave Kuhrt, Nina Korzeniewski, Amy Gardiner, Nikki Spardy, Erick Tatro, Thobba Einarsdottir, Nicolas Heluani, Michelle Wood, Ashley Way, Kristen

Scopaz, Eric Kelley, Alison Groeger, Andy Fisher, Elly Fisher, Thea Bemben, Will Bemben, Simon Wu, Sharon Messina, Trevor Lester, Kasey Eidson, Amie Eisfeld, Curtis Fenney, Anne Stetler, Ethan Block, Rob Tomko, Jason Campbell, Wiltrud Fassbinder, Ron Trible, Zeina Saliba, Brenna Bogey, Dave Werner, Mike Turner, and Jake Turner. I would also like to acknowledge all the friends from other chapters of my life that have continued to be cheerleaders through my doctoral studies: Nicole Pagano, Charina Carissimi, Steve Mahoney, Kevin Stalcup, Jen Foray, Katie Llewellyn, Cassie Farrelly, Dave Eisenberg, Prasad Adusumilli, Amit Bhargava, Francis Katai, Lisa Kehe, Jasmin Chitrakar, Jerome Covington, Rachel LeMaster, Mark Tomishima, Sereina Bodenmann, Scott Hicke, and Marina Pavic.

I would like to thank my family. My parents, who I feel did an excellent job raising me, even though we don't always see eye to eye. They along with my siblings, Patty, Paul and Matt support me through thick and thin. My siblings Patty, Paul and Matt have also been there for me when I needed them, especially Patty and Paul in Seattle, as I can call them at hours not considered normal calling hours on the East Coast. My aunt and uncle, Sybil and Ivan Baumwell and their family have been really helpful in making Pittsburgh my home. They have provided me with home cooked meals and invited me to many of the cultural events.

Lastly, I would like to thank my wife Ashley. We first met when I was applying for graduate school and she has been my rock throughout my graduate career. She has been there through the joys and frustrations of research and graduate school, cheering me up when I was down, pushing me forward when the path seemed to long and hard and helping me enjoy the successes.

## Abbreviations

ACh - acetylcholine; α-Btx - alpha-bungarotoxin; Cav-3 - caveolin-3; CBD - Caveolin Binding Domain; CMAP - Compound Muscle Action Potential; CMS - Congenital Myasthenic Syndrome; DHPR - dihydropyridine receptor; DMD - Duchenne Muscular Dystrophy; Dsh-1 - Dishevelled-1; EMG - electromyography or electromyograph; GEF - Guanine nucleotide exchange factor; GST - Glutathione S transferase; HA - Hemaglutinin; KO - knockout; LEMS - Lambert-Eaton Myasthenic Syndrome; LGMD - Limb-Girdle Muscular Dystrophy; LRP4 - LDL related receptor protein 4; MASC - Muscle associated signaling complex; MBC – Molecular Biology of the Cell; MG - Myasthenia Gravis; MuSK - Muscle Specific Kinase; nAChR - nicotinic acetylcholine receptor, NCS - nerve conduction studies; Pak1 - p21 activated kinase; PBD - Pak1 binding domain; T-tubules - Transverse Tubules; WT - wildtype

# 1.0 INTRODUCTION

## 1.1 MUSCULAR DYSTROPHY

Muscular dystrophies are a class of diseases characterized by progressive weakness and degradation of voluntary muscles. The first type of muscular dystrophy described was Duchenne Muscular Dystrophy (DMD) characterized by early onset almost exclusively in males and resulting in patient death in the second decade of life (Bogdanovich, Perkins et al. 2004). Edward Meryon first identified DMD as resulting in muscle degradation and fat replacement without nervous system defects as identified by lack of lesions in the nervous system by gross examination (Emery and Emery 1993). Dr. Meryon postulated that the disease resulted from breakdown of the sarcolemma (Emery and Emery 1993). The disease was later named Duchenne's Muscular Dystrophy after Guillame Benjamin Amand Duchenne published his research describing the same disease (Bogdanovich, Perkins et al. 2004).

Since then, eight other forms of muscular dystrophy have been documented, of which some have associated cardiac and mental developmental defects, but all present with progressive muscle weakness and wasting (Table 1). The advent of modern molecular techniques has allowed for documentation of mutated genes associated with these diseases, providing a "snapshot" into disease development. While some types of muscular dystrophy result from singular genetic changes, other dystrophy phenotypes result from one of a number of mutated

| Type | Genes | Onset | Symptoms | Progression | Inheritance |
|---|---|---|---|---|---|
| Duchenne Muscular Dystrophy (DMD) | Loss of Dystrophin | Early childhood | Effects muscle of hips, pelvic, thighs shoulders and enlarged calves | Eventually affects all voluntary muscles and heart and lungs. Death in 2nd or 3rd decade. End up in wheelchair by 12 | X-linked trait, almost exclusively confined to males |
| Becker Muscular Dystrophy (BMB) | Decreased Dystrophin | Adolescent, early adulthood | Same as above | Varied, slower then DMD Minor movement defects or wheelchair bound | X-linked trait, almost exclusively confined to males |
| Emery-Dreifuss Muscular Dystrophy (EDMD) | Emerin, Lamin A, Lamin C | Identified around 10-years-old | Stiff movements, difficultly moving joints | Later cardiomyopathy, can require a pacemaker | X-linked pattern |
| Limb-Girdle Muscular Dystrophy (LGMD) | 19 genes | Childhood to adulthood | Weakness in muscles around the shoulders and hips | Slow, may have cardiopulmonary affects | Dominant (1) Recessive (2) |
| Facioscalpulohumeral Dystrophy (FSHD) | DNA Loss on Chromosome 4 | Late teens to twenties | Weakness and Wasting of muscles around eyes, mouth, shoulders and lower legs | Slow degradation which eventually affects hip muscles also | Inherited or Sporadic |
| Myotonic Muscular Dystrophy | MMD genes insertions | Teen or adult years | Affect distal muscles, Delayed relaxation | Slow degradation, associated mental and cardiomyopathic effects | Autosomal Dominant |
| Distal Muscular dystrophy | Multiple genes | Varied, depending on type | Affects distal muscles of arms and legs | Progression into other muscles | Dominant or Recessive |
| Oculopharyngeal Muscular Dystrophy | Faulty PABPN1 gene | Late 40s or 50s | Weakness of eyelid and throat muscles | Progressive difficulty swallowing, eventually limb effects | Dominant |
| Congenital Muscular Dystrophy | Many genes | Infancy | Affecting all muscle groups, possible learning difficulties | Varied progression | Dominant or Recessive |

Table 1. Muscular Dystrophies

genes. The most common forms of muscular dystrophy arise from genetic deficiencies of the muscle protein dystrophin, collectively known as dystrophinopathies. DMD is the most severe form of dystrophinopathy, while Becker Muscular dystrophy is a milder form of dystrophinopathy (Emery and Emery 1993). Facioscapulohumeral dystrophy and myotonic dystrophy result from genetic changes that do not change translated genetic coding. (Bickmore and van der Maarel 2003). Emery-Dreifuss Muscular Dystrophy and Distal Muscular Dystrophy phenotypes result from changes in one of a number of gene sequences or the processing of the encoded protein (Emery and Emery 1993; Udd and Griggs 2001). Limb-Girdle Muscular Dystrophy is a form of muscular dystrophy affecting proximal limb and girdle muscles and has over 20 altered gene expression subtypes (Emery and Emery 1993). To date, there is no cure for muscular dystrophies, but medications and therapy can slow the course of the disease.

## 1.2 LIMB-GIRDLE MUSCULAR DYSTROPHY

The name Limb-Girdle Muscular Dystrophy (LGMD) is derived from the muscles most affected by the disease. The proximal limb muscles are the muscles afflicted in this disease, affecting movement. Degradation of the same muscle groups is the commonality in LGMD, although the subtypes vary in the time of onset, speed of progression, and severity (Mathews and Moore 2003). Due to the many genetic variations of LGMD, the classification is organized into two categories, based on whether the gene mutation is dominant (1) or recessive (2), and subsequently by the gene involved (Table 2) (Laval and Bushby 2004; Daniele, Richard et al. 2007). Not only do the subtypes have different progression characteristics, but even related

**Table 2. Limb Girdle Muscular Dystrophies**

| TYPE | GENE | ROLE | FUNCTION |
|---|---|---|---|
| 1A | Myotilin | Structure | z-disks |
| 1B | Lamin A and Lamin C | Differentiation | Nuclear envelope |
| 1C | Caveolin-3 | Structure | Membrane |
| 1D | Chromosome 7 | | |
| 1E | Chromosome 6 | | |
| 1F | Chromosome 7 | | |
| 1G | Chromosome 4 | | |
| 2A | Calpain-3 | Calcium dependant signaling | Cytoplasmic |
| 2B | Dysferlin | Membrane Repair | T-tubules, membrane |
| 2C | Gamma-Sarcoglycan | Structure | Membrane |
| 2D | Alpha-Sarcoglycan | Structure | Membrane |
| 2E | Beta-Sarcoglycan | Structure | Membrane |
| 2F | Delta-Sarcoglycan | Structure | Membrane |
| 2G | Telethonin/Titin-Cap | Regulation, Development | Z-disks |
| 2H | TRIM 32 | E3 ubiquitin ligase | Cytoplasmic |
| 2I | FKRP | Glycosyltransferase | Golgi |
| 2J | Titin | Myofibrillogenesis | Myofibrils |
| 2K | POMT1 | Glycosyltransferase | |
| 2L | Fukutin | Glycosyltransferase | |
| 2M | POMGn1 | Glycosyltransferase | |
| 2N | POMT2 | Glycosyltransferase | |

patients with the same mutation, have differences in disease onset and progression. LGMD-1C, is an autosomal dominant form of LGMD, resulting from caveolin-3 gene mutations (Minetti, Sotgia et al. 1998). Patients affected with LGMD-1C generally have one faulty caveolin-3 gene inherited from one parent. HyperCKemia, distal myopathy and rippling muscle disease are other diagnoses associated with caveolin-3 mutations (Woodman, Sotgia et al. 2004).

## 1.3 CAVEOLINS

Caveolin-3 belongs to a family of proteins known as caveolins, with three isoforms, caveolin-1, caveolin-2 and caveolin-3. The caveolins are implicated in the formation of ultrastructural plasma membrane invaginations 50 – 100nm in diameter, called caveolae (Razani and Lisanti 2001). These structures are characterized by high cholesterol and sphingolipid content. Caveolae were first identified in the mid 20$^{th}$ century by electron microscopy (Stan 2005). In the following 4 decades, biochemical techniques associated caveolae with roles in protein localization, organization and trafficking. These findings led to the postulation of the "Caveolae Signaling Hypothesis," which propounded that by compartmentalizing signaling molecules, caveolae regulate signal transduction (Song, Scherer et al. 1996). By use of modern molecular techniques, caveolin-1 was identified as an oncogenic gene important in the formation of caveolae and a substrate for v-Src (Lisanti, Scherer et al. 1994). Since then, caveolin-1 has been identified to have both oncogenic and tumor suppressor properties. Subsequently, caveolin-2 and caveolin-3 were identified and the role of caveolins in processes previously attributed to caveolae by earlier electron microscopy, were confirmed (Scherer, Okamoto et al. 1996; Tang, Scherer et al. 1996). The caveolae structure results from either 14-16 hetero-

oligomers of caveolin-1 and caveolin-2 or homo-oligomers in the case of caveolin-3 (Williams and Lisanti 2004). While caveolin-1 and caveolin-2 have been identified in many cell types such as fibroblasts, adipocytes, endothelial and epithelial cells, caveolin-3 is muscle specific and expressed in skeletal, cardiac and smooth muscle (Razani and Lisanti 2001). Caveolin-1, 2 and 3 have all been identified in arterial and bladder smooth muscle (Segal, Welsh et al. 1999; Woodman, Cheung et al. 2004).

## 1.4 CAVEOLIN-3

Caveolin-3, a muscle specific caveolin isoform, is initially expressed during myoblast differentiation into myotubes. Caveolin-1 is first expressed in myoblasts, and downregulated during myoblast differentiation (Parton, Way et al. 1997). After 48 hours of myoblast differentiation, caveolin-3 expression is initiated and replaces caveolin-1 expression. Caveolin-3 is located throughout the sarcolemma and is important for myoblast fusion into myotubes (Volonte, Peoples et al. 2003). In the cell, caveolin-3 performs structural, signaling, and trafficking capacities.

Caveolin-3 has been shown to interact with structural features and proteins in muscle cells, such as the dystrophin-glycoprotein complex, dysferlin, the T-tubules and cytoskeletal elements (Song, Scherer et al. 1996; Matsuda, Hayashi et al. 2001; Volonte, Peoples et al. 2003). The dystrophin-glycoprotein complex consists of many proteins and serves to connect the extracellular matrix to the actin cytoskeleton (Michele and Campbell 2003). Dystrophin, a major component of this conglomeration, binds beta-dystroglycan which spans the sarcolemma and through binding alpha-dystroglycan associates with the extracellular matrix (Lapidos, Kakkar et

al. 2004). Immunoprecipitation with a dystrophin antibody and blotting for caveolin-3 indicated association of caveolin-3 and dystrophin (Song, Scherer et al. 1996). Research on caveolin-3 and beta-dystroglycan suggests association through immunofluorescence, sucrose gradients and immunoprecipitation methods (Sotgia, Lee et al. 2000). The dystrophin-glycoprotein complex also consists of the transmembrane sarcospan protein and sarcoglycan family, and cytoplasmic proteins, dystrobrevin and the syntrophins. Many of these proteins are implicated in other LGMD subtypes.

Dysferlin has been identified as important in membrane repair after sheer stress (Bansal, Miyake et al. 2003). Interestingly, removal of caveolin-3 from the plasma membrane leads to increased intracellular localization of dysferlin (Capanni, Sabatelli et al. 2003; Hernandez-Deviez, Howes et al. 2008). Defects in dysferlin localization lead to concomitant disruption in caveolin-3 expression and localization found in LGMD-2B (Matsuda, Hayashi et al. 2001; Walter, Braun et al. 2003).

Caveolin-3 interacts with cytoskeletal proteins alpha-tubulin and actin. Caveolin-3 binds alpha-tubulin and loss of caveolin-3 leads to a diffuse and disoriented localization as identified in immunofluorescent staining. Likewise, caveolin-3 and actin co-localize. Lack of caveolin-3 expression in null myotubes reduces actin tubule localization along the plasma membrane and induces random localization of actin fibers (Volonte, Peoples et al. 2003).

The transverse tubules (T-tubules) are a membranous myofibular structure and the site of excitation contraction coupling (Flucher 1992). Caveolin-3 localizes to the T-tubules prenatally, although there are conflicting reports on caveolin-3 localization at the T-tubules in mature myotubes (Parton, Way et al. 1997; Ralston and Ploug 1999). A recent manuscript supports the notion of caveolin-3 continual co-localization in the T-tubules, through sarcolemma removal

from the myotube and immunofluorescent analysis (Murphy, Mollica et al. 2009). The T-tubules have an aberrant structure in caveolin-3 null myotubes as identified by electron microscopy (Galbiati, Engelman et al. 2001).

Several receptors have also been shown to associate with caveolin-3. The insulin receptor has been shown to bind caveolin-3 and traffic the activated receptor to the interior of the cell. This translocation and associated signaling pathway induces the translocation of the insulin regulated glucose transporter (GLUT-4) from intracellular vesicles to the plasma membrane (Fecchi, Volonte et al. 2006). Essential receptor tyrosine kinases, platlet derived growth factor receptor (PDGF-R) and epidermal growth factor receptor (EGF-R) have their autophosphorylation inhibited by caveolin-3 binding (Couet, Sargiacomo et al. 1997; Yamamoto, Toya et al. 1999). Caveolin-3 also inhibits autophosphorylation of the activin like receptor kinases 4 and 5 (ALK4 and ALK5), which respond to the ligand myostatin, important in negative regulation of muscle growth (Ohsawa, Hagiwara et al. 2006).

Caveolin-3 also plays a key role in intracellular signaling crucial for cellular function. As with PDGF-R and EGF-R activation, caveolin-3 inhibits autophosphorylation of c-src, of the src family kinases. In accordance with these findings, c-src has increased activation in caveolin-3 mutant or null cells (Venema, Ju et al. 1997; Smythe, Eby et al. 2003). By directly binding the nitric oxide synthase proteins, caveolin-3 inhibits nitric oxide production by all three nitric oxide synthases (Garcia-Cardena, Martasek et al. 1997; Venema, Ju et al. 1997). Oxidative stress activates movement of PI3Kinase, PDK1 and AKT signaling proteins into caveolar membranes with subsequent caveolin-3 association. Lack of caveolin-3 expression or inhibition to one of the above proteins induced abrogation of these caveolin-3 associations, and increased oxidative stress induced apoptosis (Smythe and Rando 2006).

Even though caveolin-3 plays varied roles in muscle structure and signaling, few laboratories have looked at caveolin-3 role in neuromuscular junction formation and function. Proper organization of the neuromuscular junction is essential for neuromuscular transmission required for movement.

## 1.5 NEUROMUSCULAR JUNCTION

As implied, the neuromuscular junction is where the nerve and muscle interact. The main function of this structure is conducting signals from the nerve to the muscle, inducing movement, important to the survival of all animals. While the neuromuscular junction has often served as a model for nerve to nerve signal transmission due to its size and accessibility, it is in its own right a complex structure, requiring myriad proteins and signals for proper development and efficient function.

The neuromuscular junction also known as the synapse, consists of three parts: 1) the nerve terminal, 2) the synaptic cleft, and 3) the muscle (Figure 1)(Hughes, Kusner et al. 2006). The nerve terminal, also known as the presynaptic junction, is where the action potential traveling down the axon terminates inducing the release of acetylcholine (ACh) from intracellular vesicles. The synaptic cleft is the space between the nerve and the muscle across which ACh travels and contains extracellular proteins that modulate this signaling. The muscle membrane juxtaposed to the nerve terminal, also known as the post-synaptic junction, is where nerve released ACh binds acetylcholine receptors located on the muscle membrane initiating a depolarization cascade resulting in contraction (Sanes and Lichtman 2001).

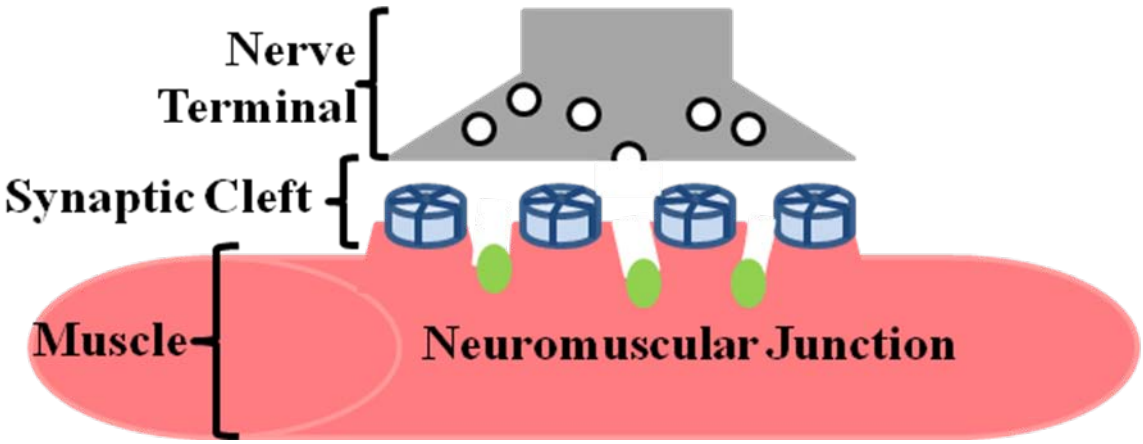


**Figure 1. Diagram of the Neuromuscular Junction Organization**

The neuromuscular junction consists of the nerve terminal, the synaptic cleft and the muscle membrane. The organization of the nerve and muscle along with the correct localization of associated proteins is important for proper neuromuscular junction transmission and muscle movement. White circles in the nerve terminal represent vesicles containing acetylcholine. Nicotinic acetylcholine receptors are represented by blue barrels and voltage gated sodium channels are represented by green dots.

The organization of the neuromuscular junction is very complex with signaling between the nerve and muscle and vice versa organizing the pre- and post-synaptic membrane and extracellular proteins in the synapse. This intercellular signaling refines the neuromuscular junction, increasing the efficiency of neuromuscular transmission (Witzemann 2006). There are many prenatal and postnatal changes modulating the organization of the acetylcholine receptor. These changes involve protein expression, protein association and structural changes leading to increased efficiency of acetylcholine receptor function.

## 1.6 ACETYLCHOLINE RECEPTOR

The two types of acetylcholine receptors present in humans and mice are the nicotinic and muscarinic acetylcholine receptors, named after their respective agonists. The muscarinic acetylcholine receptors (mAChR) are G-protein-coupled receptors initiating protein based signaling, through small g-proteins (Wessler and Kirkpatrick 2008). These receptors, found in the autonomic nervous system, are important in controlling visceral functions. Nicotinic acetylcholine receptors (nAChR) are ligand-gated ion channels, which allow sodium influx upon ACh binding. This ion influx activates a number of voltage fluctuations in the muscle leading to contraction. The speed of this signaling is much faster than that of muscarinic acetylcholine receptors due to the rapidity of depolarization (Madhavan and Peng 2005). The nicotinic acetylcholine receptor (nAChR) is essential in nerve to muscle signaling, resulting in muscle contraction.

## 1.7 NICOTINIC ACETYLCHOLINE RECEPTOR

The nicotinic acetylcholine receptor (nAChR) in muscle is a hetero-pentameric receptor. It is located on the muscle membrane and when bound by the ligand acetylcholine (ACh), induces an influx of sodium. The nAChR initially formed at the neuromuscular junction, also known as the fetal form, consists of 2α, 1β, 1γ and 1δ subunits. During neuromuscular junction maturation, receptors with the γ subunit are replaced by receptors with the ε-subunit, conferring receptor stability through increased half-life (Sanes and Lichtman 1999). Each subunit consists of 4 trans-membrane domains that associate with the other subunit transmembrane domains to

form a hydrophilic pore through which sodium ions pass (Wanamaker, Christianson et al. 2003). The association of 2 acetylcholine molecules to the receptor opens the channel by inducing removal of the transmembrane domain linkers from blocking the channel. The nAChR initially clusters at a concentration of 1000 receptors/$\mu m^2$ which increases to approximately 10,000 receptors/$\mu m^2$ in the mature neuromuscular junction (Hughes, Kusner et al. 2006). Since nAChR localization to the neuromuscular junction is essential for movement, nAChR organization and function has been extensively studied.

The muscle, before being innervated, localizes nAChR clusters along the midsection of the myotubes. This intrinsic acetylcholine receptor clustering occurs even before neuronal contact to the myotubes (Figure 2A). Around prenatal day 14 in the mouse, the nerve growth cone reaches the myotube. The nerve releases a peptide called agrin which induces the re-localization of the receptors already at the midsection of the myotubes to areas directly juxtaposed to the growing nerve (Sanes and Lichtman 2001). While there are other factors implicated in this reorganization, such as neuregulin, laminin and acetylcholine, neuronal agrin is the most potent clustering molecule (Hughes, Kusner et al. 2006). Agrin induces a signaling cascade in the muscle which induces localization and organization of the acetylcholine receptor at the neuromuscular junction. By birth, the neuromuscular junction formation is further modified to one nerve terminal per myotube (Figure 2B).

Upon birth, the neuromuscular junction undergoes further modification leading to increased efficiency of synaptic transmission. During this remodeling, folds form at the post-synaptic neuromuscular junction with the acetylcholine receptor localized at the crests and the voltage gated sodium channels located in the troughs of the folds. This differential localization provides for stronger and faster muscle depolarization for efficient contractile response. In mice,

it takes approximately a month after birth for full maturation of the neuromuscular junction (Figure 2C)(Sanes and Lichtman 2001).

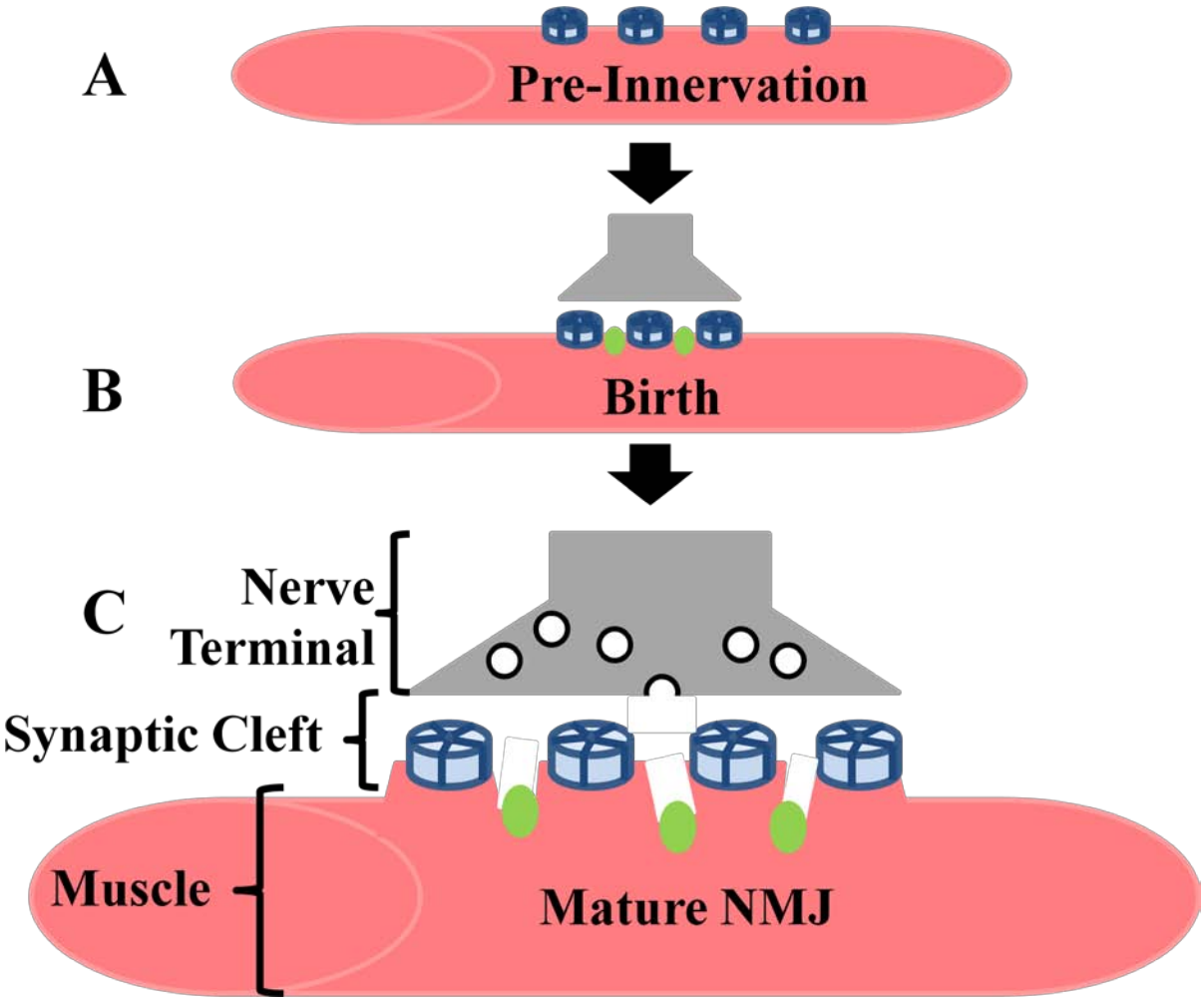


**Figure 2. Neuromuscular Junction Development**

The muscle membrane remodels over time to increase neuromuscular junction transmission efficiency. (A) In pre-innervation, the muscle has intrinsic nAChR localization at the mid-section of the myotube before nerve association with the muscle. (B) The nerve contacts the muscle and at birth one nerve has innervated each myotube and is able to function but not at full efficiency. The nAChR are located juxtaposed to the nerve terminal. (C) During postnatal development, folds form at the muscle membrane with the nAChR located at the crests (blue barrels) and the sodium channels (green dots) at the troughs of the myotube. These folds make neuromuscular transmission efficient and the neuromuscular junction (NMJ) in mice reaches maturity around 1 month of postnatal development.

The nAChR has low expression in myoblasts but is upregulated during differentiation by myogenic factors, particularly myogenin (Macpherson, Cieslak et al. 2006). During myofiber formation, the subsynaptic nuclei increase transcription of nAChR subunits, while transcription of nAChR subunits is suppressed at extrasynaptic nuclei (Macpherson, Cieslak et al. 2006).

Muscle specific kinase (MuSK) and receptor associated protein of the synapse (rapsyn) are two proteins found to be essential to nAChR clustering. Abrogation of expression of either of these proteins, results in mice that die at birth due to lack of functional neuromuscular junctions in the diaphragm required for breathing (Gautam, DeChiara et al. 1999; Wiesner and Fuhrer 2006). Many other proteins have been shown to play a role in clustering, including src family of tyrosine kinases, 14-3-3, geranyl geranyl transferase I, abl, dishevelled-1, Doc-7, Tid1, Rac1 and Rho GTPases, Pak1 and APC1 (Weston, Yee et al. 2000; Mohamed, Rivas-Plata et al. 2001; Luo, Wang et al. 2002; Luo, Je et al. 2003; Wang, Jing et al. 2003; Weston, Gordon et al. 2003; Strochlic, Cartaud et al. 2004; Weston, Teressa et al. 2007; Linnoila, Wang et al. 2008). Recent research discovered LDL related receptor 4 (LRP4) as an agrin binding protein which associates and precedes MuSK activation in the clustering signaling cascade (Kim, Stiegler et al. 2008; Zhang, Luo et al. 2008). The agrin induced signaling cascade will be discussed in further detail in chapter 4.

Since localization and stability are important for reliable signaling through the nAChR, research has focused on nAChR association with structural molecules. Vinculin, talin, paxillin, and focal adhesion kinase have been shown to link the receptor to actin and the cytoskeleton (Madhavan and Peng 2005). The receptor also associates with the dystrophin-glycoprotein complex (Banks, Fuhrer et al. 2003). This complex consists of strong associations between dystrophin, alpha and beta dystroglycan, sarcoglycans, dystrobrevin, syntrophin and nitric oxide

synthase (Michele and Campbell 2003). Utrophin replaces dystrophin in the dystrophin-glycoprotein complex at the post-synaptic membrane (Banks, Fuhrer et al. 2003). Rapsyn has been suggested to mediate nAChR linkage with beta-dystroglycan, though other research shows direct nAChR and beta-dystroglycan association (Banks, Fuhrer et al. 2003). Dystroglycan, dystrobrevin, and syntrophin mutants each exhibit disruption of neuromuscular junction organization.

## 1.8 RATIONALE

Diagnosis of muscular dystrophy occurs when patients are symptomatic with muscle weakness and degrading muscle fibers as determined by histology. This occurs after periods of unhindered movement in all but the most severe muscle pathologies. These dystrophies vary in severity and onset even when evolving from the same underlying genetic mutations. We hypothesize that this phenotypic variability could result from structural and/or functional changes at the neuromuscular junction, and be modulated by differences in patient movement over their lifetime. Following this line of thought the symptoms and diagnosis could evolve from contractile signaling degrading past a threshold in muscle signaling. Pre-symptomatic compensation may result from intrinsic supramaximal signaling involved in muscle contraction. Using a model for limb-girdle muscular dystrophy subtype 1C, we will assess the role of the neuromuscular junction structure and function in development of one form of muscular dystrophy.

The following research explores the hypothesis that loss of caveolin-3 expression leads to post-synaptic structure and function changes influencing muscular dystrophy development. This

hypothesis will be assessed using caveolin-3 null mice and derived myoblast culture in comparison to wildtype mice and derived myoblast culture. Caveolin-3 null mice and cells are a model system for LGMD-1C, a muscular dystrophy subtype resulting from dominant negative mutations of caveolin-3. This research using caveolin-3 null and wildtype mice and differentiated muscle cultures will analyze differences in formation of the post-synaptic neuromuscular junction at both the gross and molecular level and also neuromuscular junction function and contractile strength *in vivo*.

# 2.0 MATERIALS AND METHODS

## 2.1 MATERIALS

### 2.1.1 Reagents

Antibodies and their sources: nicotinic acetylcholine receptor alpha (clone 26), caveolin-3 (clone 26), HRP-conjugated goat anti-rabbit, phosphotyrosine (clone PY20), and Rac1 (clone 102), were purchased from BD transduction laboratories. Caveolin-3 (n-18), and dishevelled-1 (3F12), MuSK (C-19) were purchased from Santa Cruz Biotechnologies. MuSK and Rac1 (clone 23A8) were purchased from Affinity Bioreagents. Nicotinic acetylcholine receptor (clone 35) and beta-tubulin III (TUJ1) were obtained from Covance, while Alexa Fluor 647 conjugated alpha-bungarotoxin and unbound alpha-bungarotoxin were purchased from Invitrogen. Anti-phosphotyrosine (clone 4G10, Upstate Cell Signaling), and HRP conjugated Goat anti-mouse (Pierce) were also purchased. The construct for the GST p21 activated kinase binding domain fusion protein was kindly provided by Daniel Altschuler. pSM constructs of the nAChR subunits were kindly provided by Z. Z. Wang. All chemicals were purchased from Sigma, or Fisher Scientific.

### 2.1.2 Cell Culture

The wildtype and caveolin-3 null myoblast cell cultures were obtained as previously described (Volonte, Peoples et al. 2003). The myoblasts were grown at 33°C under a proliferation media Ham's F-10 containing 20% FBS, 2mM L-glutamine, 100 Units/ml penicillin, and 100 µg/ml streptomycin. Before using proliferation media, bFGF (2.5ng/ml) and gamma-interferon (50U/ml) were added to the media. To differentiate myoblasts into myotubes, cells at approximately 90% confluence had their media changed to differentiation media, DMEM containing 2% horse serum, 2mM l-glutamine, 100 units/ml penicillin and 100 µg/ml streptomycin at 37°C. To induce acetylcholine receptor clustering, 10ng/ml rat agrin (R & D Biosystems) was added to differentiation media. The oncogenic Ras cell line is a 3T3 line derivative expressing stable constitutively active $Ras^{G12V}$ (Koleske, Baltimore et al. 1995). Overexpression of Ras abrogates Caveolin-1 expression removing all caveolin protein expression. Ras and 3T3 cells are grown in DMEM with 10% donor bovine serum, 2mM l-glutamine, 100 units/ml penicillin, and 100 µg/ml streptomycin.

### 2.1.3 DNA Constructs

A wildtype MuSK and two MuSK constructs with mutated caveolin binding domains were inserted into a pCMV-HA vector. Using cDNA, and MuSK primers (5'- ccg gcc gtc gac aag aga gct cgt caa cat tcca and 3'- cc ggc cgc ggc cgc tta gac act cac agt tcc ctc), MuSK was amplified, and subsequently cut with Sal I and Not I and ligated into the vector. The mutants were then produced using internal primers changing aromatic residues to alanines with the original external primers. The primers for Mutant A were 5'- gat gtg gcg gcc gct ggc gtg gtc ctc gcg gag atc and

3’- gat ctc cgc gag gac cac gcc agc ggc cgc cac atc. The primers for Mutant B were 5’- gag atc gcc tcc gct ggc ctg cag ccc gcc gct ggg atg and 3’- cat ccc agc ggc ggg ctg cag gcc agc gga ggc gat ctc. The two mutated fragments were amplified with the WT MuSK vector to produce the full mutated DNA. This was also inserted into the pCMV-HA vector. A myc-tagged nAChR-alpha subunit construct was inserted into the pCAGGs vector. Using cDNA and nAChR primers (5’ - ggc cgg gaa ttc atg gag ctc tcg act gtt ctc and 3’- ggc cgg gaa ttc tta att cag atc ttc ctc gct gat cag ttt ctg ttc gcc gcc tcc ttg ttg atg taa ctc aag), nAChR-alpha-myc was amplified, cut with EcoRI and ligated into a dephosphorylated pCAGGs vector.

## 2.2 METHODS

### 2.2.1 Immunofluorescent Staining

#### 2.2.1.1 Tissue Sections

Quadriceps tissue from 22 month old wildtype and caveolin-3 null mice were dissected, snap frozen and embedded in OCT. Cross-sections, 5 micrometers thick, were placed on frosted slides, 2 sections per slide and kept frozen until stained. The slides were rehydrated in phosphate buffered saline with calcium and magnesium (PBS-CM) and rinsed with PBS-CM with 0.1% Triton-X-100 (PBS-CM-T). The tissue on the slide was placed in monoclonal mouse anti-nAChR-alpha and polyclonal anti-goat anti-caveolin-3 antibodies diluted 1:500 in PBS-CM-T and incubated at room temperature for 3 h. Slides were washed 3X in PBS-CM-T for 10 min each. Slides were incubated for 2 h in secondary antibodies, at a 1:1000 dilution in PBS-CM-T.

Slides were washed 3X in PBS-CM-T for 10 min each, rinsed in phosphate buffered saline (PBS) and a coverslip mounted over the tissue using anti-fade (Invitrogen) and sealed with nail-polish.

#### 2.2.1.2 Cells on Coverslips

Cells were grown on uncoated cover slips and treated as required for the staining experiment. The cells were washed 3x in PBS-CM and fixed with 2% paraformaldehyde in PBS solution for 30 min. Cells were permeabilized with PBS-CM-T for 10 min and peroxides quenched with ammonium chloride in PBS-CM for 10 min followed by a rinse with PBS-CM-T. The addition of the primary antibodies and subsequent steps were performed as described above for the tissue sections with the exception that the coverslips were mounted onto slides.

#### 2.2.1.3 Whole Mount Staining

This protocol is adapted from Lin *et al.* 2005. After dissecting the diaphragm tissue or EDL muscle from the mouse and washing it in PBS, it was fixed in 2% paraformaldehyde in 0.1% phosphate buffered saline (pH 7.3) overnight at 4°C. The tissue was rinsed in PBS (pH 7.3) and then incubated in a 0.1M glycine in PBS for 1 h. The tissue was rinsed again in PBS and then incubated in 0.5% Triton-X-100 solution in PBS for 1 h. The muscle was then blocked in dilution buffer (500mM NaCl, 0.01M phosphate buffer, 0.01% Thimerosal) overnight at 4°C. The tissue was then incubated with primary antibodies, caveolin-3 (1:500) and beta-tubulin III (1:500) in dilution buffer overnight at 4°C. The tissue was rinsed 3X with 0.5% Triton-X-100 in PBS for 1 h each and incubated overnight at 4°C with fluorescent secondary antibodies (1:1000) and Alex 647 alpha-bungarotoxin (1:500) in dilution buffer. The tissue was then washed 3X in 0.5% Triton-X-100 solution in PBS for 1 h each. The tissues were rinsed one last time in PBS, mounted on a slide with antifade solution and analyzed by confocal microscopy.

#### 2.2.1.4 Analysis of nAChR Clustering

Wildtype and caveolin-3 null cells were grown on uncoated glass cover slips, differentiated for 7 days and treated with agrin for 24 hours. The cells were stained for caveolin-3 and nAChR as above. The samples were analyzed by confocal microscopy, images were taken and the lengths of the clusters were measured and averaged. The clusters per field were also counted in triplicate and averaged. Statistical analysis was performed using Student's T-test.

### 2.2.2 Protein Association Procedures

#### 2.2.2.1 Immunoprecipitation

Cells were washed 2X in cold PBS, scraped in lysis buffer solution and lysed by pipeting 30 times. Tissue was placed in lysis buffer and mechanically homogenized using a tissue tearor (Biospec Products Inc.) for 30 s. Lysis buffer consisted of 10mM Tris-HCl pH 8.00, 150mM NaCl, 5mM EDTA, 1% Triton-X-100, 6mM of n-octyl glucoside (Roche) and one complete protease inhibitor tablet (Roche) per 10ml of solution. The samples were mixed on a hematology/chemistry mixer (Fisher Scientific) at 4°C for 1 h. The insoluble material was precipitated by centifugation and the supernatant was collected. The samples were pre-cleared with 10 µl of Protein A Sepharose slurry (1:1 beads:lysis buffer) and the protein content measured by BCA assay. Samples were normalized to have the same protein content and volume, and 10% of normalized solution was collected as totals. The immunoprecipitating antibody and Protein A Sepharose (Amersham Biosciences) beads were then added to the samples. The samples were put on a hematology/chemistry mixer overnight at 4°C. Beads were washed 3X with lysis buffer and once with 50mM Tris-HCl. Laemmli Buffer was added to the

beads, which were vortexed and incubated at room temperature for 10 min. Samples and corresponding totals were analyzed by western blotting.

#### 2.2.2.2 Sequential Immunoprecipitation

Followed the immunoprecipitation protocol up to the addition of Laemmli Buffer, 0.5% sodium dodecyl sulfate (SDS) solution was added to the beads and incubated at 50°C for 10 min. The supernatant was collected and diluted to 0.1% SDS in lysis buffer before continuing with the second immunoprecipitation. At the end of the experiment, the SDS removal of the proteins from the beads was performed again selectively remove the proteins leaving the antibody bound to the beads. Results were analyzed by western blot.

#### 2.2.2.3 Binding of GST-Fusion Protein to Glutathione bound Sepharose Beads

GST constructs in BL21 bacteria were grown at 37°C in ampicillin containing LB to an Optical Density between 0.3 and 0.6. IPTG was added to achieve a final concentration of 0.5mM and left shaking at 37°C for 2 h. The bacteria were centrifuged and washed in 150mM NaCl, 7.5mM Tris pH 8.00, and 3mM EDTA (STE) and resuspended in 10ml STE. 10µg/ml lysozyme was added to the bacterial solution and incubated on ice for 15 min. DTT (1M) and 10% n-lauryl sarkosyl were added to final concentrations of 5mM and 1.5%, and a crushed minicomplete protease inhibitor tablet was also added. Cells were homogenized using the tissue tearor at medium speed for 30 s and centrifuged for 20 min to remove insoluble material. The supernatant was collected and 20% Triton-X-100 in STE added to a final concentration of 2%. GST beads (500µl) were pre-washed 3X in STE buffer and then added to the GST-fusion protein solution. The beads were bound to the fusion protein on a hematology/chemistry mixer overnight at 4°C. The next day the beads were washed in STE with 1% Triton-X-100 and saved for the

experiment. The amount of protein fused to the beads was analyzed by running on a mini-gel and staining with Coomassie Blue stain.

#### 2.2.2.4 Rac1 Pull-down using GST-PBD bound Glutathione beads

Cells were washed 2X in cold PBS, scraped, and collected in lysis buffer, consisting of 50 mM Tris-HCl, 0.5% sodium deoxycholate, 0.1%SDS, 150mM sodium chloride, 10mM magnesium chloride, 1% Triton-X-100 and one Complete-Mini protease tablet per 10ml buffer for the Rac-1 pulldown. Cells were resuspended and centrifuge tube put on a hematology/chemistry mixer for 1 h. Insoluble material was precipitated by centrifugation and the supernatant collected. The samples were precleared with unbound GST beads to remove endogenous glutathione binding proteins. Sample protein expression was compared using the BCA protein assay. The same amount of protein and volume were put in each sample and 10% taken for total protein analysis. GST-PBD bound glutathione beads were then added to each sample and put on rotation overnight at 4°C. The beads were washed 3X with lysis buffer without SDS and sodium deoxycholate. Laemmli Buffer was added to the beads, which were vortexed and incubated at room temperature for 10 min. Samples and corresponding totals were analyzed by western blotting.

#### 2.2.2.5 Binding of alpha-bungarotoxin to cyanogen bromide activated sepharose beads

Unlabelled alpha-bungarotoxin was bound to cyanogen bromide activated sepharose beads (Sigma) following the protocol provided and modified for use without a column. The alpha-bungarotoxin was resuspended in coupling buffer consisting of 0.1 M $NaHCO_3$ with 0.5 M NaCl (pH 8.3) and left to dissolve until addition to the beads. Beads were reconstituted in 1 mM cold HCl for 1 h, changing every 15 min by removing the solution after letting the beads settle. The

beads were then washed 3X with distilled water and 1X with coupling buffer, before the resuspended alpha-bungarotoxin prepared above, was added to the beads. The bead-ligand solution was placed on rotation overnight at 4°C. The next day the beads were washed 3X with coupling buffer and incubated in 0.2 M glycine (pH 8.0) at room temperature for 2 h. The beads were washed in coupling buffer and then 0.1 M acetate buffer (pH 4.0) containing 0.5 M NaCl. This dual wash cycle was performed 4 times. If the beads were not used immediately, they were stored in 1.0 M NaCl at 4°C.

### 2.2.3 Western Blot

Samples analyzed by western blot were boiled for 5 min after addition of Laemmli buffer and loaded into a 12.5% Tris-HCl polyacrylamide gel with Seeblue Plus 2 markers (Invitrogen). The gel was run at 40 mAmps per gel until loading buffer ran out and transferred to nitrocellulose membranes overnight at 4°C and 150 mAmps. The nitrocellulose was stained with Ponceau S solution and the appropriate strips for specific antibodies cut out and blocked in 2% milk in Tris-Buffered Saline with Tween-20 (TBSt) for monoclonal antibodies or 2% milk, 1% BSA in TBSt solution for polyclonal antibodies. The membrane was washed with TBSt and incubated overnight with the primary antibody at required dilution in TBSt. The next day the blot was washed with TBSt and incubated with the secondary antibody in blocking solution. The blot was washed again with TBSt and then developed using Supersignal West Pico or Femto solution (Pierce) and results captured on Kodak Blue X-Omat film. Band densitometry analysis was performed using the Personal Densitometer SI (Molecular Dynamics).

### 2.2.4 Electromyography and Contractile Force Experiments

Wildtype and caveolin-3 null mice were anesthetized by IP injection of urethane. Upon anesthetization, the lower hind half and the ventral neck area of the animal was shaved. A tracheotomy was performed using 90μm diameter tubing to ease animal breathing. The Achilles tendon was exposed, tied to a force transducer, and cut proximal to the ankle. The sciatic nerve to the adjacent leg was exposed with a small skin incision and by separating the covering muscle. The nerve was covered with mineral oil to maintain the conductivity of the nerve. A stimulating electrode was placed under the nerve and the nerve cut proximal to the pelvis to remove reflex responses. A recording electrode was placed into the gastrocnemius muscle through a small incision in the skin covering the gastrocnemius muscle. The nerve was subsequently stimulated at various intensities and frequencies. Simultaneous compound muscle action potentials (CMAP) recordings and muscle contractile force data were collected and analyzed using National Instruments program Labview 7.0. If the animal maintained consistent breathing at the end of analyzing the first leg, the opposite Achilles tendon and sciatic nerve were prepared and EMG and muscle contraction experiments performed. Statistical analysis was performed by Student's T-test

# 3.0 ROLE OF CAVEOLIN-3 IN NACHR CLUSTERING

## 3.1 INTRODUCTION

While the localization of caveolin-3 and nAChR have been separately studied in muscle and myotubes, limited research on the co-localization and association of these proteins has been conducted. Published research locates caveolin-3 and nAChR to the sarcolemma, though nAChR is highly localized and caveolin-3 is globally expressed at the sarcolemma. Expression of caveolin-3 and nAChR is upregulated during myoblast differentiation. Both proteins have been localized to the high lipid microdomains known as detergent resistant membranes by sucrose gradient fractionation experiments. Co-localization and association of the dystrophin-glycoprotein complex with caveolin-3 and nAChR each has been identified by immunofluorescence and immunoprecipitation, respectively (Song, Scherer et al. 1996; Marchand, Devillers-Thiery et al. 2002).

The co-localization of caveolin-3 and the nAChR by alpha-bungarotoxin staining of single muscle fibers and muscle cross-sections was first described in rat muscle (Carlson, Carlson et al. 2003). These experiments showed caveolin-3 and nAChR co-localization, with caveolin-3 extending beyond the nAChR staining. This research also identified decreased co-localization of caveolin-3 and the nAChR in aged rats.

Caveolin-3 and the nAChR have been briefly analyzed in other studies with differing conclusions. Immunofluorescent staining of caveolin-3 and nAChR after agrin treatment for 12 h does not show any co-localization at the membrane (Trinidad and Cohen 2004). The authors suggest that nAChR and caveolin-3 co-localize internally upon removal of agrin, though no merged images identifying these conclusions were shown. Many of these experiments were also performed several hours after live cell labeling for the nAChR with alpha-bungarotoxin, an irreversible inhibitor of nAChR. Alpha-bungarotoxin binding of nAChR increases internalization and degradation of the receptor (Pumplin and Fambrough 1982). The role of alpha-bungarotoxin in the internalization of the nAChR taken may explain the assertions and conclusions of Trinidad *et al.* (2004). The internal co-localization of caveolin-3 and nAChR may be further explained as caveolin-3 has been shown to assist in the internalization of the insulin receptor after insulin activation, and this may be the role caveolin-3 is playing upon binding of the nAChR by the antagonist alpha-bungarotoxin (Fecchi, Volonte et al. 2006).

Caveolins have been shown to localize to high cholesterol and sphingolipid membrane microdomains, and can be isolated from other cellular proteins by Triton-X-100 lysis and separated by discontinuous sucrose gradient fractionation (Lisanti, Scherer et al. 1994). The high lipid containing particulate floats at the interface of layered 5% and 30% sucrose solutions, containing 2-5% of total cellular protein. This process first described to separate caveolae, also separates out other non-caveolin associated lipid microdomains or lipid rafts, as proteins reside in the buoyant fraction in the absence of caveolin expression. The nAChR and associated protein rapsyn were shown to co-localize to lipid raft fractions with endogenous caveolin-1 when heterologously expressed in immortalized African green monkey cells (Cos). Each of these proteins is still localized to the lipid raft domain when expressed alone (Marchand, Devillers-

Thiery et al. 2002). Stetzkowski *et al.* found that nAChR localized in the lipid fraction of differentiated myotubes both with and without agrin stimulation (2006). An additional study found that agrin treatment of C2C12 myotubes led to translocation of nAChR to the lipid raft domains as identified by sucrose gradient fractionation. Immunofluorescent imaging showed that the nAChR co-localizes with lipid raft marker GM1 in both myotubes and diaphragm tissue (Zhu, Xiong et al. 2006). The reagent, methyl beta cyclodextrin, is employed to deplete cholesterol from cell membranes. Since lipid rafts and caveolae are cholesterol rich domains, this treatment disrupts the localization of proteins to detergent resistant membrane domains. Treatment of rapsyn expressing Cos cells with methyl beta cyclodextrin disrupted the punctate membrane localization of rapsyn in a concentration dependent manner (Marchand, Devillers-Thiery et al. 2002). Methyl beta cyclodextrin treatment of C2C12 myotubes disrupted the stability of nAChR clustering, decreased the nAChR half-life and removed caveolin-3 and nAChR from the buoyant fractions of sucrose gradients. (Zhu, Xiong et al. 2006) Cholesterol depletion of C2C12 cells both before agrin treatment and after nAChR clustering attenuated cluster size. *In vivo* methyl beta cyclodextrin treatment of prenatal mice decreased overall nAChR clustering in the diaphragm at birth (Stetzkowski-Marden, Gaus et al. 2006).

While prior research touches on the potential of caveolin-3 associating with the nAChR or playing a role in nAChR clustering, no conclusive results have been determined. We hypothesize that there is a caveolin-3 and nAChR association, and that lack of caveolin-3 expression affects nAChR clustering and neuromuscular junction formation. With wildtype and caveolin-3 null mice and derived myoblast cultures, we further explored caveolin-3 and nAChR co-localization and association.

## 3.2 RESULTS

### 3.2.1 nAChR and Caveolin-3 Co-localize in Wildtype Mouse Muscle

To assess the physiological relevance of nAChR and caveolin-3 association, immunofluorescent staining was performed on 22 month old gastrocnemius muscle cross-sections from wildtype and caveolin-3 null mice. LGMD-1C is a subtype of limb-girdle muscular dystrophy caused by mutations in the caveolin-3 gene. By staining older mice, we hypothesized that phenotypic changes would be more pronounced, due to a generally more

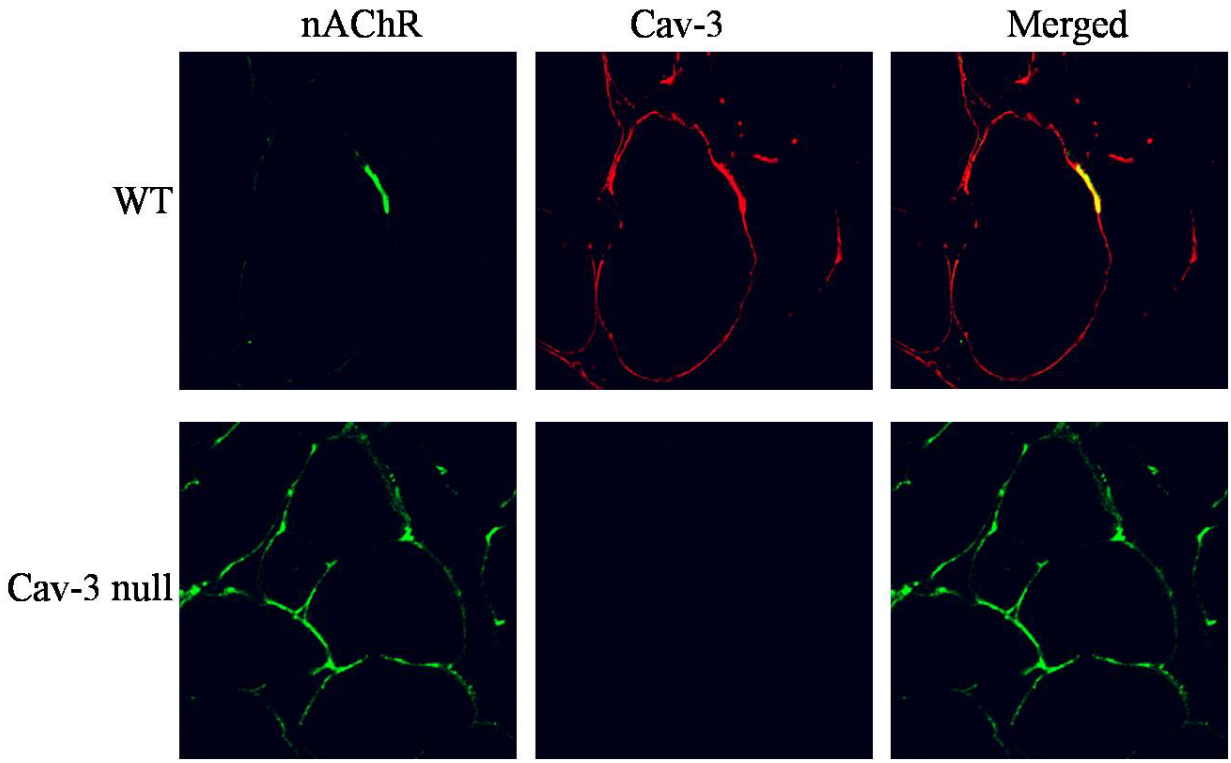


**Figure 3. Caveolin-3 and nAChR Co-localize in Wildtype Mouse Muscle**

Quadriceps muscles were dissected from 22 month-old wildtype and caveolin-3 null mouse muscle, embedded in OCT, cross-sectioned, stained and imaged by confocal microscopy. Images representative of 3 or more experiments were stained for nAChR-alpha (green) and caveolin-3 (red) and co-localization is signified by yellow. Figure was originally published in the journal, Molecular Biology of the Cell (MBC)(Hezel, de Groat et al. 2009).

distinct movement disability phenotype. In Figure 3, wildtype muscle staining shows caveolin-3 located along the sarcolemma of the myofiber, while nAChR co-localized to a distinct portion of the sarcolemma. The nAChR localization is consistent with the literature reporting one innervation per myofiber. In contrast, staining of caveolin-3 null muscle cross-sections had diffuse nAChR expression along the sarcolemma (Figure 3). The caveolin-3 null image is over-exposed in order to identify the myofiber structure. Figures 3a and 3b are flattened Z-stacks images of the nAChR clustering from wildtype and caveolin-3 null muscle cross-sections. Notice the high level of nAChR and caveolin-3 co-localization indicated by yellow in the wildtype sample (Figure 4A). The caveolin-3 null image is very planar and longer, representing distinct changes from the wildtype image (Figure 4B).

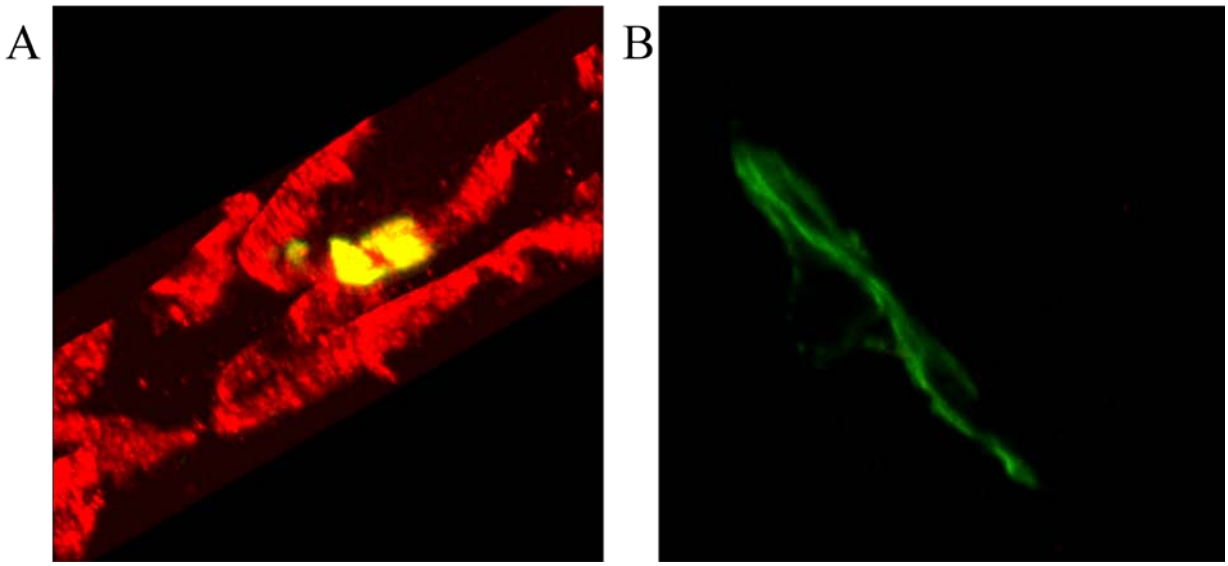


**Figure 4. Flattened Z-Stack Images of Wildtype and Caveolin-3 Null Mouse Cross-Sections**

Flattened Z-stack images from,wildtype (A) and caveolin-3 null (B) mouse quadriceps muscle, embedded in OCT, cross-sectioned, and stained for nAChR-alpha (green) and caveolin-3 (red). Confocal microscopy images representative from 3 or more experiments. Overlap is in yellow.

### 3.2.2 Caveolin-3 and nAChR Co-localization at the Wildtype Neuromuscular Junction

Figures 3 and 4 identify co-localization of nAChR and caveolin-3, but there is no neuronal staining to confirm that this co-localization occurs at the neuromuscular junction. Confirmation of co-localization of nAChR and caveolin-3 was accomplished by triple fluorescent whole-mount staining of wildtype Extensor Digitorum Longus muscle. The dissected muscle was incubated in an antibody for neuronal marker beta-tubulin 3, and caveolin-3 followed by the appropriate secondary antibodies and with Alexa 647 labeled alpha-bungarotoxin. The muscle was mounted on a slide and analyzed by confocal imaging. Caveolin-3 in red and nAChR in blue co-localize in pink juxtaposed to the nerve terminal labeled in green (Figure 4). This juxtaposition is more prominent in the flattened Z-stack image identified where the most of the nAChR co-localizes with caveolin-3 and one can see the nerve innervating the neuromuscular junction (Figure 5).

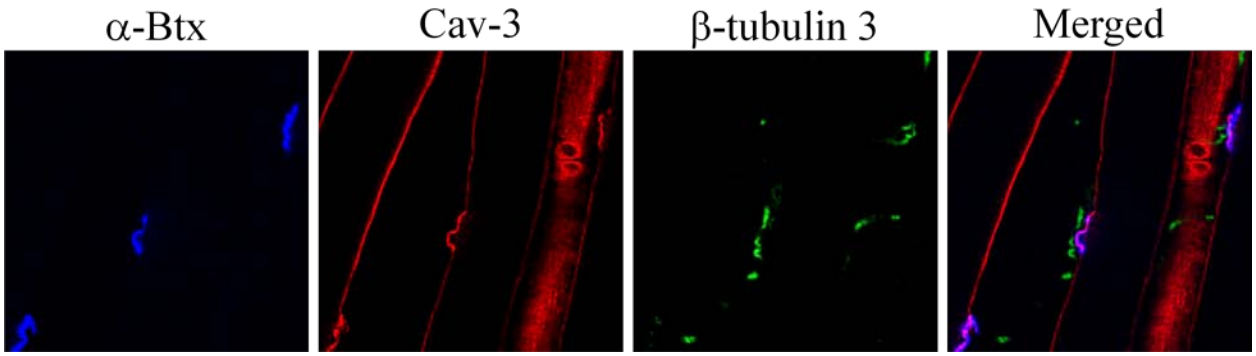


**Figure 5. Caveolin-3 and nAChR Co-localization at the Wildtype Neuromuscular Junction**

The extensor digitorum longus muscle was dissected from a wildtype mouse and stained for nAChR (blue), caveolin-3 (red), and the motor neuron with beta-tubulin-3 (green) and imaged using confocal microscopy. In the merged images, nAChR and caveolin-3 co-localization is represented in pink. Images are representative of 3 or more experiments. Figure was originally published in MBC (Hezel, de Groat et al. 2009).

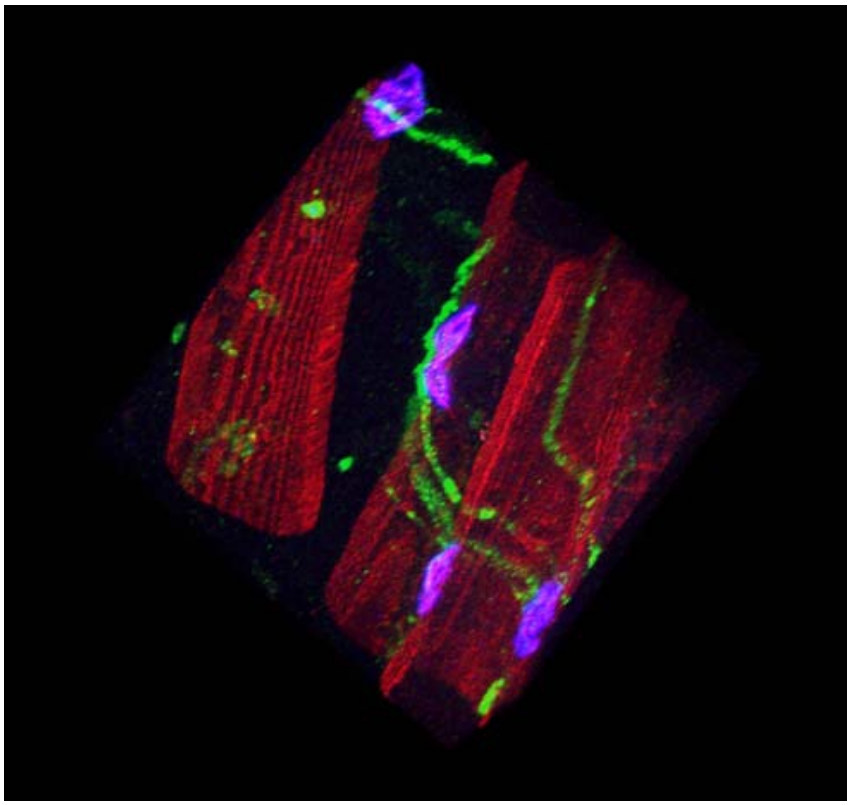

**Figure 6. Flattened Z-stack of Neuromuscular Junction Staining in Wildtype Mouse Tissue**

The extensor digitorum longus muscle was dissected from a wildtype mouse and stained for nAChR (blue), caveolin-3 (red), and the motor neuron with beta-tubulin-3 (green). Tissue was imaged using confocal microscopy and is representative of 3 or more experiments. For this image a Z-stack was flattened. Caveolin-3 and nAChR association is represented in pink. Figure was originally published in MBC (Hezel, de Groat et al. 2009).

### 3.2.3 Upregulation of Caveolin-3 and nAChR Expression during Myoblast Differentiation

The observations in mouse tissue are supportive of nAChR and caveolin-3 association and of an effect of caveolin-3 on nAChR clustering. The goal was to analyze caveolin-3 and nAChR expression during differentiation of our myoblast cultures. Our myoblast cultures are derived from mouse muscle resulting from the immorto-mouse being crossed with either wildtype or caveolin-3 null mice. Cells of the immorto-mouse lineage contain a temperature

sensitive gene, causing the cells to proliferate when grown at 33°C under treatment with interferon-gamma. The cells stop dividing and start differentiating when placed at 37°C without interferon-gamma. This system allows for initiating proliferative cell lines of tissue lineages which have low replicating power in primary culture.

Caveolin-3 and nAChR protein expression are upregulated during myoblast differentiation into myotubes. To confirm the upregulation time course of these proteins in our myoblast cultures, whole cell lysates were collected at 0, 12, 24, 48, and 96 h and the subsequent western blots were probed for nAChR and caveolin-3 protein expression (Figure 7). The results of this time course indicate that nAChR is expressed beginning at 12 h in wildtype cells and increases through 96 h. Caveolin-3 null cells express some nAChR during proliferation which increases during differentiation with more robust expression than in wildtype cells at 96 hours of differentiation. Caveolin-3 is expressed after 48 hours and robustly at 96 hours in wildtype cells only. The wildtype upregulation schedule of nAChR and caveolin-3 in our culture system is consistent with the literature (Capanni, Sabatelli et al. 2003; Macpherson, Cieslak et al. 2006).

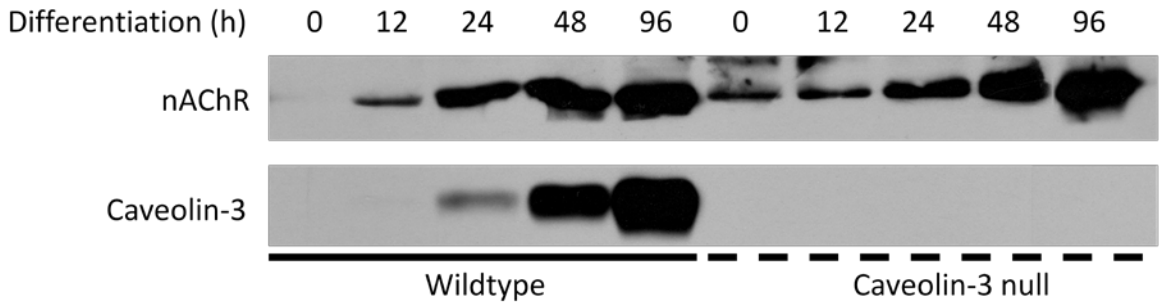


**Figure 7. Upregulation of Caveolin-3 and nAChR Expression during Myoblast Differentiation**

Wildtype and caveolin-3 null mouse derived myoblasts were differentiated for 0, 12, 24, 48 and 96 h. Cells were lysed and total protein content normalized. Whole lysates were analyzed by western blot and probed with caveolin-3 and nAChR-alpha antibodies to identify protein expression. Image is representative of 3 experiments.

### 3.2.4 Agrin induced Clustering of nAChR in Differentiated Wildtype Myotubes

Nerve released agrin induces clustering of nAChR in muscle which can be recapitulated *in vitro* by recombinant neural agrin treatment of differentiated myotubes. In wildtype muscle, there was co-localization of caveolin-3 and nAChR, does this occur in cells after agrin treatment. Wildtype myotubes differentiated for 7 days were treated with 10ng/ml agrin for 24 h. The myotubes were fixed with paraformaldehyde and stained using antibodies against caveolin-3 and nAChR-alpha followed by fluorescent tagged secondary antibodies. Confocal microscopy of the myotubes indicated nAChR clustering similar to that found in mouse muscle with discrete sarcolemma nAChR clustering (Figure 8). This indicates that agrin treatment of cells can be used to induce nAChR clustering.

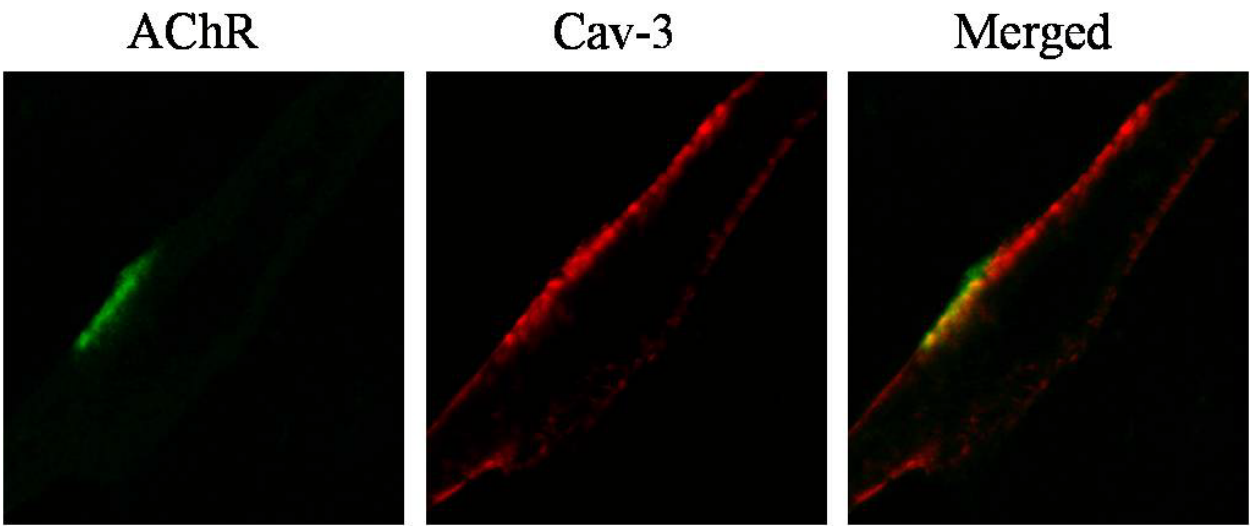


**Figure 8. Agrin induced Clustering of nAChR in Differentiated Wildtype Myotubes**

Wildtype myoblasts, grown on untreated coverslips, differentiated for 7 days and treated with agrin for 24 h. Myotubes were probed with nAChR (green) and caveolin-3 (red) antibodies and appropriate fluorescent secondary antibodies. Confocal microscopy images are representative of 3 or more experiments. Co-localization is indicated by yellow in the merged image. Figure was originally published in MBC (Hezel, de Groat et al. 2009).

### 3.2.5 Agrin induced nAChR Clustering Disrupted in Caveolin-3 Null Myotubes

As agrin treatment of wildtype myotubes led to nAChR clustering, we wanted to see if caveolin-3 played a role in nAChR clustering by comparing clustering in wildtype and caveolin-3 null differentiated myotubes. Wildtype and caveolin-3 null myoblasts were differentiated for 7 days, treated with agrin for 24 h, and probed for localization of caveolin-3 and nAChR. Agrin treated wildtype myotubes form more discrete clusters, while agrin treatment of caveolin-3 null myotubes induces diffuse nAChR sarcolemmal localization (Figure 9). This indicates that agrin treatment of cells can be used to delineate the role of caveolin-3 in nAChR clustering and neuromuscular junction formation.

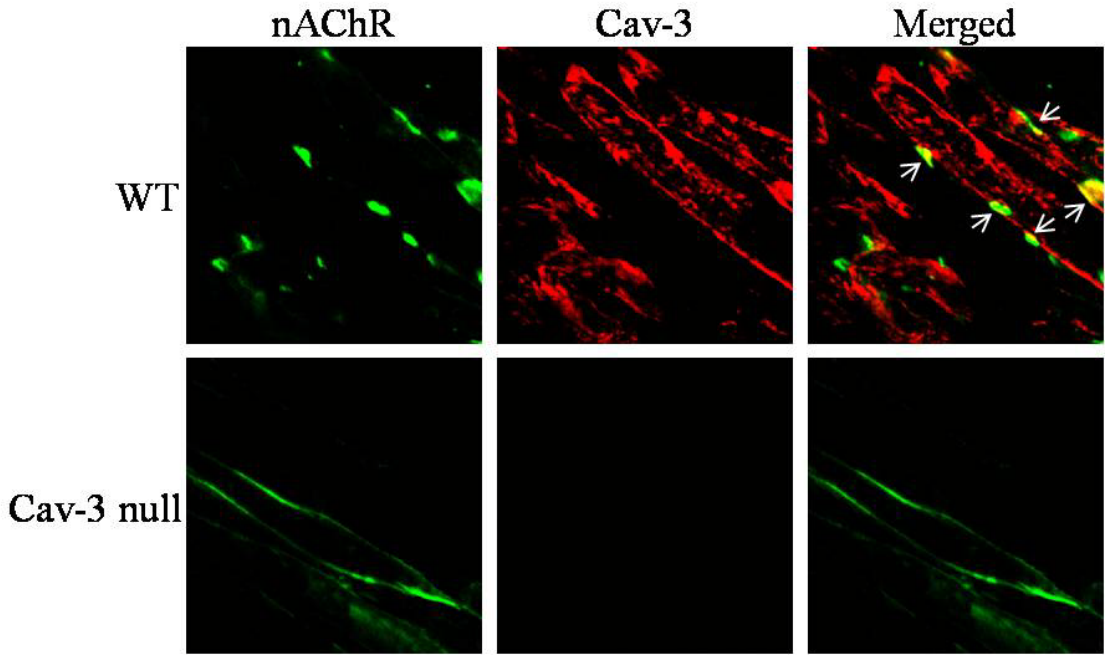


**Figure 9. Agrin induced nAChR Clustering Disrupted in Caveolin-3 Null Myotubes**

Wildtype and caveolin-3 null mouse derived myoblasts were differentiated for 7 days and treated with neural agrin (10ng/ml) for 24 h. Cells were fixed, stained and imaged using confocal microscopy. Representative figures of 3 or more experiments with nAChR-alpha in green, caveolin-3 in red and co-localization represented in yellow (arrows). Figure was originally published in MBC (Hezel, de Groat et al. 2009).

### 3.2.6 Quantification of Abrogated nAChR Clustering in Caveolin-3 Null Myotubes

The clustering differences were quantified by two analyses. One analysis compared the length of the clusters between the agrin treated wildtype and caveolin-3 null cells and the other looked at the number of clusters per field. Agrin induced nAChR clusters in wildtype cells were 2/3rds the size of nAChR clusters in caveolin-3 null cells, indicating changes in clustering of the nAChR (Figure 10A). Agrin induced clustering per field was normalized by comparing to intrinsic clustering of non-agrin treated wildtype and caveolin-3 null myotubes. Agrin induced 60% less clusters in caveolin-3 null myotubes as compared to agrin treated wildtype cells (Figure10B). This quantification suggests that caveolin-3 plays a role in nAChR clustering and that lack of caveolin-3 expression attenuates nAChR clustering.

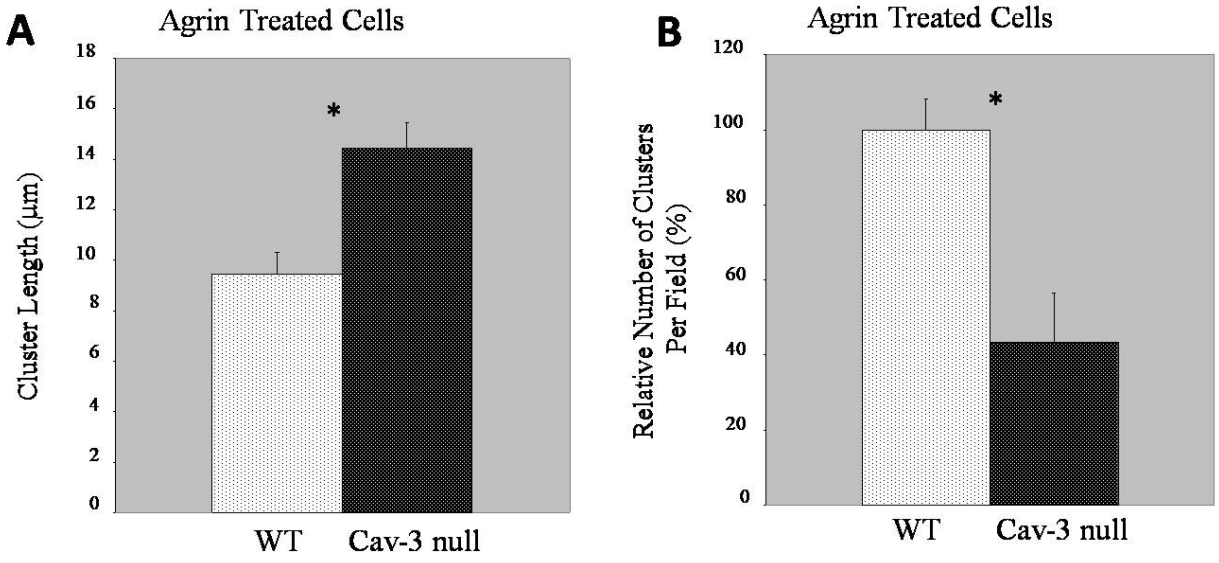


**Figure 10. Quantification of Abrogated nAChR Clustering in Caveolin-3 Null Myotubes**

Analysis of the (A) average length of nAChR clusters in agrin treated differentiated myotubes; and (B) the average number of clusters per field as quantified using confocal microscopy. (A) n=2 *p<0.0029 (B) n=3 *p<0.025. Figure was originally published in MBC (Hezel, de Groat et al. 2009).

### 3.2.7 Caveolin-3 and nAChR Associate in Wildtype Mouse Muscle

The immunofluorescent co-localization experiments show co-localization but have no bearing on whether the proteins actually associate due to the resolution limits of confocal microscopy. Immunoprecipitation is a method to assess protein association. In this method, antibodies are bound by their conserved regions to beads leaving the hyper-variable region exposed to bind the protein of interest. The bead-antibody complex is used to precipitate the antibody targeted protein with associated proteins. The associated proteins are then separated from each other by SDS treatment and analyzed by western blotting. Muscle tissue from wildtype and caveolin-3 null mice was homogenized and the nAChR immunoprecipitated using alpha-bungarotoxin bound Sepharose beads. Figure 11 indicates that caveolin-3 is immunoprecipitated with nAChR in wildtype muscle homogenates. While a large piece of muscle tissue was homogenized, total nAChR expression was undetectable. This lack of nAChR detection stems from nAChR expression only being at the neuromuscular junction of each myofiber, which is only 0.1% of the total muscle surface area. A reciprocal immunoprecipitation

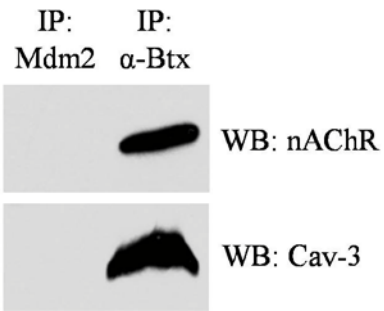


**Figure 11. Caveolin-3 and nAChR Associate in Wildtype Mouse Muscle**

Wildtype quadriceps muscle was excised, homogenized and the nAChR immunoprecipitated using alpha-bungarotoxin (α-Btx) bound beads or MDM2, an unrelated antibody, bound to Protein A Sepharose beads. The immunoprecipitates were analyzed by western blot probed with nAChR and caveolin-3 antibodies. Images are representative of 3 or more experiments. Figure was originally published in MBC (Hezel, de Groat et al. 2009).

using a caveolin-3 antibody was not successful. This may result from the differential expression between the proteins with caveolin-3 being much more prevalent than the nAChR, possibly saturating the antibodies without enough bound nAChR for successful western blot detection.

### 3.2.8 Agrin Induces Association of Caveolin-3 and nAChR in Wildtype Myotubes

To finish validating that agrin treatment after myoblast differentiation mimics the nAChR organization process in mouse muscle, an immunoprecipitation of nAChR was performed on differentiated wildtype myotubes treated with and without agrin. In agrin treated myotubes, as in muscle, caveolin-3 immunoprecipitated with the nAChR (Figure 12). Interestingly, agrin treatment for 24 hours increased the association of these proteins. While there was some association between caveolin-3 and nAChR in differentiated myotubes, agrin treatment increased the association of these proteins.

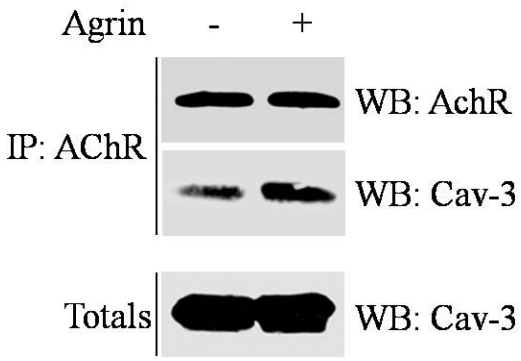


**Figure 12. Agrin Induces Association of Caveolin-3 and nAChR in Wildtype Myotubes**

Differentiated wildtype myotubes were treated with and without agrin for 24 h. Myotubes were lysed, immunoprecipitations performed using a nAChR antibody, analyzed by western blot, and probed with nAChR and caveolin-3 antibodies. Figure is representative of 3 or more experiments.

### 3.2.9 Agrin Induces Caveolin-3 Association with nAChR 20 Fold

Since the above immunoprecipitations are descriptive, quantification of the association was warranted to better understand the binding dynamics of these proteins. To this end, an immunoprecipitation in wildtype myotubes was performed using alpha-bungarotoxin bound Sepharose beads and analyzed by western blot. To better understand the relative amounts of protein immunoprecipitated to the total protein expression, the immunoprecipitates were analyzed with varying concentrations of total proteins by western blot to mimic the amount of protein immunoprecipitated (Figure 13). The immunoprecipitated proteins and corresponding portion of

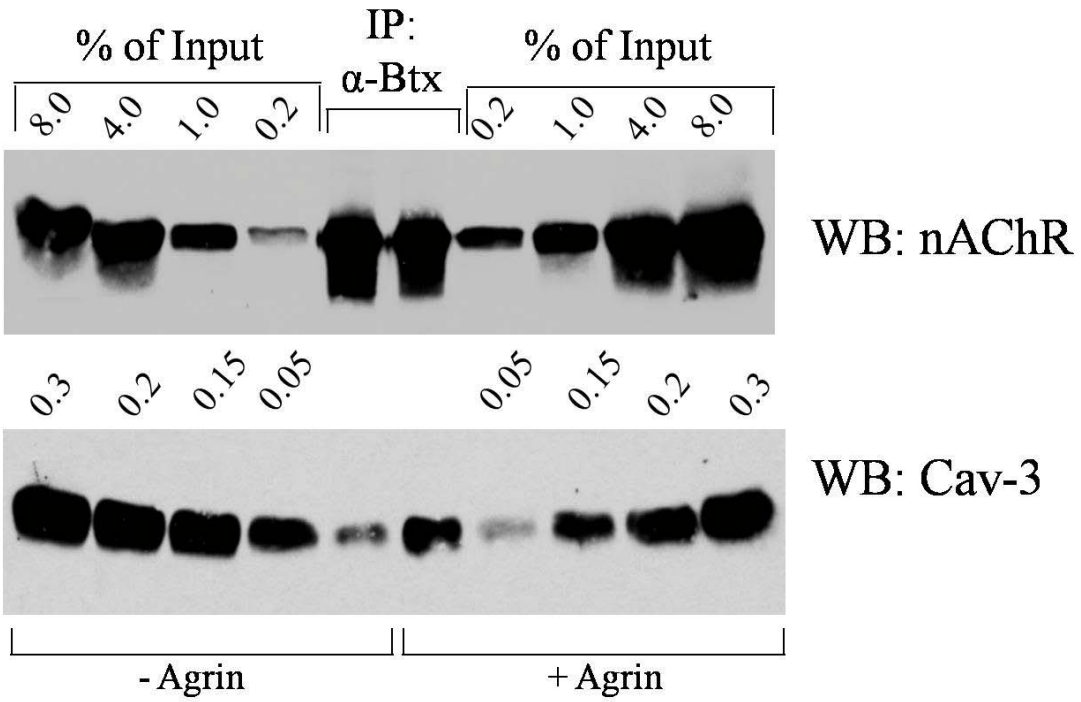


**Figure 13. Agrin Induces Caveolin-3 Association with nAChR 20 Fold**

Differentiated wildtype myotubes treated with or without agrin for 24 h. Cells were lysed and nAChR pulled-down with alpha-bungarotoxin bound beads. Analyzed by western blot and comparing the amount pulled down with total concentrations. Representative results from 2 experiments. Figure was originally published in MBC (Hezel, de Groat et al. 2009).

totals were then extrapolated to understand the total amount of protein association, a technique performed by Zhu *et al.* (2006). As before, these experiments were carried out only by immunoprecipitating nAChR. Again there was an increase in nAChR and caveolin-3 association upon agrin treatment. Through comparison of immunoprecipitate with the concentrations of total protein there was a 20 fold increase in caveolin-3 and nAChR association. To understand this calculation, this western blot indicates that only 4% of the total nAChR expression was immunoprecipitated with the alpha-bungarotoxin bound beads in both the agrin treated and untreated samples. The agrin untreated immunoprecipitates pulled down around 0.01% of total caveolin-3 expression, while the agrin treated immunoprecipitates appeared to be similar to about 0.2% of total caveolin-3 expression. As only 4% of total nAChR was immunoprecipitated, a correction of 25 was applied to all calculations. When 100% of the nAChR is immunoprecipitated 0.25% of total caveolin-3 is also pulled down in agrin untreated myotubes. While in the agrin treated myotubes 5% of the total caveolin-3 is immunoprecipitated with nAChR, yielding a 20 fold change. This corresponds to the co-localization found in agrin treated myotubes where most of the nAChR co-localizes with caveolin-3. Since caveolin-3 is expressed globally in the myotubes only a portion of caveolin-3 actually associates with nAChR.

### 3.2.10 Caveolin-3 and nAChR Associate at a Ratio of 14:1 after heterologous transfection

The above nAChR and caveolin-3 association was quantified in differentiated cultured myotubes. To further determine whether these proteins interact, several heterologous transfection experiments were performed. Using nAChR subunit constructs kindly shared by Z. Z. Wang, nAChR and caveolin-3 were transfected into 3T3 cells. Immunoprecipitation with alpha-bungarotoxin bound beads or a nAChR antibody immunoprecipitated caveolin-3 was

performed (data not shown). Immunoprecipitation of caveolin-3 with the reconstituted nAChR occurred with both whole fetal and adult nAChR forms.

Quantification of protein association by western blot is possible when using the same antibody for detection to eliminate the variability of antibody affinity. This can be accomplished by transfecting DNA constructs coding similarly tagged proteins. Thus, nAChR-alpha-myc subunit was cloned as outlined in the methods. Our lab already had a myc-tagged caveolin-3. These myc-tagged caveolin-3 and nAChR-alpha constructs were co-transfected into 3T3 cells and a sequential immunoprecipitation was performed after 48 h (Figure 14). A sequential immunoprecipitation is where two immunoprecipitations are performed one after another. After 48 h, the cells were lysed and a caveolin-3 immunoprecipitation performed. The

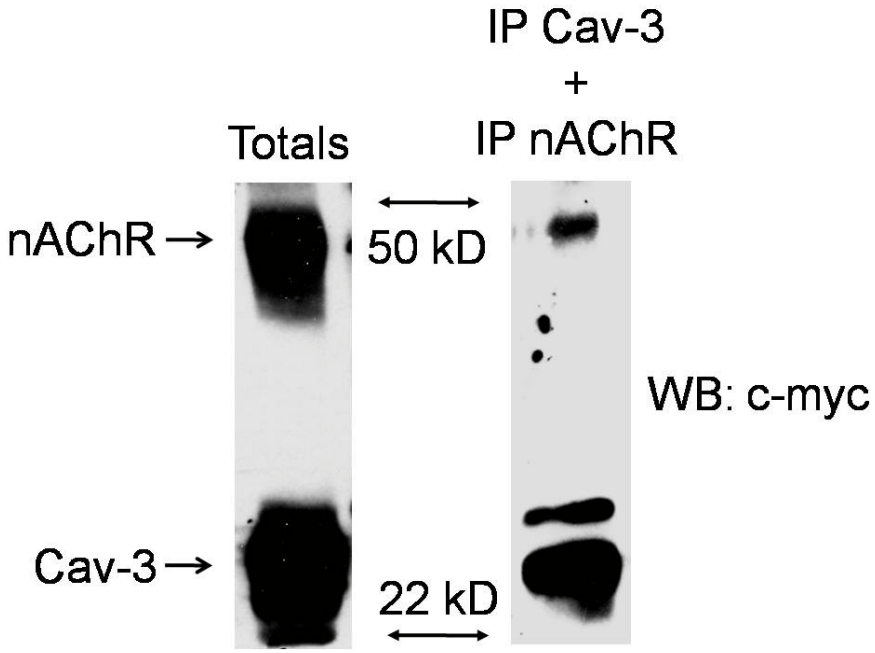


**Figure 14. Caveolin-3 and nAChR Associate at a Ratio of 14:1 after Heterologous Transfection**

3T3 cells were heterologously transfected with myc tagged caveolin-3 and nAChR-alpha constructs. 48 h later the lysates were collected and a sequential immunoprecipitation performed and analyzed by western blot. Densitometry analysis indicated a 14:1 ratio of caveolin-3 to nAChR-alpha. Representative results from 3 experiments. Figure was originally published in MBC (Hezel, de Groat et al. 2009).

immunoprecipitated proteins were isolated from the beads and antibodies by addition of 0.5% SDS in lysis buffer and incubating the samples at 50°C for 10 m. The protein solution was collected and diluted to 0.1% with lysis buffer and immunoprecipitation with a nAChR antibody was performed. Again the proteins were isolated and collected from the beads and antibodies as before. Lammeli buffer was added to the isolated proteins and analyzed by western blot and probing with a c-myc antibody. Band analysis by densitometry indicated that there were approximately 14 times more caveolin-3 bound to the nAChR-alpha subunit (Figure 14). As caveolae consist of 14-16 caveolin-3 proteins bound together, this suggests one nAChR-alpha subunit per caveolae. This may indicate that caveolae function as a platform for nAChR signaling and protein associations.

## 3.3 DISCUSSION

While other research has touched on the possibility of caveolin-3 association with nAChR, this research provides definitive answers by using tools well suited for this task. Caveolin-3 co-localizes and associates with nAChR in muscle and in agrin treated differentiated myotubes. Lack of caveolin-3 appears to change the attributes of the nAChR clustering in caveolin-3 null muscle and differentiated myotubes. This research suggests that caveolin-3 is important in nAChR clustering and that nAChR-alpha subunits and caveolin-3 associate.

There are distinct differences in nAChR and caveolin-3 co-localization from muscle to differentiated myotubes in culture. The co-localization appears much stronger in the muscle as compared to our culture model. This could result from the cell culture model not containing the whole complement of signals for neuromuscular junction formation. Since these experiments

were performed using only muscle cells treated with a soluble form of agrin and without the associated nerve cells, it is most likely that post-synaptic junction formation is not as robust or directed *in vitro* as *in vivo*. In muscle, the synaptic localization of the nucleus induces increased transcription and translation of the nAChR and associated proteins, leading to higher expression. Various other differences between muscle and cultured myotubes could also affect association. For example, agrin is anchored to the extra cellular matrix after neuronal release *in vivo* though in culture a soluble agrin form is used. Research has shown that agrin bound to substrate can induce clustering even without MuSK kinase activation (Bromann, Zhou et al. 2004). The lack of interplay between the nerve and muscle is also thought to play a role, as ACh release has been shown to disperse clusters not fully anchored at the membrane (Madhavan, Zhao et al. 2003). The lack of nerve induced contraction in the cell culture also may play a role in the maturation of the muscle neuromuscular junction which is not found in cell culture.

The immunofluorescent staining of agrin induced differentiated wildtype and caveolin-3 null myotubes indicates more diffuse nAChR localization in the caveolin-3 lacking myotubes. The caveolin-3 null myotubes form some clusters but not as distinctly as wildtype myotubes suggesting an inability to carry out the full clustering signal pathway. This is further confirmed by the decreased number of clusters per view in the agrin treated null myotubes. As with the differentiated myotube co-localization above, this model system does not contain all signaling mechanisms found in the *in vivo* muscle system. It must also be considered that caveolin-3 null mice are viable but live slightly shortened lives, suggesting that while the neuromuscular junction formation is impaired, it definitely is not dysfunctional.

The analysis of caveolin-3 and nAChR-alpha protein association in cultured myotubes was difficult due to uneven protein expression, with caveolin-3 being more prevalent than the

nAChR-alpha subunit. Our immunofluorescence data indicate nAChR and caveolin-3 localize to the plasma membrane, while the immunoprecipitation experiments reflect whole cell protein expression. Immunoprecipitation using biotin bound alpha-bungarotoxin applied to the cell culture media and subsequent streptavidin immunoprecipitation might yield higher association results by isolating only the nAChR located at the membrane. It has been suggested that only 30% of the full nAChR is trafficked to the membrane, and so whole cell nAChR immunoprecipitation may skew the results (Wanamaker, Christianson et al. 2003). Caveolin-3 to nAChR ratios are estimated from myotubes treated with agrin for 24 h. This does not take into account the affinity of the antibodies that were used to probe for each protein and the length of time ECL was incubated on the membrane before developing.

Immunofluorescence and immunoprecipitation experiments indicate similar interactions between caveolin-3 and nAChR with only a portion of caveolin-3 co-localizing and associating with nAChR. As noted before the immunoprecipitation experiments using whole lysates do not differentiate between cytoplasmic and membrane localized protein. If these proteins only associate in one part of the cell and have other non-associating protein pools it may skew the association ratio calculation. Another way to further confirm the ratio of nAChR and caveolin-3 association in heterologously transfected cells would be through Forster energy resonance transfer. This technique uses co-transfection of differentially labeled fluorescent proteins, where excitation of the chromophore on one protein induces a fluorescent emittance which consequentially activates the fluorophore on the associated protein. The proximity of the fluorophores on the proteins cannot be farther than 10nm apart to use this technique. This imaging experiment would further confirm protein association, while eliminating the possibility of data skewing due to differential protein localization.

Sequential immunoprecipitation of caveolin-3 followed by immunoprecipitation of the nAChR-alpha subunit indicated a 1:14 ratio of caveolin-3 to nAChR, fitting well in the role of each nAChR alpha-subunit interacting with a full caveolae. These results do have some pitfalls. The sequential immunoprecipitation may have artifacts resulting from the use of SDS to remove the bound proteins from the antibody and bead complex. This treatment could potentially remove the antibody from the beads, carrying over to the second immunoprecipitation skewing the data. As caveolin-3 proteins form large structures by binding one another, the caveolin-3 pulled-down but not bound to nAChR in the first immunoprecipitation may bind caveolin-3 molecules already bound to nAChR, skewing the ratio results from the second immunoprecipitation. In both the fetal and adult nAChR, there are 2 nAChR-alpha subunits in the full structure. The sequential immunoprecipitation results suggest that only one nAChR-alpha subunit must associate with a caveolae, this may be different with the all the nAChR subunits expressed.

Our results indicate an association between caveolin-3 and nAChR. More importantly, there are differences in the formation of nAChR clusters in caveolin-3 null and wildtype animals and derived agrin-treated differentiated myotubes. Whether these changes actually affect neuromuscular junction function or not remains to be seen. The role caveolin-3 plays in the signaling cascade leading to nAChR clustering needs to be delineated to identify how caveolin-3 changes the nAChR localization and neuromuscular junction as shown above.

# 4.0 CAVEOLIN-3 ROLE AT THE MOLECULAR LEVEL IN NACHR CLUSTERING

## 4.1 INTRODUCTION

The neuromuscular junction undergoes many changes in producing a highly efficient signaling synapse. The muscle without input from the nerve produces nAChR clusters along the midline of differentiated myofibers (Lin, Burgess et al. 2001). During muscle innervation by the motorneuron, these clusters are modified by neuronal agrin release, inducing nAChR cluster translocation to juxtaposition with the nerve terminal. The synapse then undergoes further structural modifications to enhance the efficiency of synaptic transmission (Wiesner and Fuhrer 2006).

For many years experiments were performed to identify proteins that induce clustering of the nAChR. While laminin, neuregulin, fibroblast growth factor (FGF), midkine and acetylcholine were probed for nAChR clustering ability, agrin has been determined as the most potent nAChR clustering inducing ligand (Sanes and Lichtman 2001). Agrin is produced and released in different forms by both the nerve and muscle. The muscle form has no nAChR clustering activity. Neural agrin is different from muscle agrin in that it contains 2 inserted amino acid sequences. These inserts confer activity to agrin, which can be used *in vitro* to stimulate nAChR clustering in differentiated myotubes (Ferns, Campanelli et al. 1993).

Since the Torpedo electric organ is a modified neuromuscular junction expressing the nicotinic acetylcholine receptor, it has served as a model for determining important protein

associations and signals. Many of the essential proteins found to bind the nAChR, or those that, due to proximity, are otherwise involved in nAChR clustering result from studying this model system. These proteins include MuSK, which is involved in the initiation of clustering signaling and Rapsyn, an important binding protein of nAChR. These proteins have formed the basis for clustering research. Both, MuSK and Rapsyn null mice die at birth, due to dysfunctional diaphragm neuromuscular junctions leading to asphyxiation of the pups (Gautam, DeChiara et al. 1999).

The signaling pathway initiated by agrin acting on proteins in the sarcolemma and leading to nAChR clustering has been extensively studied. The sequence of these protein associations and their role in signaling is currently unknown. Many proteins have been identified as being involved in nAChR organization though the order of their associations and path of signal transduction has not been clarified (Figure 11). Since many of these proteins have been identified as binding MuSK, or Rapsyn, it is not known whether these proteins are involved with primary clustering signaling or signaling induced by agrin treatment but not directly affecting clustering.

Until recently, MuSK had been considered the protein initiating nAChR clustering pathway. This receptor tyrosine kinase is activated by agrin treatment inducing auto-phosphorylation and a subsequent signaling cascade. Due to a lack of direct agrin association, it was long hypothesized that MuSK activation requires an associated protein for signaling nicknamed muscle associated signaling complex (MASC) (Glass, Bowen et al. 1996). MASC was recently identified to be LDL receptor related protein 4 (LRP4), which is also essential for neuromuscular junction formation and animal survival upon birth (Kim, Stiegler et al. 2008; Zhang, Luo et al. 2008).

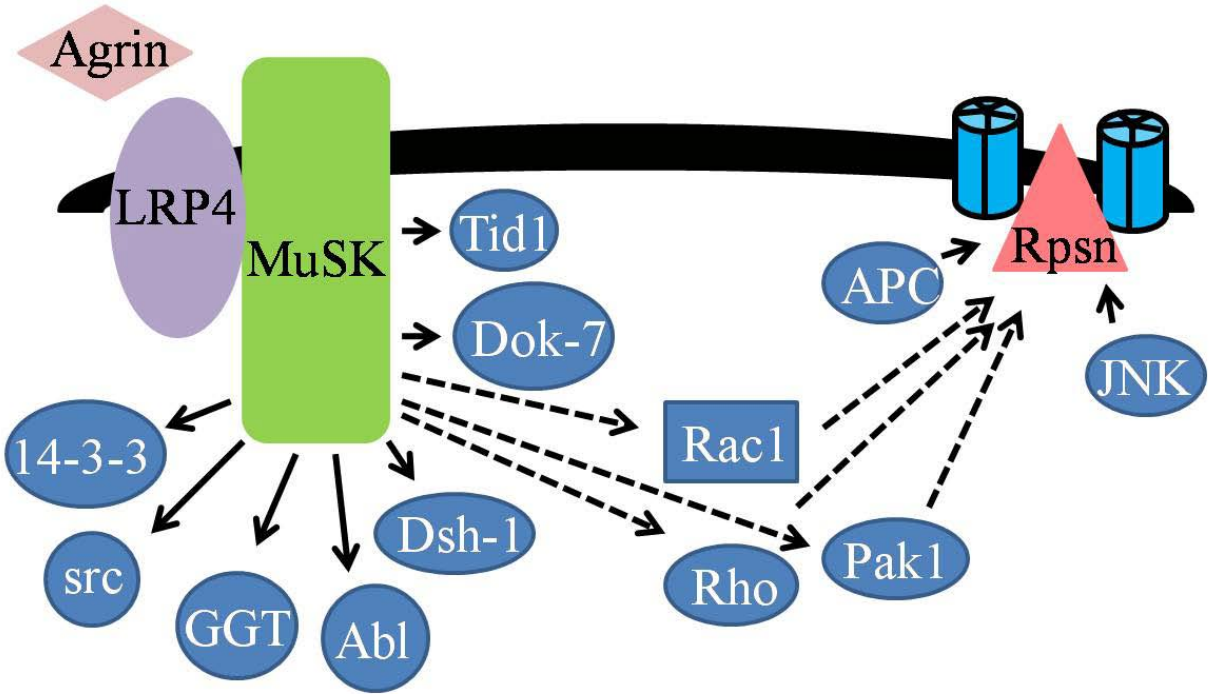


**Figure 15. Model of Protein Signaling Relevant to nAChR Clustering**

The pathway for nAChR clustering has not been fully elucidated. The pathway is initiated by neural agrin binding to LRP4 and inducing MuSK phosphorylation leading to eventual localization of Rapsyn (Rpsn) and the nAChR (blue barrels around rapsyn) at the neuromuscular junction. Agrin, LRP4, MuSK, Rapsyn and nAChR subunits are all essential proteins and removal of any of these proteins results in animals that die at birth. Research has focused on proteins that, after agrin activation, bind MuSK (Tid1, Dok-7, Dsh-1, Abl, GGT, src, 14-3-3) and Rapsyn (APC and JNK). How these proteins fit into a nAChR cluster inducing pathway is still undetermined. Likewise Rac1, Rho and Pak1 are essential but how agrin leads to activation and transmission of their activation is not clear. Solid arrows are identified associations while the dashed arrows are implied signaling processes.

Since the discovery of MuSK, much research has focused on identification of proteins bound to and activated by MuSK after agrin treatment. Proteins found to bind MuSK and be activated by agrin treatment are the src family kinases, geranyl geranyl transferase I, dishevelled, abl, Doc-7, 14-3-3 and recently identified TID1 (Mohamed, Rivas-Plata et al. 2001; Luo, Wang et al. 2002; Luo, Je et al. 2003; Strochlic, Cartaud et al. 2004; Okada, Inoue et al. 2006; Linnoila, Wang et al. 2008). Many of these proteins have been shown to be essential in clustering through knockdown by interference RNA or by signal abrogation by protein specific inhibitors. Whether

and how these proteins fit into the nAChR clustering signaling scheme or structure is not fully understood.

Rapsyn has been found to be at a 1:1 stoichiometry with nAChR in myotubes (LaRochelle and Froehner 1986; Hughes, Kusner et al. 2006). Originally discovered in the electric organ of the electric eel, co-expression of rapsyn and nAChR is required for nAChR clustering (Sealock, Wray et al. 1984). By also binding beta-dystroglycan in the dystrophin glycoprotein complex, rapsyn is involved in the stabilization of the nAChR clusters (Dobbins, Zhang et al. 2006). Laminin, which is a weak alternative signaling pathway for nAChR clustering, also signals through rapsyn (Banks, Fuhrer et al. 2003). Simultaneous expression of rapsyn with src family kinases leads to nAChR subunit phosphorylation (Banks, Fuhrer et al. 2003).

Other proteins identified as essential for nAChR clustering include the small GTPases, Rac1 and Rho, and other signaling proteins Pak1 and APC. (Weston, Yee et al. 2000; Wang, Jing et al. 2003; Weston, Gordon et al. 2003; Weston, Teressa et al. 2007) Most likely these signaling proteins fall between MuSK activation and nAChR clustering though their position in the clustering pathway has not been determined.

Since our results show association and co-localization of caveolin-3 and nAChR and suggest modified clustering in caveolin-3 knockout mice and differentiated myotubes (Chapter 3), the next step was to look at whether caveolin-3 played a role in the signaling cascade of nAChR clustering. As the distinct pathway is not yet defined, this research focused on proteins essential in nAChR clustering.

## 4.2 RESULTS

### 4.2.1 Agrin induced Rac1 activation in Wildtype Myotubes

To understand the abrogation of clustering in the caveolin-3 null myotubes, proteins identified in nAChR clustering were compared to those that associate with the caveolin family. Rac1 was a strong candidate, as it is essential to nAChR clustering and requires binding to caveolin-1 for successful signaling in vascular endothelial cells (Zuo, Ushio-Fukai et al. 2005). Rac1 is a small GTP binding protein involved in cell mediated cytoskeletal reorganization, cell growth and kinase activation pathways. Rac1 has been shown to be an essential intermediary in nAChR clustering, which is abrogated after expression of dominant negative Rac1 (Weston, Yee et al. 2000). Rac1 localized to the cytoplasm, translocates with caveolin-1 to the plasma membrane after angiotension II treatment of vascular smooth muscle cells (Zuo, Ushio-Fukai et al. 2005). Several papers show that knockdown of caveolin-1in vascular endothelial cells disrupts Rac1 activation and the eventual signaling endpoint (Cho, Ryu et al. 2004; Zuo, Ushio-Fukai et al. 2005; Hu, Ye et al. 2008; Singleton, Chatchavalvanich et al. 2009). Due to 85% similarity between caveolin-1 and caveolin-3, it is likely that both proteins have similar interactions with Rac1. Rac1 may be the link that is disrupted in caveolin-3 null myotubes during nAChR clustering.

To determine whether lack of caveolin-3 affects agrin induced Rac1 activation, Rac1 activation was assessed over an agrin treatment time course in wildtype and caveolin-3 null myotubes. Agrin treatment induces activation of Rac1, and Cdc42 (Weston, Yee et al. 2000). Activated Rac1 can be isolated and assessed through pulling down the binding domain of p21 activated kinase 1 (Pak1) to which activated Rac1 binds (Weston, Yee et al. 2000). Using a fused GST-

Pak1 binding domain (PBD) construct from Dr. Daniel Altschuler's laboratory, a GST-PBD fusion protein was produced and bound to glutathione-bound agarose beads. Activation of Rac1 was analyzed in wildtype and caveolin-3 null myotubes treated with 10ng agrin per ml of agrin for 0, 15, 60 or 240 min. In wildtype myotubes, activated Rac1 peaked after 1 h of agrin treatment, while caveolin-3 null myotubes maintained basal expression of activated Rac1 without any agrin induced activation (Figure 16). The lack of Rac1 activation corresponds to the differences in nAChR clustering seen in caveolin-3 null myotubes.

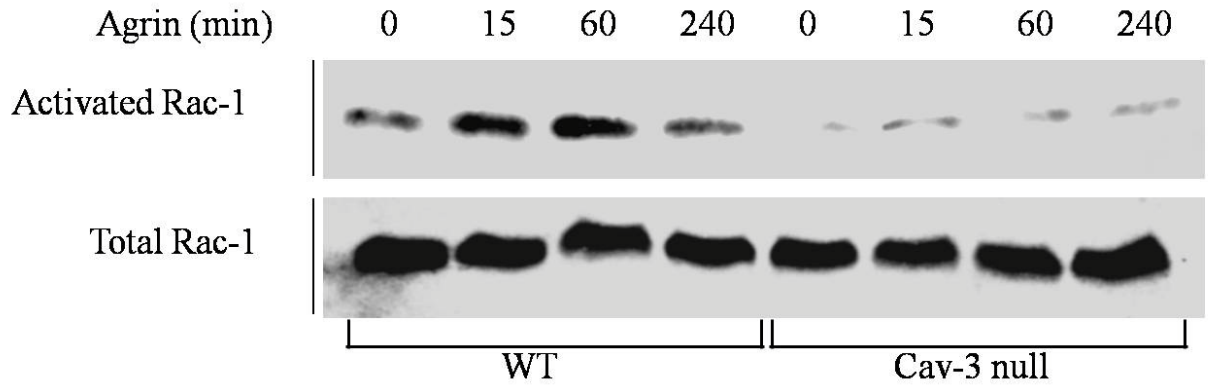


**Figure 16. Agrin induced Rac1 Activation in Wildtype Myotubes**

Wildtype and caveolin-3 null mouse derived myoblasts were differentiated for 7 days and treated with agrin for 0, 15, 60 and 240 min. Cells were lysed and activated Rac1 was pulled down using a glutathione S-transferase-Pak1 binding domain fusion protein bound to glutathione sepharose beads. Western blot analysis probed with Rac1 antibody indicated activated Rac1. Total expression of Rac1 in lysates is located below. Representative results from 3 or more experiments. Figure was originally published in MBC (Hezel, de Groat et al. 2009).

### 4.2.2 Agrin induces Caveolin-3 and Rac1 Association

Our previous data indicate that Rac1 is not activated in agrin treated caveolin-3 null myotubes in contrast to the activation in wildtype cells. Whether this occurs due to lack of caveolin-3 binding is not known, but probably due to the effect of caveolin-1 on Rac1 activation.

Immunoprecipitation of caveolin-3 in agrin treated myotubes was performed to identify whether caveolin-3 interacts with Rac1. Figure 17 shows that agrin induces the association of caveolin-3 and Rac1 with the association peaking at a 15 min but remaining elevated at 4 h. These data directly support the requirement of caveolin-3 for Rac1 activation and nAChR clustering.

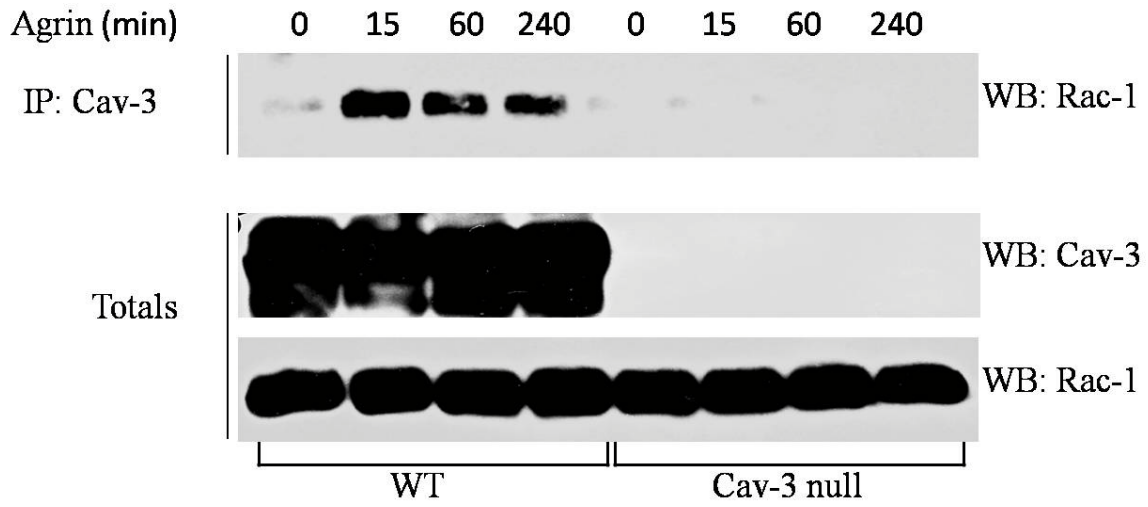


**Figure 17. Agrin induces Caveolin-3 and Rac1 Association**

Wildtype and caveolin-3 null mouse derived myoblasts were differentiated for 7 days and treated with agrin for 0, 15, 60 and 240 min. Cells were lysed and caveolin-3 pulled down using caveolin-3 antibody and Protein A Sepharose beads. Western blot analysis probed with Rac1 antibody indicated association. Total expression of Rac1 and caveolin-3 is located below. n=3. Figure was originally published in MBC (Hezel, de Groat et al. 2009).

### 4.2.3 What activates Rac1

Rac1, as a small G-protein is activated by the exchange of bound GDP for GTP. This exchange is catalyzed by Guanine nucleotide exchange factors (GEFs). There are a large number of proteins that act as GEFs, and due to their transient interaction with the G-proteins, it is difficult to determine which GEF is involved with activation. Immunoprecipitations for Rac1 and associated GEFs were performed in an attempt to identify the GEF responsible for agrin

induced Rac1 activation in myotubes. Sos-1, the first GEF identified also called son of sevenless, has been shown to activate Rac1 in response to angiotension II in vascular smooth muscle cells (Zuo, Ushio-Fukai et al. 2005). Caveolin-3 binding to Sos-1 was identified but Rac1 association with Sos-1 was elusive (Data not shown). Geft is a muscle specific GEF protein that has been identified to activate Ras family proteins (Bryan, Mitchell et al. 2005). Association between GEFT and Rac1 was also not observed (Data not shown).

### 4.2.4 Agrin induced JNK Activation is not Affected in Caveolin-3 Null Myotubes

JNK activation is required for expression of the epsilon subunit of nAChR (Si, Wang et al. 1999). JNK phosphorylation results from activated Rac1 and Cdc42 expression, and this phosphorylation is abrogated by expression of Rac1 and Cdc42 kinase null constructs (Weston, Yee et al. 2000). Due to the implication that JNK phosphorylation occurs after Rac1 activation, JNK activation was assessed in whole cell lysates over an agrin treatment time course of 0, 15, 60, and 240 min. Lysates were analyzed by western blots probed for phospho-JNK. There was JNK activation at 15 min in both wildtype and caveolin-3 null myotubes treated with agrin (Figure 18). These results show activation which does not follow the time course of agrin

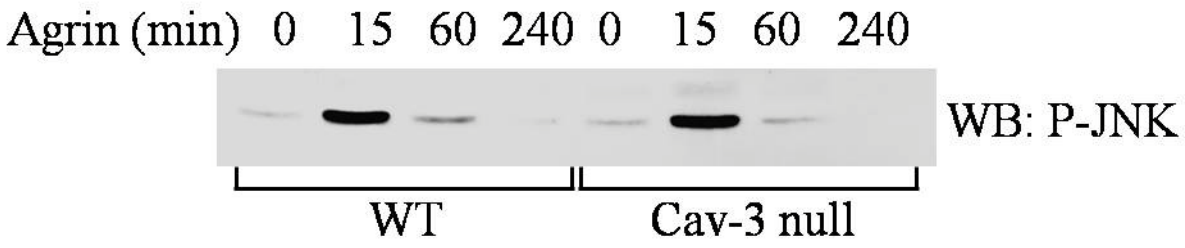


**Figure 18. Agrin induced JNK Activation is not Affected in Caveolin-3 Null Myotubes**

Wildtype and caveolin-3 null mouse derived myoblasts were differentiated for 7 days and treated with agrin for 0, 15, 60 and 240 min. Cells were lysed, and protein content normalized. Western blot analysis of total lysate was probed with a phospho-JNK antibody. n=2. Figure was originally published in MBC (Hezel, de Groat et al. 2009).

activation of Rac1, implying that agrin induced JNK activation occurs through a different pathway.

### 4.2.5 Caveolin-3 is important for MuSK Phosphorylation

Results presented earlier (Figure12), found abrogation of nAChR clustering signaling at the point of Rac1 activation. Rac1 activation is recognized as an intermediate step in nAChR clustering. Since subsequent experiments were unable to delineate whether signal abrogation occurred at Rac1 activation through localization of GEFs for Rac1, we focused on upstream signaling important for nAChR clustering. MuSK, the protein located at the beginning of signaling cascade, was an appropriate starting point.

MuSK has long been determined to be part of a protein complex involved in the initiation of clustering signaling. MuSK is a receptor tyrosine kinase, whose kinase domain consists of most of the cytoplasmic domain and contains 6 tyrosines which have been shown to be phosphorylated upon agrin induced activation (Watty, Neubauer et al. 2000). While there is no direct interaction between agrin and MuSK, agrin treatment induces MuSK autophosphorylation initiating the nAChR clustering pathway. Analysis of agrin induced MuSK phosphorylation in myotubes was the next logical step. Wildtype and caveolin-3 differentiated myotubes were treated with agrin for 0, 15, 60 or 240 min. The cells were lysed and MuSK immunoprecipitated using a combination of polyclonal MuSK antibodies. The samples were analyzed on a western blot and probed with a phospho-tyrosine antibody. There was a peak in MuSK phosphorylation after 1 h of agrin treatment in both wildtype and caveolin-3 null cells, but the MuSK activation was stronger in the wildtype as compared to the caveolin-3 null myotubes (Figure 19). The

caveolin-3 null myotubes had less MuSK overall than the wildtype myotubes, as found in analysis of total lysates. Density analysis of the western blot results, indicate that overall MuSK expression was decreased by 1/3, while phosphorylation decreased 3/5 between wildtype and caveolin-3 null myotubes. This suggests that loss of caveolin-3 results in not only decreased MuSK expression or stability but also changes in the level of MuSK activation.

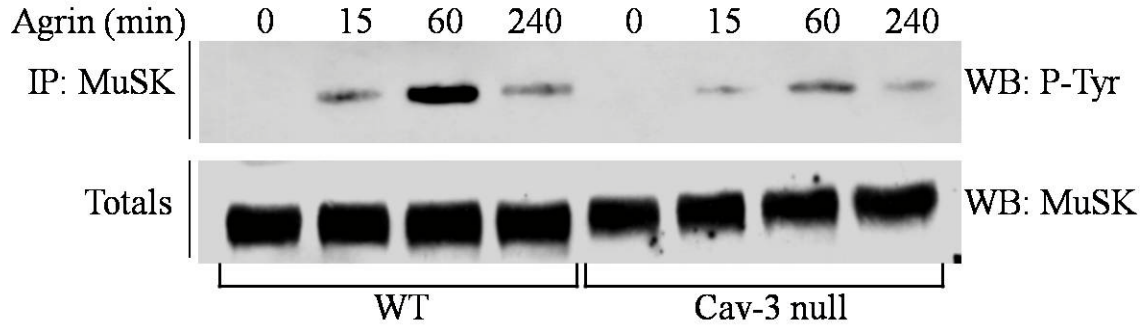


**Figure 19. Caveolin-3 is important for MuSK Activation**

Wildtype and caveolin-3 null mouse derived myoblasts were differentiated for 7 days and treated with agrin for 0, 15, 60 and 240 min. Cells were lysed and MuSK pulled down using MuSK antibody bound to Protein A Sepharose beads. Western blot analysis probed with a phospho-tyrosine antibody indicates MuSK activation. Total expression of MuSK in lysates is located below. Representative results of 3 or more experiments. Figure was originally published in MBC (Hezel, de Groat et al. 2009).

### 4.2.6 Agrin induces MuSK and Caveolin-3 Association in Differentiated Myotubes

Our research shows distinct differences in agrin activation of MuSK and overall MuSK expression between wildtype and Caveolin-3 null myotubes, suggesting that Caveolin-3 is important in the stability of MuSK. The next step was to assess whether caveolin-3 and MuSK interact. Using differentiated myotubes treated with 10ng/ml agrin for 0, 15, 60, and 240 min, MuSK was immunoprecipitated as before. Western blot analysis of associated proteins was probed with an anti-caveolin-3 antibody. The results indicated a basal level of caveolin-3 and

MuSK association with peaks after 1 h of agrin treatment in wildtype myotubes (Figure 20). This peak matches the peak activation of Rac1 found earlier and the peak in MuSK phosphorylation. Overall MuSK expression was again decreased in the caveolin-3 null cells.

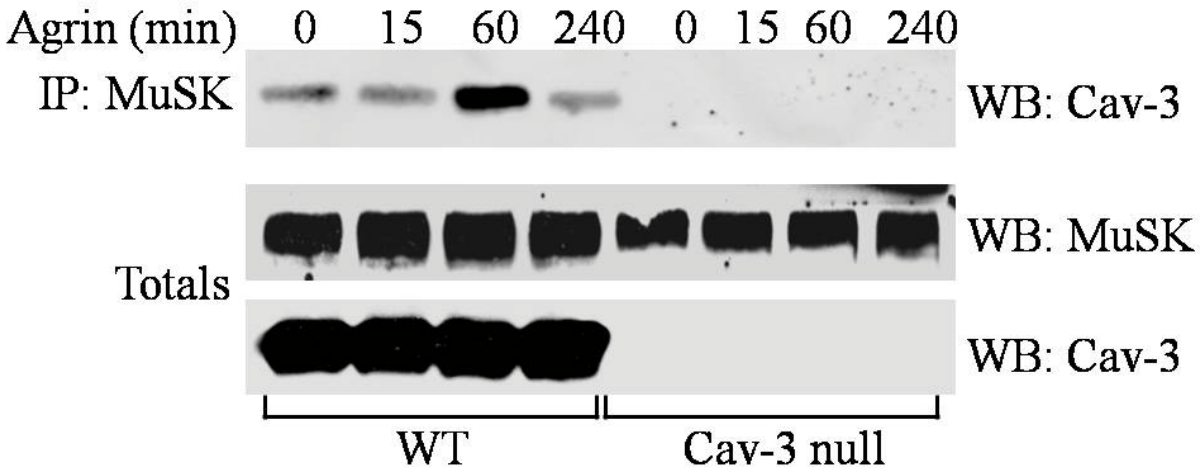


**Figure 20. Agrin induces MuSK and Caveolin-3 Association in Differentiated Myotubes**

Wildtype and caveolin-3 null mouse derived myoblasts were differentiated for 7 days, and treated with agrin for 0, 15, 60 and 240 min. Cells were lysed and MuSK was pulled down using MuSK antibody and Protein A Sepharose beads. Western blot analysis probed with caveolin-3 antibody indicated association. Total expression of MuSK and caveolin-3 in lysates is located below. Representative results of 3 or more experiments. Figure was originally published in MBC (Hezel, de Groat et al. 2009).

### 4.2.7 MuSK binds Caveolin-3 at the MuSK Caveolin Binding Domain

The MuSK immunoprecipitation indicated association of MuSK with caveolin-3, but did not confirm that this interaction is direct. There is the possibility of an adapter protein binding to both of them, which is not discriminated from actual protein-protein binding by immunoprecipitation. The amino acid sequence of MuSK contains 2 putative caveolin-3 binding domains (CBD) consisting of the sequence OXOXXXXO, where Os are aromatic residues and Xs are other amino acids (Figure 21). These binding domains, located in the kinase domain,

contain similar sequences to the sequences first identified as caveolin binding domains (Couet, Li et al. 1997). The tyrosine residues contained in the caveolin-3 binding domains are not phosphorylated in MuSK activation (Watty, Neubauer et al. 2000).

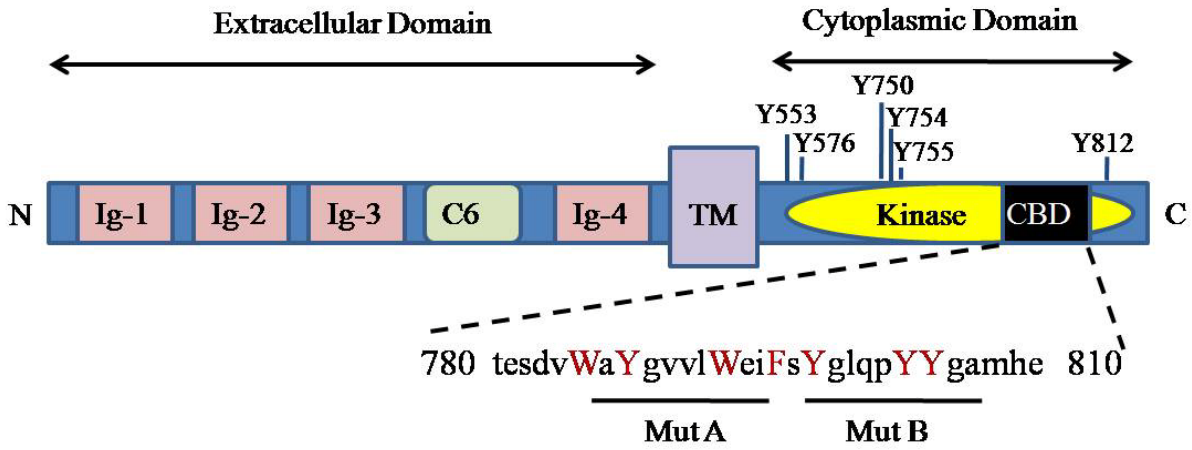


**Figure 21. Diagram of MuSK Protein**

This diagram characterizes the known functional domains of the MuSK protein. The tyrosines shown in the cytoplasmic domain represent tyrosines phosphorylated after agrin activation. There are 2 caveolin-binding domains (CBD) within the kinase domain. The important aromatic residues highlighted in red, are mutated in our Mutant A (MutA) and Mutant B (MutB) constructs. Figure was originally published in MBC (Hezel, de Groat et al. 2009).

To further determine whether caveolin-3 and MuSK directly bind each other at the MuSK CBD, MuSK was cloned into an hemaglutinin (HA) tagged constitutively expressed vector. Using internal primers, PCR directed mutagenesis to alanine residues was performed on each of the caveolin binding domains. The mutated MuSK sequences were cloned into the same vector as the wildtype MuSK sequence. To understand caveolin-3 and MuSK binding, each MuSK vector in conjunction with a wildtype caveolin-3 vector were transfected into Ras transformed 3T3 fibroblasts. The overexpression of Ras suppresses endogenous caveolin-1 expression, removing the chance of caveolin-1 contamination. Two days after transfection, the cells were lysed and immunoprecipitation with caveolin-3 antibodies performed. MuSK binding to

caveolin-3 was analyzed by western blot and probed for the HA tag (Figure 22). While there was strong affinity between caveolin-3 and wildtype MuSK, caveolin-3 binding to MuSK with mutated caveolin binding domain A, was highly reduced and binding between caveolin-3 and MuSK caveolin binding domain B was not detected by western blotting. These results support a direct interaction between caveolin-3 and MuSK which requires the MuSK caveolin binding domains.

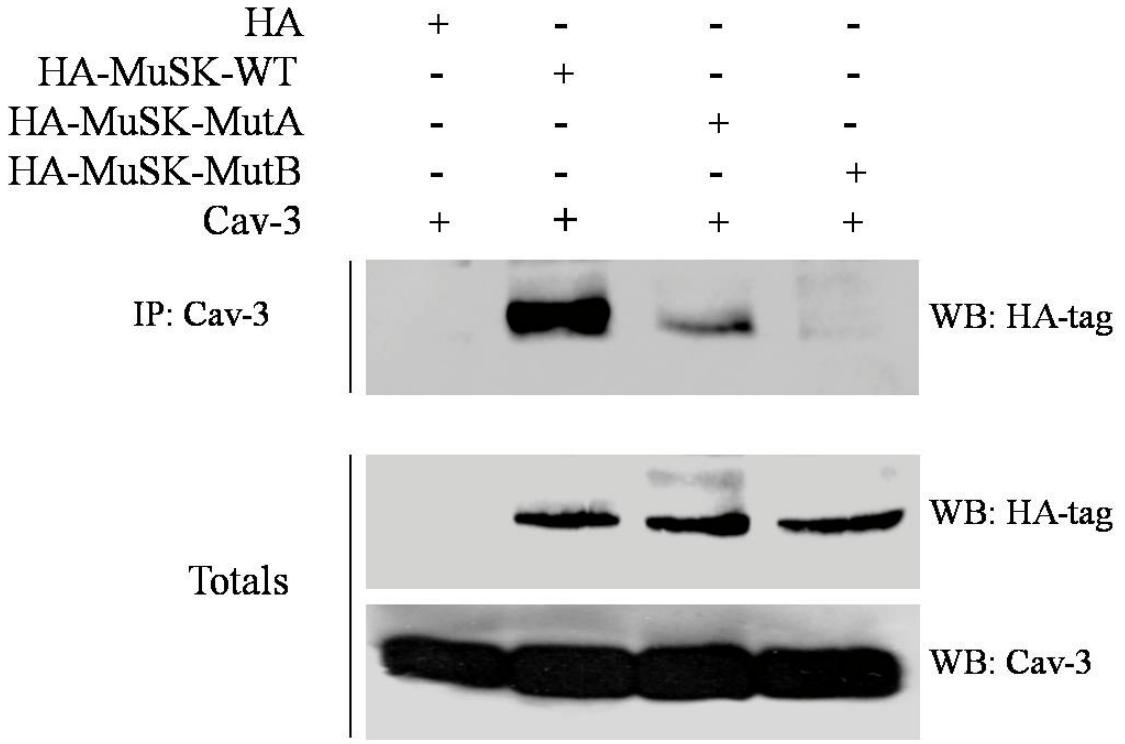


**Figure 22. Caveolin-3 binds MuSK at the MuSK Caveolin Binding Domains**

Ras cells were transfected with caveolin-3 and empty HA, HA-MuSK-WT, HA-MuSK-MutA, or HA-MuSK-MutB vectors. 48 h later, cells were lysed and caveolin-3 pulled down using a caveolin-3 antibody with Protein A Sepharose beads. Western blot analysis probed with an HA antibody indicated association. Total expression for HA and caveolin-3 in lysates is located below. Figure is representative of 3 experiments. Figure was originally published in MBC (Hezel, de Groat et al. 2009).

### 4.2.8 MuSK consistently Associates with Dishevelled-1

The role that lack of caveolin-3 expression plays on proteins associated with MuSK remains to be tested. Dishevelled-1 has been identified as a MuSK binding protein essential to nAChR clustering (Luo, Wang et al. 2002). Disruption of dishevelled-1 expression through expression of a dominant negative construct disrupts spontaneous currents and attenuates agrin induced clustering but not intrinsic clustering. Dishevelled-1 was found to co-immunoprecipitate with MuSK which is unchanged by agrin treatment (Luo, Wang et al. 2002). Our results are consistent with those published by Luo *et al.* which show continuous association between MuSK and dishevelled-1 regardless of agrin treatment (Figure 23)(2002). Lack of caveolin-3 does not influence MuSK and dishevelled-1 association.

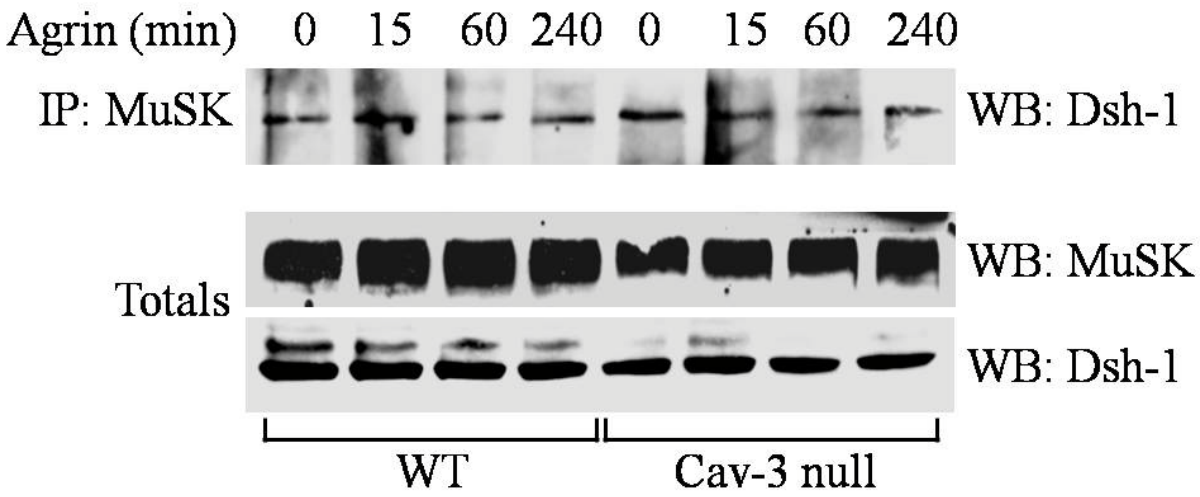


**Figure 23. MuSK consistently Associates with Dishevelled-1**

Wildtype and caveolin-3 null mouse derived myoblasts were differentiated for 7 days and treated with agrin for 0, 15, 60 and 240 min. Cells were lysed and MuSK pulled down using a MuSK antibody and Protein A Sepharose beads. Western blot analysis probed with dishevelled-1 (Dsh-1) antibody indicated association. Total expression of MuSK and dishevelled-1 found in whole lysates is located below. Figure is representative of 3 or more experiments.

### 4.2.9 Agrin induces Caveolin-3 Association with Dishevelled-1

Analysis of dishevelled-1 association with caveolin-3 by immunoprecipitation after differentiated myotube treatment with agrin, showed that caveolin-3 and dishevelled-1 association peaks 15 min after agrin treatment and remains elevated at 1h (Figure 24). This time course corresponds with agrin-induced MuSK activation and MuSK and caveolin-3 association suggesting a signaling complex.

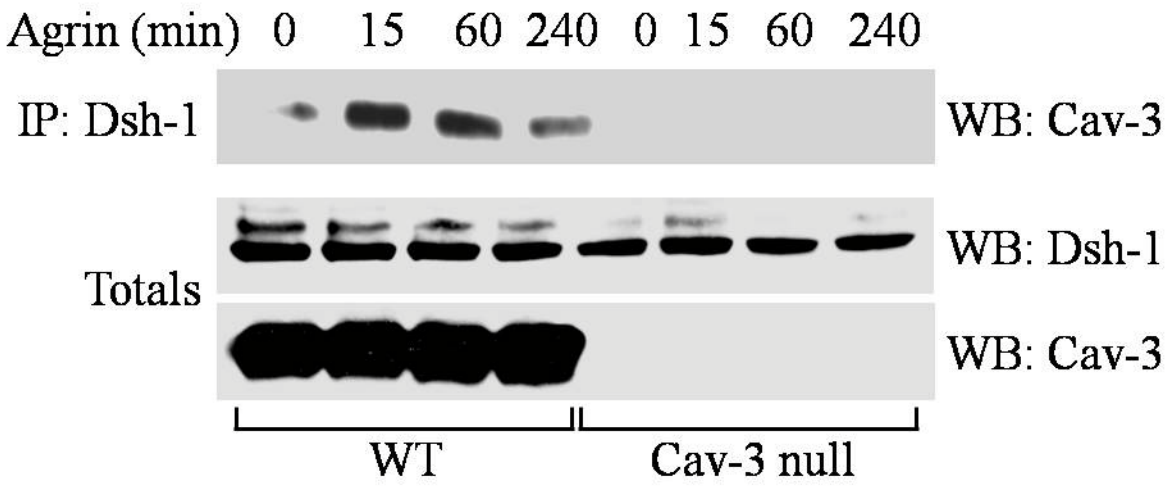


**Figure 24. Agrin induces Caveolin-3 Association with Dishevelled-1**

Wildtype and caveolin-3 null mouse derived myoblasts were differentiated for 7 days and treated with agrin for 0, 15, 60 and 240 min. Cells were lysed and dishevelled-1 (Dsh-1) pulled down using a dishevelled-1 antibody and Protein A Sepharose beads. Western blot analysis probed with caveolin-3 (Cav-3) antibody indicated association. Total expression of dishevelled-1 and caveolin-3 in whole lysates is located below. Figure is representative of 3 experiments.

## 4.3 DISCUSSION

This chapter addresses the role of caveolin-3 in the signaling cascade culminating in nAChR clustering. This research, while attempting to be comprehensive, is hindered by the lack of a fully defined signaling pathway for nAChR clustering. Lack of caveolin-3 expression disrupts activation of several proteins involved with signaling for nAChR clustering. There is highly reduced Rac1 and MuSK activation in agrin treated caveolin-3 null myotubes. The caveolin-3 null cells also have reduced overall MuSK expression. The MuSK and caveolin-3 interaction is direct and can be abrogated through directed mutagenesis of the caveolin binding domains on MuSK. Interestingly, MuSK binding to its partner dishevelled-1 is unchanged.

While limited agrin induced Rac1 activation in the caveolin-3 null myotubes is observed, there is still some Rac1 activation. This activation may result from alternate pathways which signal through Rac1**.** Induction of Rac1 activation has been shown to occur upon agrin treatment and the pathway converges with laminin activation (Weston, Teressa et al. 2007). Rac1 is also implicated in cytoskeletal organization and may reflect a basal level of cytoskeletal reorganization in some cells. Since our myotube cultures still contain undifferentiated myoblasts, it is possible that these cells contain Rac1 activation. Rac1 activation is induced by mechanical stretch, though this is unlikely to be the cause, as there were contractions occurring in both differentiated myotube cultures and all cultures were treated similarly (Kawamura, Miyamoto et al. 2003).

Rac1 and Rho are activated sequentially for successful cluster formation. Myoblast transfection with constitutively active Rac1 and Rho constructs, induces nAChR clustering with normal characteristics (Weston, Gordon et al. 2003). Abrogation of either Rac1 or Rho by expression of dominant negative constructs, disrupts clustering of the nAChR. Attempts to look

at Rho activation in wildtype and caveolin-3 null myotubes were unsuccessful, but most likely mirror the Rac1 activation results, since Rac1 signaling is upstream of Rho (Weston, Gordon et al. 2003).

The similar activation profile of JNK in both wildtype and caveolin-3 null cells, does not correspond to the requirement of Rac1 activation ahead of JNK activation as put forth by Weston *et al*. (2000). These findings were refuted by Luo *et al*. (2002) which showed that expression of dominant negative JNK does not affect intrinsic or agrin induced clustering. This research also found that Pak1 can be activated through MuSK and dishevelled-1 independently of Rac1 (Luo, Wang et al. 2002). Additionally, JNK can be activated through a neuregulin activated ErbB2 pathway predominantly upregulated in cell culture, occurring at the same levels induced by simultaneous agrin and neuregulin treatment (Si, Wang et al. 1999; Lacazette, Le Calvez et al. 2003). JNK activation may not be as important in nAChR clustering as first identified. However, it still may be required for nAChR-epsilon subunit phosphorylation, though the activation shown here does not occur through Rac1 (Si, Wang et al. 1999).

MuSK was considered the known step in agrin induced signaling of nAChR clustering. There was a theoretical, but unidentified protein postulated to bind agrin and assist in the signal transduction through MuSK (Glass, Bowen et al. 1996). This protein, originally called the muscle accessory specificity component (MASC), has been recently identified as LDL receptor related protein 4 (LRP4). This protein was identified as mutated in polysyndactyly which is a condition of webbed fingers and toes and implicated in other development dysfunctions (Simon-Chazottes, Tutois et al. 2006). By an N-ethyl-N-nitrosourea mutagenesis mouse screen, LRP4 was identified as essential for neuromuscular junction formation in which mutated mice die at birth (Weatherbee, Anderson et al. 2006). Myotubes derived from myoblasts of LRP4 mutant

embryonic mice do not respond to agrin treatment implicating this gene in clustering (Weatherbee, Anderson et al. 2006). Subsequent research found that LRP4 binds agrin and MuSK and is phosphorylated identifying LRP4 as the theoretical MASC in nAChR clustering signaling (Kim, Stiegler et al. 2008; Zhang, Luo et al. 2008). Additionally, the expression of MuSK and LRP4 follow the same pattern during differentiation (Zhang, Luo et al. 2008).

Our research focuses on MuSK through which LRP4 is known to signal. While it is unknown whether caveolin-3 expression affects LRP4 in agrin activation and signal transduction, it is likely. There are 3 putative caveolin binding domains on LRP4, which if LRP4 also binds to caveolin-3, support the idea of a caveolin-3 forming a scaffold and sequestering proteins required for efficient nAChR clustering. Based on the results shown above (Figure 19), caveolin-3 is important for MuSK expression stability and agrin activation. Thus, caveolin-3 may assist in the binding between and co-localization of MuSK and LRP4.

Dishevelled-1 was another protein identified as essential for nAChR clustering resulting from interactions with MuSK (Luo, Wang et al. 2002). While there is no difference in MuSK and dishevelled-1 association (Figure 23), it is feasible that lack of caveolin-3 affects the localization of both MuSK and disshevelled-1. This would allow for association while still affecting signal transduction and MuSK phosphorylation. This theory is supported by the strong association of MuSK and dishevelled-1 with caveolin-3 following 1 h of agrin treatment. Interestingly, antisense dishevelled-1 treatment led to a 40% decrease in nAChR clustering, which is not as strong as the 60% change found in caveolin-3 null myotube experiments (Figure 10)(Luo, Wang et al. 2002). Many other isoforms of LRPs are involved in the Wnt signaling pathway, as this is the canonical pathway though which dishevelled-1 acts. The LRP4 ectodomain does not bind to the Wnt1 ligand, but this does not preclude Wnt signaling through

MuSK (Zhang, Luo et al. 2008). Further research is required to delineate a potential caveolin-3 and MuSK signaling complex.

The above research answers some questions while raising some new ones. The results suggest a mechanism for the role of caveolin-3 in the signaling cascade leading to nAChR clustering (Figure 25). In this model there is only full clustering in the agrin treated wildtype cells as evidenced by MuSK phosphorylation and MuSK and dishevelled-1 localization to the caveolae along with Rac1 which is activated as represented by binding GTP. In agrin treated caveolin-3 null myotubes, there is some MuSK phosphorylation and association with dishevelled-1, but this never localizes to the same domain as Rac1 which remains unactivated. In the non-treated wildtype and nAChR there is no agrin signal to organize the co-localization and association of MuSK, dishevelled-1, and Rac1 with caveolin-3.

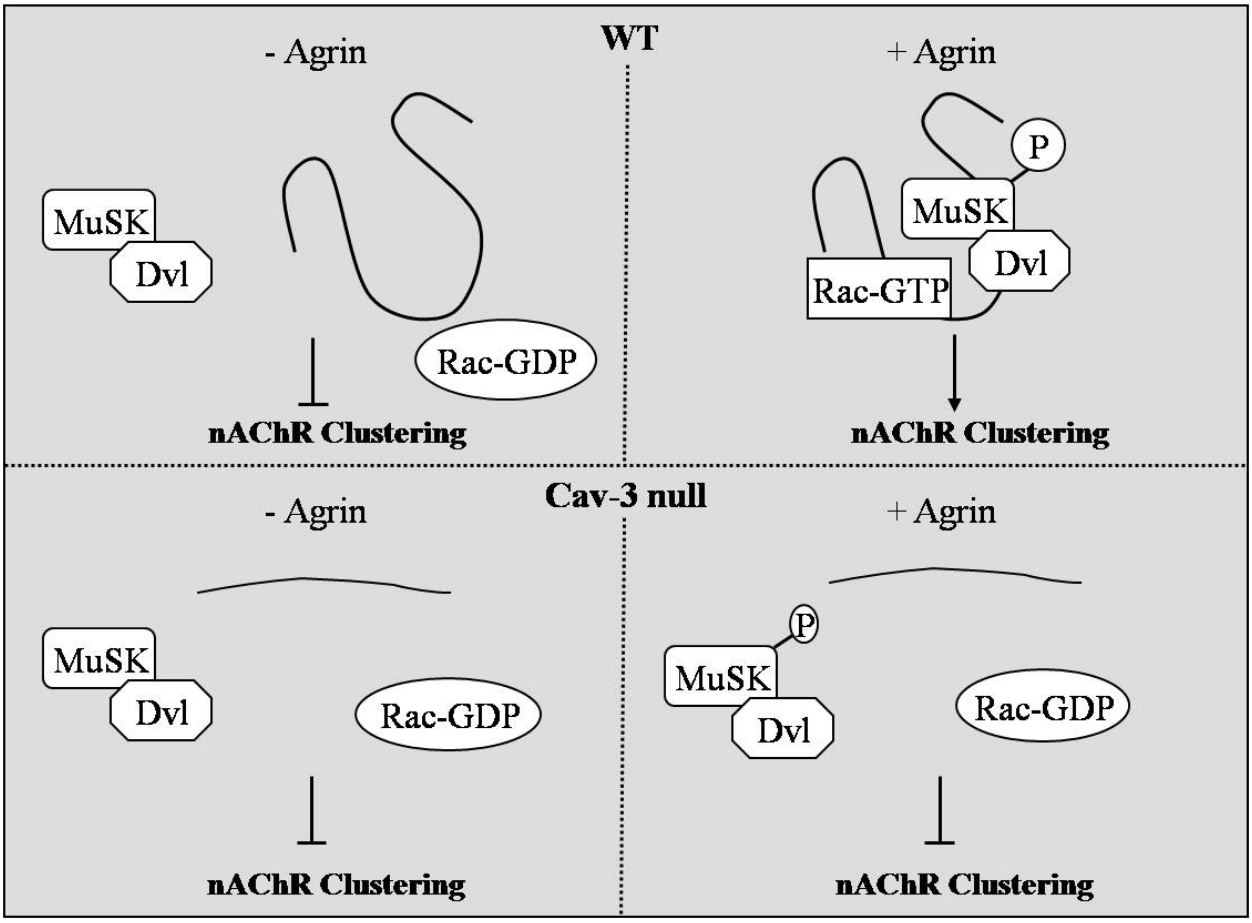


**Figure 25. Proposed Model of nAChR Clustering**

These proposed mechanisms indicate the importance of caveolin-3 for MuSK and Rac1 activation and nAChR clustering, as identified in experiments in wildtype myotubes. Non-agrin treated wildtype and agrin treated and untreated caveolin-3 null myotubes accordingly have abrogated nAChR clustering.

This model is one dimensional and only looks at agrin signaling and myotubes, glossing over the complexity that actually occurs in neuromuscular junction organization. As already stated, caveolin-3 null mice are viable but do not live as long as wildtype mice (Galbiati, Engelman et al. 2001). The ability for forming functional neuromuscular junctions in these mice, probably results from the plethora of signals that have been identified as having small affects on nAChR clustering. In muscle, neural agrin release leads to agrin embedding in the extracellular matrix, which does not occur when using the soluble agrin used in these experiments. The effect of the cell media, especially the presence of serum may also alter

signaling pathways, would normally counterbalance each other or function simultaneously. Likewise, ACh signaling may reinforce nAChR localization and stability allowing for neuromuscular junction function. These are all limitations of our model and most models used for nAChR clustering and organization of the post-synaptic membrane.

The time course of nAChR clustering in our model is different from other published research. MuSK phosphorylation and Rac1 activation occur between 15 m and 30 m in other studies (Luo, Wang et al. 2002; Weston, Gordon et al. 2003). This may result from a number of factors. Most nAChR clustering research uses only 1 or 2 cell lines that have been in culture for years. This length of culturing may have enhanced some signaling processes, while eliminating redundant signaling. Our immortalized cell lines are used with less than 30 passages. The background of our myoblast lines may also alter signaling pathways. Our cell culture model originates from crosses of either wildtype or caveolin-3 null transgenic animal with an immorto-mouse containing a temperature sensitive SV40 large T antigen gene under an interferon-gamma promoter (Volonte, Peoples et al. 2003). The immorto-mouse background myoblasts are conditionally proliferative when maintained at 33°C and under interferon-gamma. Ubiquitous expression of this gene may interfere with some signaling pathways, especially if it is not fully inactivated at 37°C (Whitehead, VanEeden et al. 1993). The signaling differences may also result from the age of the mice from which the cultures are taken. The wildtype and caveolin-3 null myoblasts were obtained from adult mice between 8 and 10 months old, which may affect the overall speed of signal induction. In both our cell culture model and previously studied cell culture models, the activation of certain proteins follows the same pathway even if there is a delay in the activation time course. The delay in the nAChR clustering signal gives the benefit of identifying signaling patterns, correlating to ligand treatment but that do not fit the new

system. JNK activation remains on par with JNK activation in other systems, suggesting an activation that is not through the agrin induction of the MuSK-Rac1 signaling cascade.

The research in this chapter has delineated a role of caveolin-3 in signaling for nAChR clustering at the neuromuscular junction. The varied associations of caveolin-3 with proteins involved in nAChR clustering, suggests a role for caveolin-3 in stability, localization, and efficiency of signaling pathway proteins. This research implies changes in the formation of the post-synaptic membrane, but does not address if there are changes in actual neuromuscular junction function.

# 5.0 FUNCTIONAL CHANGES AT THE NEUROMUSCULAR JUNCTION

## 5.1 INTRODUCTION

The preceding chapters identify the loss of caveolin-3 expression as changing the organization of nAChR through disturbed nAChR clustering signaling. While the lack of caveolin-3 expression visually changes the structure and localization of the post-synaptic membrane, there are limited data suggesting a functional significance. Most neuromuscular junction functional data comes from case studies with EMG recordings and nerve conduction studies in patients with caveolin-3 mutations. The identified structural neuromuscular junction changes may be: 1) cosmetic and not affecting function, 2) compensated for by subsequent structure changes, or 3) cause direct dysfunction of neuromuscular junction signaling. The research presented here attempts to parse out the role of caveolin-3 in neuromuscular junction function.

### 5.1.1 Limb-Girdle Muscular Dystrophy-1C

Patients with caveolin-3 mutations have been diagnosed with LGMD-1C, rippling muscle disease, distal myopathy and hyperCKemia (Woodman, Sotgia et al. 2004). EMG analysis of some patients with caveolin-3 mutations indicated myopathic characteristics, while other patients are described with unremarkable EMG results, as published in case studies. The reported nerve

conduction studies (NCS) have been generally characterized as normal. Myopathic EMGs are characterized by decreased amplitude and duration (Preston and Shapiro 2002).

### 5.1.2 Caveolin-3 at the Neuromuscular Junction in *Caenorhabditis elegans*

Research in *Caenorhabditis elegans* (*C. elegans*) with conserved caveolin-3 mutations has identified changes in nAChR activation after treatment with pharmacologic agents. There are 2 caveolin isoforms in *C. elegans*. *C. elegans* caveolin-2 is similar to mammalian caveolin-2, while *C. elegans* caveolin-1 gene is equally homologous to both mammalian caveolin-1 and caveolin-3. Caveolin-1 was found to co-localize with the *C. elegans* nAChR-alpha subunit UNC-63 at the post-synaptic membrane and does not co-localization with pre-synaptic membrane markers. While there is also expression of C. elegan's caveolin-1 protein in the worm nervous system, it is not localized to the neuromuscular junction. Levamisole treatment of caveolin-1 mutated worms hastened the paralytic response. Caveolin-1 null worms replicated the levamisole response, though siRNA knockdown of caveolin-1 had no effect supporting a caveolin-1 role in neuromuscular junction formation. Disruption or abrogation of caveolin-1 expression in worms leads to a compromised neuromuscular junction as identified by faster paralysis from nAChR agonists. The effect of caveolin-1 on the worm neuromuscular junction is not delineated, but caveolin gene conservation from worms to mice and humans supports the idea of a mammalian caveolin-3 affect on neuromuscular junction function (Parker, Peterkin et al. 2007).

### 5.1.3 Neuromuscular Regulation of Muscle Contraction

While these experiments will focus most on nerve to muscle signaling it is important to understand the whole signaling process from the action potential in the nerve to muscle contraction (Figure 26). Signal transduction from the motor neuron to muscle contraction is highly efficient but also very complex. It achieves both of these characteristics primarily with voltage fluctuation. To outline the process, an action potential travels from the motor-neuronal cell body down the motor neuron axon by successive sodium influx depolarization. Upon reaching the nerve terminal, the depolarization signal changes from sodium influx to calcium influx. This calcium influx induces ACh release from neurotransmitter filled vesicles fusing with the membrane at the active zones of the nerve terminal. The ACh diffuses across the synapse and binds to nAChR which initiates sodium influx through the nAChR channel. This influx is enhanced by activation of the voltage gated sodium channels at the troughs of the neuromuscular junction. The sodium depolarization spreads along the sarcolemma, eventually reaching the T-tubules. The T-tubules are membranous tubules that facilitate simultaneous signaling to all the myofibrils in the myofiber, propagating coordinated contractions. Depolarization originating at the sarcolemma induces calcium release at the T-tubules through the dihydropyridine receptor (DHPR). The DHPR calcium release induces a stronger subsequent calcium release from the sarcoplasmic reticulum through a voltage gated calcium receptor also known as ryanodine receptor. This high calcium concentration causes removal of tropomyosin from binding myosin, freeing the myosin and actin filaments which by using adenosine triphosphate energy, slide across each other contracting the muscle.

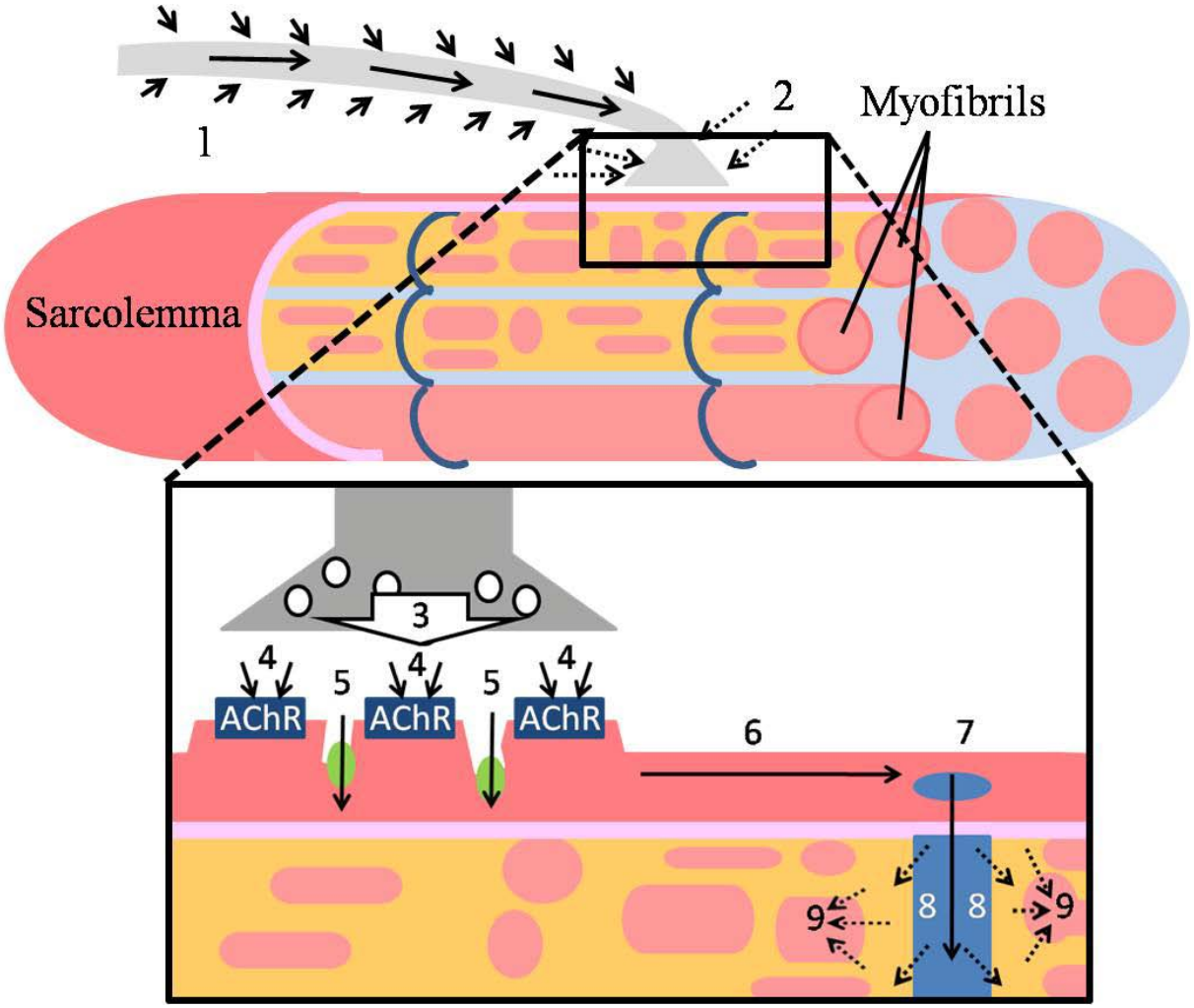


**Figure 26. Diagram depicting the Neuromuscular Regulation of Muscle Contraction**

The complex signaling of muscle contraction. 1) The action potential travels down the nerve axon by sodium depolarization. 2) At the nerve terminal the sodium depolarization induces calcium depolarization. 3) The calcium influx induces ACh release from vesicles in the nerve terminal. 4) The ACh travels across the synapse and binds the nAChR causing sodium influx through the nAChR. 5) nAChR sodium influx activates the sodium depolarization through voltage gated channels (green dots). 6 and 7) Sodium depolarization continues down the sarcolemma and into the T-tubules (dark blue) by voltage gated sodium channels. 8) Sodium depolarization in the T-tubules induces dihydropyridine receptor calcium release 9) Dihydropyridine receptor calcium release induces calcium release from the sarcoplasmic reticulum (orange covering the myofibrils) through voltage gated calcium channels called ryanodine receptors. This calcium release induces muscle contraction by allowing actin and myosin fibers to associate and slide against each other in the myofibril. Solid arrows = sodium depolarization, Dotted arrows = Calcium depolarization

### 5.1.4 Diseases of the Neuromuscular Junction

Several diseases found to directly affect neuromuscular junction signaling are Lambert-Eaton Myasthenic Syndrome (LEMS), Myasthenia Gravis (MG) and Congenital Myasthenia Syndrome (CMS). These diseases are characterized by weakness, but unlike muscular dystrophies, there is not progressive muscle wasting. The severity of LEMS and MG symptoms fluctuates daily (Vincent 2008).

MG and CMS are similar diseases resulting in easy muscle weakness and fatigue, but differ in disease origination. MG is an autoimmune syndrome targeting proteins involved in the clustering of the nAChR at the post-synaptic muscle membrane. MuSK, rapsyn and nAChR are often the targeted proteins. Antibody binding of these proteins induces degradation, disruption of the nAChR organization, and decrease the overall number of nAChR for neuromuscular signaling. The loss of nAChR makes the muscle more susceptible to fatiguing during repetitive movement. CMS has the same results of MG except that the disease characteristics result from protein mutations affecting nAChR clustering and not from auto-immune disruption (Boonyapisit, Kaminski et al. 1999).

LEMS disrupts the pre-synaptic terminal by autoimmune response, disrupting ACh release. Most of the time the protein targeted by the disease is the voltage gated calcium channel, which is required for ACh release. This channel responds to axonal depolarization reaching the nerve terminal. This calcium influx induces proportional acetylcholine release which activates the post-synaptic muscle contraction signal. The loss of these pre-synaptic calcium channels leads to decreased acetylcholine release and weak or non-existent muscle response. Continual nerve firing plies the nerve terminal with extra calcium leading to increased acetylcholine release and increased strength of contraction (Takamori 2008).

### 5.1.5 Analysis of Neuromuscular Diseases

EMG is often used to delineate the characteristics of neuromuscular diseases. The readout is the electromyogram (EMG), or depiction of voltage change over time in a wave form, which can be quantified. EMG procedure in patients refers to electrode placement in the muscle and also measuring muscle depolarization after voluntary contraction or intramuscular nerve stimulation. Nerve conduction studies are studies measuring traveling of the action potential along the nerve and are done to discount neuropathic disease. EMG and NCS are performed simultaneously to get a full picture of muscle depolarization and nerve signaling in neuromuscular diseases (Preston and Shapiro 2002). Repetitive low frequency stimulation in MG and CMS patients, often yields a decrease of 10% or larger from the $1^{st}$ to the $5^{th}$ stimuli of the EMG amplitude or area under the curve (Vincent 2008). This generally results from an overall decrease in nAChR at the neuromuscular junction due to an autoimmune reaction or disrupted nAChR clustering. Under these conditions there is not enough nAChR available for subsequent activation due to inactivation of the recently activated nAChR leading to a decrement in signaling. In LEMS electromyography, there is an increment in the EMG amplitude under high intensity and frequency stimulation (Takamori 2008). Increased calcium influx at the nerve terminal under high frequency stimulation primes the nerve terminal with calcium allowing excessive release of acetylcholine. This increment is highest after exercise.

Using EMG studies along with concomitant measurement of contractile force, these next experiments will analyze neuromuscular junction function and the subsequent contraction in wildtype and caveolin-3 null mice.

### 5.1.6 Experimental Set-up

Differences in the neuromuscular function between wildtype and caveolin-3 null mice were analyzed by EMG. For these experiments, the mice were anesthetized using urethane and shaved at the neck and the hind half of the mouse to maintain aseptic conditions (Figure 27). First, the trachea was isolated and a tracheotomy tube inserted to assist in breathing. Next, the skin around the ankle was cut and the Achilles tendon exposed. This tendon was cut and tied by string to a force transducer to measure contractile force. The foot was restrained to have maximal muscle contractile strength readings. The skin covering the hind left quarter was opened in a horizontal laceration and by spreading the muscle the sciatic nerve was isolated. The skin flaps were tied up forming a pool for mineral oil to maintain viability of the nerve. A bipolar stimulating electrode was placed under the nerve and the nerve was cut at the most proximal point to eliminate reflex responses. A recording electrode was inserted into the gastrocnemius muscle through a slit in the skin. In these experiments the nerve was stimulated at the sciatic nerve, and the subsequent muscle electromyogram and force of muscle contraction measured.

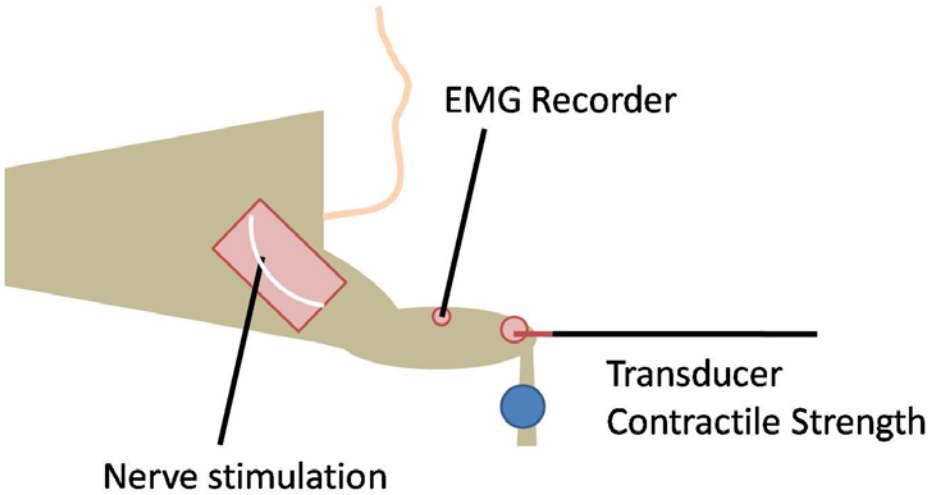


**Figure 27. Diagram of the mouse Set-up for EMG and Contractile Strength Experiments**

## 5.2 RESULTS

### 5.2.1 EMG Data Analysis

The EMG results can be analyzed individually per stimulation or as a series of events. In terms of the MG, CMS, and LEMS, the most telling results are the series of stimulations which show either decreased or potentiation of muscle depolarization (Vincent 2008). The experimental results did not provide distinct differences found in MG, CMS, and LEMS, in terms of a decrease or increase upon repetitive nerve stimulation (Data not shown). The EMG data were analyzed for a number of factors including latency, amplitude, area under the curve, stimulation to peak and the ratio of amplitude to area under the curve (Figure 28).

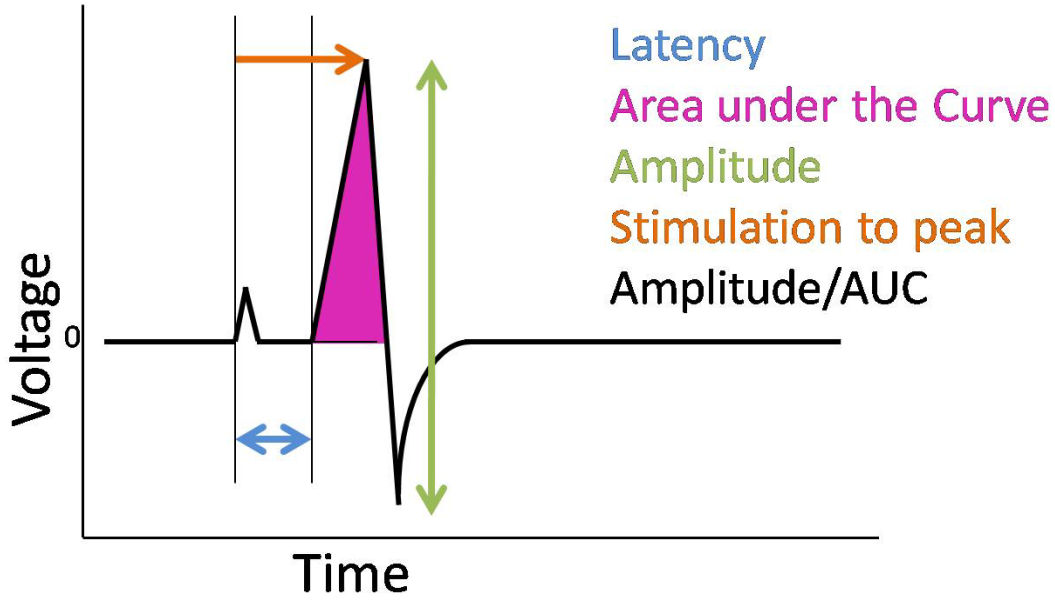


**Figure 28. Representative EMG Wave and Associated Data**

Low frequency nerve stimulation induces subsequent muscle depolarizations, which produces a wave form such as the representative wave above. This research analyzes data points collected from each wave including the latency, (blue arrow) area under the curve (purple fill), amplitude (green arrow), stimulation to peak (orange arrow) and the ratio of amplitude to area under the curve.

### 5.2.2 Latency of EMG Stimulation

Latency is the measure of time from nerve stimulation to the beginning of muscle depolarization. The time of the stimulus is identified as the EMG artifact that shows up in the EMG recording ahead of actual muscle depolarization. Comparison of the latency between wildtype and caveolin-3 null animals indicated a significant delay between stimulation and muscle depolarization in the caveolin-3 null animals (Figure 29). As this time period covers the time from nerve stimulation to muscle sarcolemma depolarization, this may be representative of changes at the neuromuscular junction. If these neuromuscular junctions are differentially organized then it should affect the latency and therefore the efficiency of transmission.

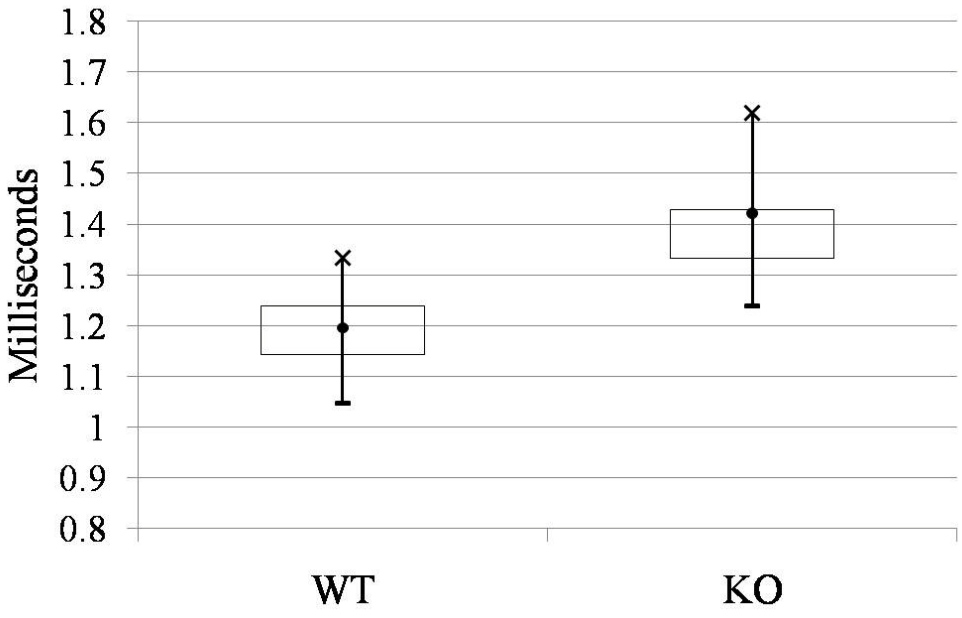


**Figure 29. Latency of EMG Stimulation**

EMG analysis of the latency of stimulation at 10V and 1Hz in wildtype (WT) and caveolin-3 null (KO) animals. Box and whisker plots, where the box represents the interquartile range, while the top and bottom of the bar, represents the full range. The dot indicates the average latency length. WT n=2, KO n=4 Student's T-test * $p < 0.0001$. Figure was originally published in MBC (Hezel, de Groat et al. 2009).

### 5.2.3 Amplitude of the EMG

The amplitude represents the total voltage change during the depolarization and repolarization. The amplitude was calculated as the voltage change below and above baseline. While the amplitude in the wildtype mice was well conserved across specimens, the caveolin-3 null mice had significant variability (Figure 30). The voltage decrease resulted from less muscle depolarization in the area of the recording electrode, which may come from sub-maximal activation through the neuromuscular junction. There is a possibility that this is an artifact from muscle wasting with a loss of depolarization in neighboring myofibers.

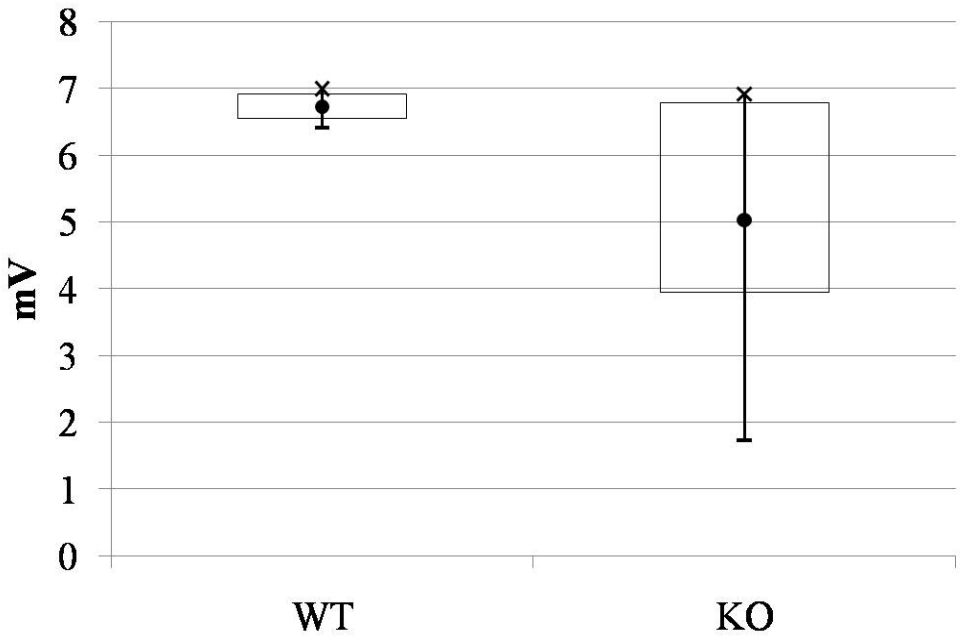


**Figure 30. Amplitude of the EMG**

EMG analysis of the amplitude of the muscle depolarization at 10V and 1Hz in wildtype (WT) and caveolin-3 null (KO) animals. Box and whisker plots, where the box represents the interquartile range, while the top and bottom of the bar, represents the full range. The dot indicates the average latency length. WT n=2, KO n=4 Student's T-test * $p < 0.0004$. Figure was originally published in MBC (Hezel, de Groat et al. 2009).

### 5.2.4 Area Under the Curve of the EMG

The area under the curve is a composite of the time period of the depolarization and the amplitude of the first peak. This is a correlate of the strength of depolarization over depolarization time in muscle fiber analyzed. There is significantly less depolarization in the caveolin-3 null mice (Figure 31). This may result from the decreased activation in correlation to the amplitude changes. This may also represent changes in the depolarization characteristics of the muscle, with decreased opening of the voltage gated sodium channels activated by sodium influx through the nAChR.

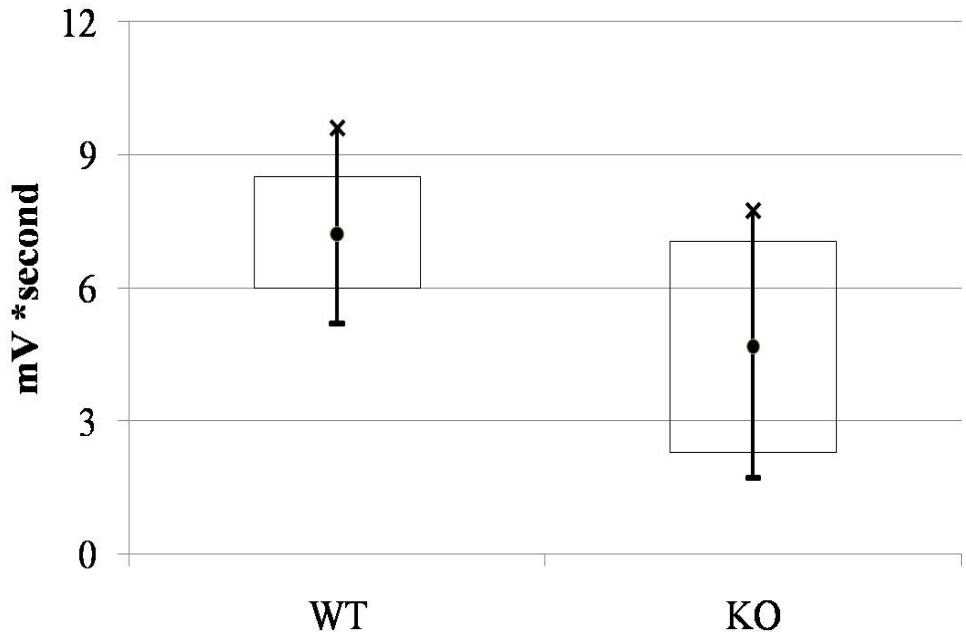


**Figure 31. Area Under the Curve of the EMG**

EMG analysis of the area under the curve at 10V and 1Hz in wildtype (WT) and caveolin-3 null (KO) animals. Box and whisker plots, where the box represents the interquartile range, while the top and bottom of the bar, represents the full range. The dot indicates the average latency length. WT n=2, KO n=4 Students's T-test * $p < 0.0001$. Figure was originally published in MBC (Hezel, de Groat et al. 2009).

### 5.2.5 Time from Stimulation to Peak

Stimulation to peak analyzes the activation characteristics of the muscle depolarization. Since there is a longer latency in the caveolin-3 null mice, if all other characteristics were the same one would expect this to be reflected in the time from stimulation to peak (Figure 29). There is no significant difference in the time from latency to peak between wildtype and caveolin-3 null mice (Figure 32). These results further confirm changes found in the amplitude and area under the curve as affecting depolarization.

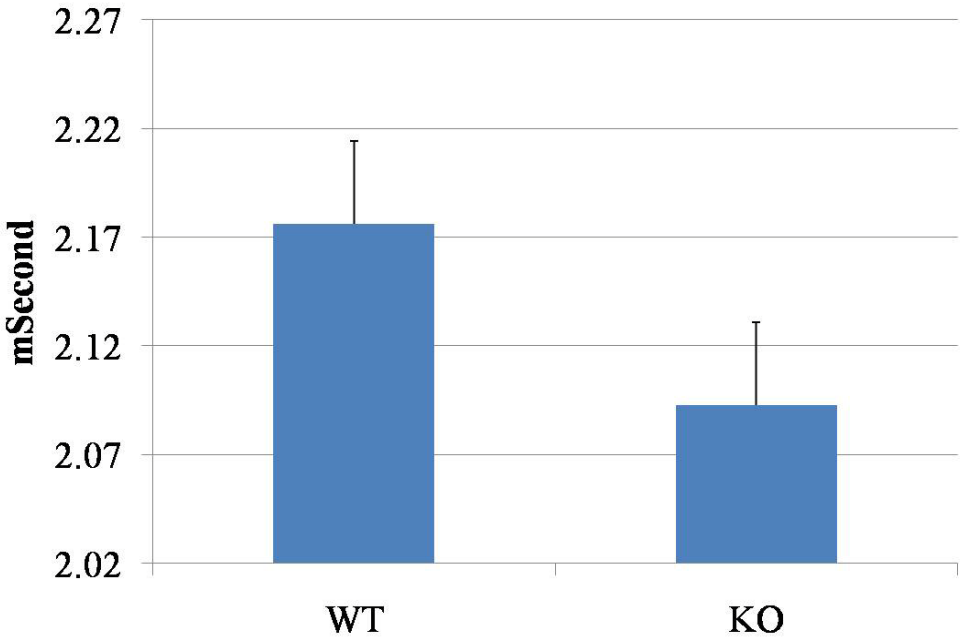


**Figure 32. Average Time from Stimulation to Peak of the EMG**

EMG analysis of the average time from the nerve stimulation until the peak in muscle depolarization at 10V and 1Hz in wildtype (WT) and caveolin-3 null (KO) animals. Height of the column represents the average. Error bars are standard error of measure (SEM). WT n=2 SEM = 0.038, KO n=4 SEM = 0.038, Student's T-test * $p < 0.1711$.

### 5.2.6 Ratio of Amplitude to Area Under the Curve

The ratio of amplitude to area under the curve analyzes changes in the EMG wave characteristics. The ratio reflects the correlation between the amplitude and area under the curve. When amplitude decreases a consequent decrease in area under the curve is expected. Our results show that the overall waves have similar characteristics reflecting the strength of depolarization (Figure 33). Though insignificant the changes in area of caveolin-3 null animals are not directly proportional to the amplitude, as exemplified by a ratio of 1.2 as opposed to a ratio of 1 in wildtype.

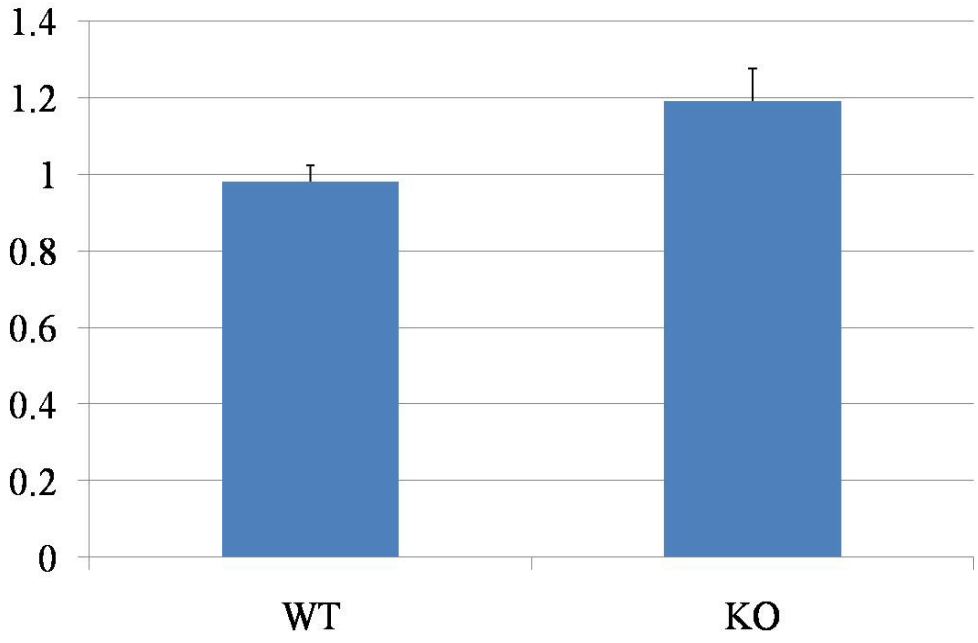


**Figure 33. Ratio of Amplitude to Area Under the Curve of the EMG**

Ratio of the amplitude to the area under the curve of the EMG at 10V and 1Hz in wildtype (WT) and caveolin-3 null (KO) animals. Height of the column represents the average. Error bars are standard error of measure (SEM). WT n=2 SEM = 0.042, KO n=4 SEM = 0.082, Student's T-test * $p < 0.1711$.

### 5.2.7 Overall EMG Analysis

Compiled in Table 3 is the numerical data for the EMG results represented above. The latency, amplitude and area under the curve results were significant. The latency difference between wildtype and caveolin-3 null animals suggests a delay in muscle depolarization following nerve stimulation potentially representing changes in neuromuscular junction transmission. The changes in amplitude and area under the curve could reflect neuromuscular transmission changes or subsequent changes in the process of muscle depolarization. The changes in the amplitude and area under the curve may also reflect changes in channel activation and inactivation in muscle as alternative effects of the loss of caveolin-3 expression.

**Table 3. EMG Results**

| | Wildtype | | Caveolin-3 null | | |
|---|---|---|---|---|---|
| | Average | SEM | Average | SEM | p-value |
| Latency | 1.1952 ms | 0.016 | 1.4214 ms | 0.014 | <.0001 |
| Amplitude | 6.7227 mV | 0.042 | 5.0293 mV | 0.314 | <.0004 |
| AUC | 7.2194 mV*s | 0.329 | 4.6765 mV*s | 0.394 | <.0001 |
| Stim to peak | 2.1762 ms | 0.038 | 2.0928 ms | 0.038 | .1711 |
| AMP/AUC | 0.9799 | 0.042 | 1.1918 | 0.082 | .0830 |

### 5.2.8 Contraction Results

Muscular dystrophies are characterized by muscle weakness therefore concomitant analysis of contractile strength with NCS seemed appropriate. These animals are a model of LGMD-1C, a mild form of muscular dystrophy.

While data were collected at different intensities and frequencies of activation, muscle contraction was mostly similar between wildtype and caveolin-3 null mice. Distinct differences in the contractile consistency were identified under tetanic stimulation (Figure 34). Under continuous 50 Hz stimulation, there are stability differences between wildtype and caveolin-3 null mice. The wildtype contraction peaks and plateaus for 5-6 s and then runs down. The contraction tension is relatively steady with only slight variability in contractile force. In the caveolin-3 null mouse, contractile force reaches an initial peak, continues to climb over the next 6-8 s and then runs down. The force of this contraction is unstable as evidenced by the variation in contraction tension. This is easily identifiable in the snippet from the first 2 seconds of the contractile force measurement (Figure 35). Calculation of the area of the contraction variability identifies the caveolin-3 null mice tetanic contraction as being twice as unstable as the wildtype contractions (Figure 36).

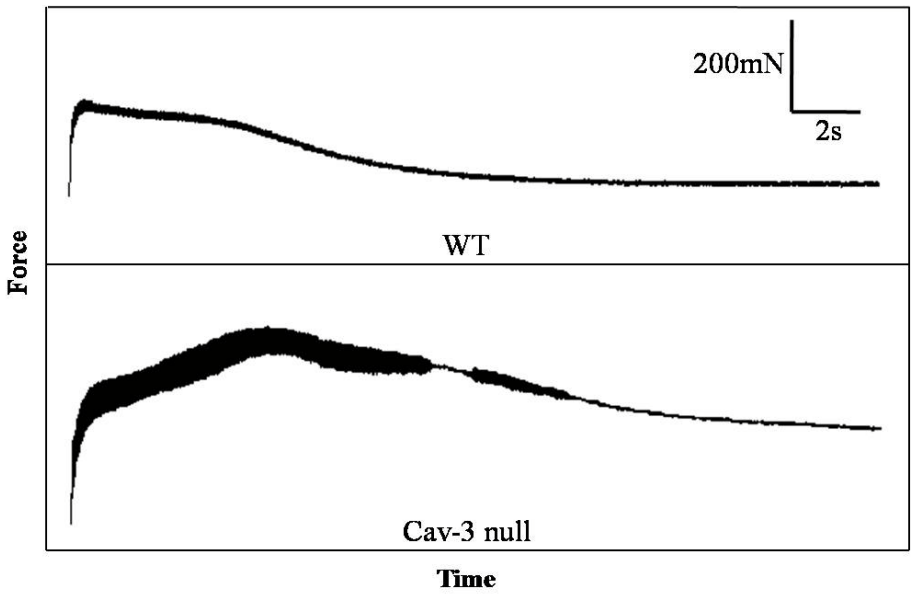


**Figure 34. Tetanic Muscle Contractions at 100V and 50Hz for 20 seconds.**

Representative contractile force recordings from the gastrocnemius muscle of wildtype (WT) and caveolin-3 null (Cav-3 null) animals obtained during 20 s of 100V and 50 Hz continuous sciatic nerve stimulation. Figure was originally published in MBC (Hezel, de Groat et al. 2009).

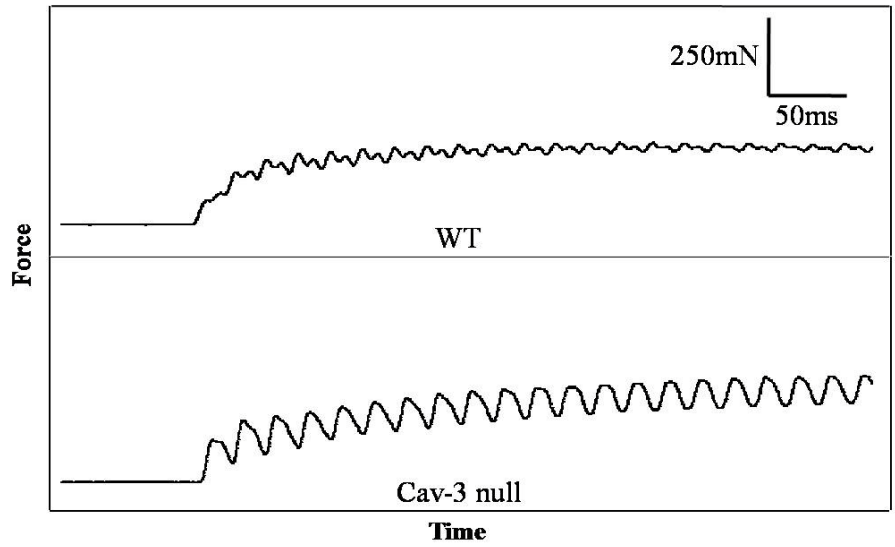


**Figure 35. Snippet of the first 500 ms of the above Tetanic Contractions**

This is a short snippet of the above continuous contraction, showing the variability in continuous muscle strength in the caveolin-3 null (Cav-3 null) tetanic contraction as compared to wildtype (WT). Figure was originally published in MBC (Hezel, de Groat et al. 2009).

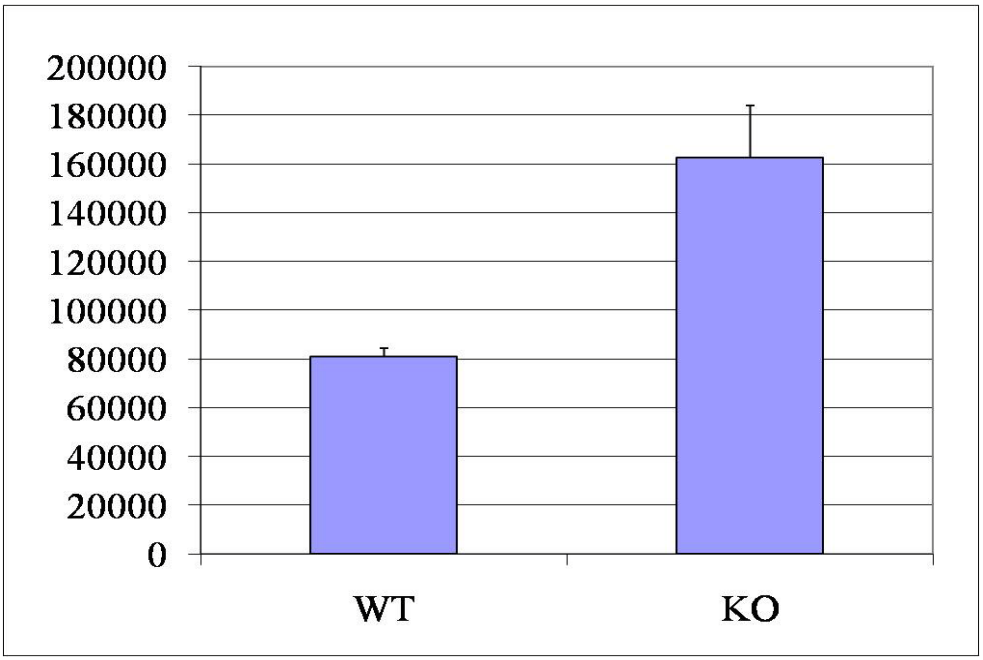


**Figure 36. Quantification of the Instability of Tetanic Muscle Contraction**

The variable portion of the tetanic contraction recording was measured as the average trace area per second of recording and compared between wildtype (WT) and caveolin-3 null (KO) animals. Error bars represent SEM. n=7 Student's T-test * $p < 0.0034$. Figure was originally published in MBC (Hezel, de Groat et al. 2009).

## 5.3 DISCUSSION

The research presented here analyzes the functional characteristics of the neuromuscular junction. The stimulation latency, the amplitude, and area under the curve of the EMG are significantly changed between wildtype and caveolin-3 null mice. Two other factors, stimulation to peak and the ratio of the amplitude to area under the curve are not significant but further our understanding of neuromuscular junction transmission. Analysis of the contractile differences between wildtype and caveolin-3 null mice showed decreased stability of tetanic contraction in caveolin-3 null animals. While the whole of muscle contraction signaling occurs before contraction, this indicates a disruption in contractile signaling, though not specific to the neuromuscular junction. There is also potentiation of contractile strength in the tetanic contraction of the caveolin-3 null mice, which is discussed later in this chapter.

These experiments were conducted in animals, housed under identical conditions and were also non-survival, which is not acceptable for humans. The animals were all age matched in the C57BL/6 background and had identical cage conditions throughout life. The standardized conditions allowed for the detection of subtle differences. While the results between these animal strains are distinct, these differences might not be detectable in humans, where patient variability is larger. Isolation of the nerve and removal of reflex signaling were also important to parsing out the subtle differences and these techniques would need to be modified for patients.

Latency also reflects the length of the sciatic nerve to the nerve terminal and the conduction characteristics. While there may be slight variations in this length from muscle innervations at the knee to the nerve terminal, the stimulating electrode was placed directly between the knee innervations and the nerve threading through the pelvic bone. The differences in latency between wildtype and caveolin-3 null animals are indicative of signal disruption

before muscle depolarization. It is possible that this could be resultant of pre-synaptic signaling differences, but since there is no caveolin-3 expression in the nerves it is unlikely that lack of caveolin-3 would affect neuronal signaling. Caveolin-3 immunoreactivity is found in the Schwann cells forming the myelin sheath around the axon, but caveolin-1 is the predominant caveolin expressed (Kawahara 2004).

The myasthenic syndromes described above are easily identified by EMG tests, since the results are based on internal controls. The results compare the amplitude or area under the curve of the 5$^{th}$ EMG to the first EMG, removing variability between subjects. The EMG differences identified in our experiments unlike with the myasthenic syndromes would require a control group for comparison. Human variability may not allow subtle differences of this nature to be readily determined. More research will need to be done to resolve whether these changes can actually be detected in humans. This may require new testing techniques, the use of pharmacological agents, or both for testing viability in human subjects. Procedures removing the requirement of a control group such as those already used in the neuromuscular junction analysis of the various myasthenia diseases, would be ideal.

The determination of neuromuscular junction diseases depends on a decrement or increment in EMG amplitude or area under the curve during repetitive stimulation. Myopathic diseases are diagnosed by EMG changes in amplitude, duration and jitter. There is overlap in the data used in determination of neuromuscular junction diseases and myopathic diseases. Whether the EMG data is really describing neuromuscular transmission differences or muscle degradation remains to be reevaluated (Chapter 6).

Analysis of muscle contraction found distinct differences under tetanic, or constant contraction. This raises several questions. Does this result from changes in neuromuscular

junction structure? What is the reason behind the differences in contractile stability? What is the meaning of the potentiation in the muscle contraction? Are there subcellular locations where caveolin-3 loss affects signaling from nerve to muscle contraction and potentiation?

The answer to these questions will require further research, but based on current research we can draw some conclusions. Our research on the structural differences of the nAChR clusters found more diffuse distribution of nAChR in the caveolin-3 null mice as compared to wildtype. If the nAChR is diffusely spread along the sarcolemma at the neuromuscular junction and the nerve terminal doesn't compensate with a larger nerve terminal then it would place some nAChR outside juxtaposition from the nerve terminal. Under tetanic contraction with continual ACh release, ACh would leak outside of the synapse and localization of acetylcholineesterase, activating extra-synaptic nAChRs not activated under regular contractions. Activation of extra-synaptic nAChR might explain the contractile potentiation in caveolin-3 null mice. The instability of contractile tension may also result from overall disruption of the nAChR clustering structure. These structural changes may stem from changes in protein localization and more importantly, nAChR in relation to the voltage gated sodium channels and changes in the mature neuromuscular junction post-synaptic membrane folding characteristics. Analysis of the ultra-structure of the neuromuscular junction in caveolin-3 null mice could identify neuromuscular junction structural changes.

In the introduction of this chapter the signaling leading to muscle contraction was diagrammed. There are other places outside of the neuromuscular junction where loss of caveolin-3 may affect contractile signaling.

Caveolin-3 is located along the sarcolemma so it may affect the muscle depolarization. Caveolin-3 has been shown to bind several ion channels. Since many of the signals involved in

muscle contraction involve ion flux, lack of caveolin-3 may also affect this signaling. Caveolin-3 has been indentified to associate with the sodium potassium pump in the sarcolemma (Kristensen, Rasmussen et al. 2008). Exercise induced greater localization of caveolin-3 and the alpha-subunits of the sodium pump to the sarcolemma. Potassium voltage dependant channels, Kv1.3 and Kv1.5 have been shown to co-fractionate and co-localize with caveolin-3 (Folco, Liu et al. 2004; Martinez-Marmol, Villalonga et al. 2008). Sodium voltage dependant channel Nav1.5 has also been seen to co-localize with caveolin-3 in cardiomyocytes (Palygin, Pettus et al. 2008). Changes in the opening and closing characteristics of the voltage gated sodium channels would change amplitude and area under the curve data of the EMG. It is possible that lack of caveolin-3 affects channel dynamics.

Caveolin-3 localization to the T-tubules in mice throughout life, may also affect contractile signaling. Parton et al. (1997) show caveolin-3 involvement in T-tubule formation in cultured myotubes and muscle, with a postnatal co-localization decrease as determined by immunofluorescence. Consequently, dihydropyridine receptor co-localization with caveolin-3 was lost as differentiation progressed (Parton, Way et al. 1997). Research also suggests caveolin-3 T-tubule localization in mature muscle fibers by immunofluorescence and electron microscopy (Ralston and Ploug 1999). This was confirmed by stripping off the sarcolemma to find caveolin-3 localization at the T-tubules in the myofibrils that make up the muscle (Murphy, Mollica et al. 2009). The localization of dihydropyridine receptors at the T-tubule is disturbed in caveolin-3 null muscle. Ultra-structural analysis of T-tubules shows a change from a transverse linear localization in wildtype muscle to a disordered cluster form in caveolin-3 null muscle respectively (Galbiati, Engelman et al. 2001).

Caveolin-3 mutations are also associated with rippling muscle disease. In this disease, severe contraction will lead to a rippling contraction through the muscle. EMG analysis of rippling muscle has determined that rippling muscle is electrically silent, pointing to a defect in the T-tubules as muscle depolarization is not recorded by EMG. This supports a caveolin-3 role in T-tubule signaling in addition to the changes at the neuromuscular junction.

Calcium channels are important to the last signaling steps in muscle contraction with sequential calcium release from the dihydropyridine receptors then the ryanodine receptor induced by T-tubule depolarization. Both isoforms CaV1.1 and CaV1.2 of the dihydropyridine sensitive voltage gated L-type calcium channels are expressed in muscle. CaV1.2, which is not particular to skeletal muscle cells, is expressed at the plasma membrane and functions in calcium signaling by activating calcium binding proteins (Jeftinija, Wang et al. 2007). Of these slow activating and inactivating channels, CaV 1.2 is localized to type I and type IIa fibers but not type IIb, while CaV1.1 is ubiquitous throughout the muscle fibers (Couchoux, Allard et al. 2007; Jeftinija, Wang et al. 2007). Immunofluorescence indicated that CaV1.2 partially co-localized with caveolin-3 and partially co-localized with dystrophin (Jeftinija, Wang et al. 2007). Immunofluorescence of wildtype myotubes and caveolin-3 transfected myoblasts shows co-localization of CaV1.1 and caveolin-3 at the plasma membrane and the developing T-tubules. Myotubes expressing the dominant negative caveolin-3 mutant have decreased CaV1.1 expression and decreased current permeability (Couchoux, Allard et al. 2007; Weiss, Couchoux et al. 2008). Caveolin-3 mutant transfected myotubes had varied current required for channel activation but overall the current was decreased (Weiss, Couchoux et al. 2008).

Our experiments find EMG and contractile force differences between wildtype and caveolin-3 null mice. EMG analysis indicates differences in the latency, amplitude and area

under the curve between the animal strains. This supports the findings of disrupted nAChR clustering and disrupted mechanism leading to nAChR clustering identified in the previous chapters. These results will need to be independently verified.

# 6.0 CONCLUSION

The data presented here identify a role for caveolin-3 in nAChR clustering. Agrin treatment of wildtype myotubes leads to essential nAChR clustering steps of MuSK phosphorylation and Rac1 activation. These signaling processes occur when temporally bound to caveolin-3. Agrin treatment of caveolin-3 null myotubes induces some phosphorylation of MuSK, while Rac1 activation by agrin is abrogated. These changes in signaling are reflected in the clustering differences between wildtype and caveolin-3 null myotubes. Agrin induced clustering in caveolin-3 null myotubes is reduced by more than half and the clusters are more diffuse across the membrane. This *in vitro* research indicated distinct differences in nAChR clustering and organization of the neuromuscular junction between wildtype and caveolin-3 null myotubes. The results of figure 5, modeled the differences in the nAChR clusters at the muscle sarcolemma, where the nAChR is distinct in wildtype mice and more diffuse in caveolin-3 null mice (Figure 2 and 3). These changes indicated differences in the neuromuscular junction function between wildtype and caveolin-3 null mice. Subsequent, EMG studies indicated a significant longer latency from the stimulation artifact to the EMG recording as well as decreased amplitude and area under the curve in caveolin-3 null mice as compared to wildtype mice. These differences correspond to a myopathic disease.

If the differences identified appear to be specific to the neuromuscular junction, why do these results fall under myopathies instead of neuromuscular junction diseases such as LEMS,

MG and CMS, which also have changes in the pre- or postsynaptic junction? To answer this it is important to look at the whole neuromuscular junction structure and function to understand the EMG results.

Revisiting the muscle contraction signaling diagram, the EMG recording reflects half of the signaling in the muscle up to depolarization of the sarcolemma. It is unlikely that EMG changes in caveolin-3 null mice reflected the nerve action potential leading to pre-synaptic ACh release. There was no caveolin-3 expression in the nerve and stimulation was supra-maximal, or well above the nerve transmission threshold. The EMG differences could therefore result from nAChR activation or subsequent muscle depolarization.

While there do not appear to be differences in the number of nAChR, it is possible that ACh binding to the receptor and subsequent activation is delayed. This hypothesis would correspond to the increased latency. Other studies have analyzed nAChR activation by patch clamp in myotubes cultured from biopsies obtained from normal and DMD patients. The DMD cultures did not have any changes in the influx and opening characteristics but there was an overall increase in frequency of channel opening. These results are attributed to increased ACh release, but possibly suggest changes in depolarization and repolarization characteristics (Mancinelli, Sardini et al. 1989). It is possible that the caveolin-3 mutation disrupts the channel mechanics, through changed characteristics of the nAChR clustering.

Alternatively, the changes in EMG results are derived from altered sodium depolarization of the myotube. Since nAChR activation is required to reach threshold before opening of the voltage gated ion channel, this may play a role in the change in the latency and depolarization. The change could also result from decreased numbers of voltage gated sodium channels at the neuromuscular junction. A recently published manuscript by Banks *et al*. (2009), suggests that

reduction in the folds at the neuromuscular junction membrane reduces the number of sodium channels. Caveolin-3 null mouse muscle 3D images of nAChR localization in muscle cross-sections, support this occurrence in decreased amplitude and area under the curve by EMG. The 3D image of wildtype NMJ is much more dynamic then the very planar caveolin-3 null mouse neuromuscular junction (Figure 3). Caveolin-3 has been shown to assist in sodium depolarization in cardiomyocytes. Addition of caveolin-3 antibodies to the cytoplasm of cardiac myocytes abrogated isoproterenol induction of the voltage gated sodium channel (Yarbrough, Lu et al. 2002). Another factor that may play a role in the EMG results is myofiber size variability. There are multiple possibilities for the weaker depolarization in some caveolin-3 null cells.

Overall, the loss of caveolin-3 decreases sarcolemma sodium depolarization either through changes in nAChR activation characteristics or changes in the number or resistance of voltage gated sodium channels in the sarcolemma. This leaves open the question of whether the structural and signaling deficiencies shown here contribute to muscle degradation, or if neuromuscular junction structural and transmission changes and muscle degradation are 2 separate occurrences.

This research uses these caveolin-3 null mice as a model for LGMD-1C. LGMD-1C results from an autosomal dominant mutation of caveolin-3. In published case studies, patients with caveolin-3 mutations have been shown to have both normal and myopathic EMGs, and present with or without muscle weakness. Progression heterogeneity in this disease could arise for many reasons. This heterogeneity could result from genotypic variability, the caveolin-3 mutations themselves, or differences in the lifetime of movement reflecting neuromuscular transmission changes. In several studies the patients, do not present with weakness but do have myopathic changes. This was found in both younger patients and some older patients. This

supports our findings in mice of different EMG results without definitive weakness, and also corresponds with our muscle contractile results which are not weakened. Due to the heterogeneity of the mutations involved, this may be mutation specific.

This research finds structural disruption at the neuromuscular junction leading to myopathic EMGs. There are other proteins which lead to disruption in the neuromuscular junction formation. Many of the genes associated with the dystrophin-glycoprotein complex, lead to structural changes in the neuromuscular junction. Loss of dystrophin which is characteristic of DMD leads to disrupted neuromuscular junction formation (Lyons and Slater 1991). Truncated dystrophins identified to prevent muscle degeneration were analyzed for their effect on neuromuscular junction formation in transgenic mice. The truncated protein called minidystrophin led to proper neuromuscular junction formation, while the other, microdystrophin still underwent neuromuscular junction fragmentation, though temporally with formation of ringed fibers (Banks, Chamberlain et al. 2009). Ringed fibers are a normal occurrence found in muscle as people age. Utrophin, is the protein homologous to dystrophin and is associated with the neuromuscular junction. Mice deficient in utrophin develop decreases in the density of the neuromuscular junction and associated membrane folding (Grady, Merlie et al. 1997). Analysis of alpha-dystrobrevin, a cytoplasmic protein of the dystrophin glycoprotein complex, indicates a requirement for neuromuscular junction maturation (Grady, Zhou et al. 2000). Loss of these genes leads to neuromuscular junction structure disruption. These animal models would be a good place to start identifying whether general neuromuscular junction changes lead to myopathic EMG.

The other possibility is that caveolin-3 is the driving factor behind the myogenic changes at the neuromuscular junction. This is supported by the disruption of nAChR and the potential

association of caveolin-3 with voltage-gated sodium channels. The EMG results could be a singular result due to the ubiquitous expression of caveolin-3 in the sarcolemma and muscle. Caveolin-3 binds to several proteins implicated in other forms of muscular dystrophy, such as Trim 32, dysferlin and proteins associated with the dystrophin-glycoprotein complex. Some of these proteins also fall in the disruption of the neuromuscular junction category. There is the possibility that these proteins could also affect the EMG results.

Our research indicates that lack of caveolin-3 disrupts the post-synaptic membrane of the neuromuscular junction and that this is also associated with myopathic EMG. Further research will need to be done to determine if this is a precursor to muscular degeneration and if this is applicable to multiple forms of muscular dystrophy. If this is a common precursor to muscular degeneration, then treatments which rectify EMG efficiency should be a future target for treatment of muscular dystrophies. These treatments may require delineation of whether EMG changes result from changes in nAChR channel functioning characteristics and/or muscle depolarization.

## BIBLIOGRAPHY


Banks, G. B., J. S. Chamberlain, et al. (2009). "Truncated dystrophins can influence neuromuscular synapse structure." Mol Cell Neurosci **40**(4): 433-41.

Banks, G. B., C. Fuhrer, et al. (2003). "The postsynaptic submembrane machinery at the neuromuscular junction: requirement for rapsyn and the utrophin/dystrophin-associated complex." J Neurocytol **32**(5-8): 709-26.

Bansal, D., K. Miyake, et al. (2003). "Defective membrane repair in dysferlin-deficient muscular dystrophy." Nature **423**(6936): 168-72.

Bickmore, W. A. and S. M. van der Maarel (2003). "Perturbations of chromatin structure in human genetic disease: recent advances." Hum Mol Genet **12 Spec No 2**: R207-13.

Bogdanovich, S., K. J. Perkins, et al. (2004). "Therapeutics for Duchenne muscular dystrophy: current approaches and future directions." J Mol Med **82**(2): 102-15.

Boonyapisit, K., H. J. Kaminski, et al. (1999). "Disorders of neuromuscular junction ion channels." Am J Med **106**(1): 97-113.

Bromann, P. A., H. Zhou, et al. (2004). "Kinase- and rapsyn-independent activities of the muscle-specific kinase (MuSK)." Neuroscience **125**(2): 417-26.

Bryan, B. A., D. C. Mitchell, et al. (2005). "Modulation of muscle regeneration, myogenesis, and adipogenesis by the Rho family guanine nucleotide exchange factor GEFT." Mol Cell Biol **25**(24): 11089-101.

Capanni, C., P. Sabatelli, et al. (2003). "Dysferlin in a hyperCKaemic patient with caveolin 3 mutation and in C2C12 cells after p38 MAP kinase inhibition." Exp Mol Med **35**(6): 538-44.

Carlson, B. M., J. A. Carlson, et al. (2003). "Concentration of caveolin-3 at the neuromuscular junction in young and old rat skeletal muscle fibers." J Histochem Cytochem **51**(9): 1113-8.

Cho, K. A., S. J. Ryu, et al. (2004). "Morphological adjustment of senescent cells by modulating caveolin-1 status." J Biol Chem **279**(40): 42270-8.

Couchoux, H., B. Allard, et al. (2007). "Loss of caveolin-3 induced by the dystrophy-associated P104L mutation impairs L-type calcium channel function in mouse skeletal muscle cells." J Physiol **580**(Pt.3): 745-54.

Couet, J., S. Li, et al. (1997). "Identification of peptide and protein ligands for the caveolin-scaffolding domain. Implications for the interaction of caveolin with caveolae-associated proteins." J Biol Chem **272**(10): 6525-33.

Couet, J., M. Sargiacomo, et al. (1997). "Interaction of a receptor tyrosine kinase, EGF-R, with caveolins. Caveolin binding negatively regulates tyrosine and serine/threonine kinase activities." J Biol Chem **272**(48): 30429-38.

Daniele, N., I. Richard, et al. (2007). "Ins and outs of therapy in limb girdle muscular dystrophies." Int J Biochem Cell Biol **39**(9): 1608-24.

Dobbins, G. C., B. Zhang, et al. (2006). "The role of the cytoskeleton in neuromuscular junction formation." J Mol Neurosci **30**(1-2): 115-8.

Emery, A. E. and M. L. Emery (1993). "Edward Meryon (1809-1880) and muscular dystrophy." J Med Genet **30**(6): 506-11.

Fecchi, K., D. Volonte, et al. (2006). "Spatial and temporal regulation of GLUT4 translocation by flotillin-1 and caveolin-3 in skeletal muscle cells." FASEB J **20**(6): 705-7.

Ferns, M. J., J. T. Campanelli, et al. (1993). "The ability of agrin to cluster AChRs depends on alternative splicing and on cell surface proteoglycans." Neuron **11**(3): 491-502.

Flucher, B. E. (1992). "Structural analysis of muscle development: transverse tubules, sarcoplasmic reticulum, and the triad." Dev Biol **154**(2): 245-60.

Folco, E. J., G. X. Liu, et al. (2004). "Caveolin-3 and SAP97 form a scaffolding protein complex that regulates the voltage-gated potassium channel Kv1.5." Am J Physiol Heart Circ Physiol **287**(2): H681-90.

Galbiati, F., J. A. Engelman, et al. (2001). "Caveolin-3 null mice show a loss of caveolae, changes in the microdomain distribution of the dystrophin-glycoprotein complex, and t-tubule abnormalities." J Biol Chem **276**(24): 21425-33.

Garcia-Cardena, G., P. Martasek, et al. (1997). "Dissecting the interaction between nitric oxide synthase (NOS) and caveolin. Functional significance of the nos caveolin binding domain in vivo." J Biol Chem **272**(41): 25437-40.

Gautam, M., T. M. DeChiara, et al. (1999). "Distinct phenotypes of mutant mice lacking agrin, MuSK, or rapsyn." Brain Res Dev Brain Res **114**(2): 171-8.

Glass, D. J., D. C. Bowen, et al. (1996). "Agrin acts via a MuSK receptor complex." Cell **85**(4): 513-23.

Grady, R. M., J. P. Merlie, et al. (1997). "Subtle neuromuscular defects in utrophin-deficient mice." J Cell Biol **136**(4): 871-82.

Grady, R. M., H. Zhou, et al. (2000). "Maturation and maintenance of the neuromuscular synapse: genetic evidence for roles of the dystrophin--glycoprotein complex." Neuron **25**(2): 279-93.

Hernandez-Deviez, D. J., M. T. Howes, et al. (2008). "Caveolin regulates endocytosis of the muscle repair protein, dysferlin." J Biol Chem **283**(10): 6476-88.

Hezel, M., W. C. de Groat, et al. (2009). "Caveolin-3 Promotes Nicotinic Acetylcholine Receptor Clustering and Regulates Neuromuscular Junction Activity." Mol Biol Cell.

Hu, G., R. D. Ye, et al. (2008). "Neutrophil caveolin-1 expression contributes to mechanism of lung inflammation and injury." Am J Physiol Lung Cell Mol Physiol **294**(2): L178-86.

Hughes, B. W., L. L. Kusner, et al. (2006). "Molecular architecture of the neuromuscular junction." Muscle Nerve **33**(4): 445-61.

Jeftinija, D. M., Q. B. Wang, et al. (2007). "The Ca(V) 1.2 Ca(2+) channel is expressed in sarcolemma of type I and IIa myofibers of adult skeletal muscle." Muscle Nerve **36**(4): 482-90.

Kawahara, T. (2004). "Caveolae localization and caveolin expressions in Schwann cells of mature rat spinal nerves." Kurume Med J **51**(3-4): 263-71.

Kawamura, S., S. Miyamoto, et al. (2003). "Initiation and transduction of stretch-induced RhoA and Rac1 activation through caveolae: cytoskeletal regulation of ERK translocation." J Biol Chem **278**(33): 31111-7.

Kim, N., A. L. Stiegler, et al. (2008). "Lrp4 is a receptor for Agrin and forms a complex with MuSK." Cell **135**(2): 334-42.

Koleske, A. J., D. Baltimore, et al. (1995). "Reduction of caveolin and caveolae in oncogenically transformed cells." Proc Natl Acad Sci U S A **92**(5): 1381-5.

Kristensen, M., M. K. Rasmussen, et al. (2008). "Na(+)-K (+) pump location and translocation during muscle contraction in rat skeletal muscle." Pflugers Arch **456**(5): 979-89.

Lacazette, E., S. Le Calvez, et al. (2003). "A novel pathway for MuSK to induce key genes in neuromuscular synapse formation." J Cell Biol **161**(4): 727-36.

Lapidos, K. A., R. Kakkar, et al. (2004). "The dystrophin glycoprotein complex: signaling strength and integrity for the sarcolemma." Circ Res **94**(8): 1023-31.

LaRochelle, W. J. and S. C. Froehner (1986). "Determination of the tissue distributions and relative concentrations of the postsynaptic 43-kDa protein and the acetylcholine receptor in Torpedo." J Biol Chem **261**(12): 5270-4.

Laval, S. H. and K. M. Bushby (2004). "Limb-girdle muscular dystrophies--from genetics to molecular pathology." Neuropathol Appl Neurobiol **30**(2): 91-105.

Lin, W., R. W. Burgess, et al. (2001). "Distinct roles of nerve and muscle in postsynaptic differentiation of the neuromuscular synapse." Nature **410**(6832): 1057-64.

Linnoila, J., Y. Wang, et al. (2008). "A mammalian homolog of Drosophila tumorous imaginal discs, Tid1, mediates agrin signaling at the neuromuscular junction." Neuron **60**(4): 625-41.

Lisanti, M. P., P. E. Scherer, et al. (1994). "Characterization of caveolin-rich membrane domains isolated from an endothelial-rich source: implications for human disease." J Cell Biol **126**(1): 111-26.

Luo, Z. G., H. S. Je, et al. (2003). "Implication of geranylgeranyltransferase I in synapse formation." Neuron **40**(4): 703-17.

Luo, Z. G., Q. Wang, et al. (2002). "Regulation of AChR clustering by Dishevelled interacting with MuSK and PAK1." Neuron **35**(3): 489-505.

Lyons, P. R. and C. R. Slater (1991). "Structure and function of the neuromuscular junction in young adult mdx mice." J Neurocytol **20**(12): 969-81.

Macpherson, P. C., D. Cieslak, et al. (2006). "Myogenin-dependent nAChR clustering in aneural myotubes." Mol Cell Neurosci **31**(4): 649-60.

Madhavan, R. and H. B. Peng (2005). "Molecular regulation of postsynaptic differentiation at the neuromuscular junction." IUBMB Life **57**(11): 719-30.

Madhavan, R., X. T. Zhao, et al. (2003). "The involvement of calcineurin in acetylcholine receptor redistribution in muscle." Mol Cell Neurosci **23**(4): 587-99.

Mancinelli, E., A. Sardini, et al. (1989). "Properties of acetylcholine-receptor activation in human Duchenne muscular dystrophy myotubes." Proc R Soc Lond B Biol Sci **237**(1287): 247-57.

Marchand, S., A. Devillers-Thiery, et al. (2002). "Rapsyn escorts the nicotinic acetylcholine receptor along the exocytic pathway via association with lipid rafts." J Neurosci **22**(20): 8891-901.

Martinez-Marmol, R., N. Villalonga, et al. (2008). "Multiple Kv1.5 targeting to membrane surface microdomains." J Cell Physiol **217**(3): 667-73.

Mathews, K. D. and S. A. Moore (2003). "Limb-girdle muscular dystrophy." Curr Neurol Neurosci Rep **3**(1): 78-85.

Matsuda, C., Y. K. Hayashi, et al. (2001). "The sarcolemmal proteins dysferlin and caveolin-3 interact in skeletal muscle." Hum Mol Genet **10**(17): 1761-6.

Michele, D. E. and K. P. Campbell (2003). "Dystrophin-glycoprotein complex: post-translational processing and dystroglycan function." J Biol Chem **278**(18): 15457-60.

Minetti, C., F. Sotgia, et al. (1998). "Mutations in the caveolin-3 gene cause autosomal dominant limb-girdle muscular dystrophy." Nat Genet **18**(4): 365-8.

Mohamed, A. S., K. A. Rivas-Plata, et al. (2001). "Src-class kinases act within the agrin/MuSK pathway to regulate acetylcholine receptor phosphorylation, cytoskeletal anchoring, and clustering." J Neurosci **21**(11): 3806-18.

Murphy, R. M., J. P. Mollica, et al. (2009). "Plasma membrane removal in rat skeletal muscle fibers reveals caveolin-3 hot-spots at the necks of transverse tubules." Exp Cell Res **315**(6): 1015-28.

Ohsawa, Y., H. Hagiwara, et al. (2006). "Muscular atrophy of caveolin-3-deficient mice is rescued by myostatin inhibition." J Clin Invest **116**(11): 2924-34.

Okada, K., A. Inoue, et al. (2006). "The muscle protein Dok-7 is essential for neuromuscular synaptogenesis." Science **312**(5781): 1802-5.

Palygin, O. A., J. M. Pettus, et al. (2008). "Regulation of caveolar cardiac sodium current by a single Gsalpha histidine residue." Am J Physiol Heart Circ Physiol **294**(4): H1693-9.

Parker, S., H. S. Peterkin, et al. (2007). "Muscular dystrophy associated mutations in caveolin-1 induce neurotransmission and locomotion defects in Caenorhabditis elegans." Invert Neurosci **7**(3): 157-64.

Parton, R. G., M. Way, et al. (1997). "Caveolin-3 associates with developing T-tubules during muscle differentiation." J Cell Biol **136**(1): 137-54.

Preston, D. C. and B. E. Shapiro (2002). "Needle electromyography. Fundamentals, normal and abnormal patterns." Neurol Clin **20**(2): 361-96, vi.

Pumplin, D. W. and D. M. Fambrough (1982). "Turnover of acetylcholine receptors in skeletal muscle." Annu Rev Physiol **44**: 319-35.

Ralston, E. and T. Ploug (1999). "Caveolin-3 is associated with the T-tubules of mature skeletal muscle fibers." Exp Cell Res **246**(2): 510-5.

Razani, B. and M. P. Lisanti (2001). "Caveolins and caveolae: molecular and functional relationships." Exp Cell Res **271**(1): 36-44.

Sanes, J. R. and J. W. Lichtman (1999). "Development of the vertebrate neuromuscular junction." Annu Rev Neurosci **22**: 389-442.

Sanes, J. R. and J. W. Lichtman (2001). "Induction, assembly, maturation and maintenance of a postsynaptic apparatus." Nat Rev Neurosci **2**(11): 791-805.

Scherer, P. E., T. Okamoto, et al. (1996). "Identification, sequence, and expression of caveolin-2 defines a caveolin gene family." Proc Natl Acad Sci U S A **93**(1): 131-5.

Sealock, R., B. E. Wray, et al. (1984). "Ultrastructural localization of the Mr 43,000 protein and the acetylcholine receptor in Torpedo postsynaptic membranes using monoclonal antibodies." J Cell Biol **98**(6): 2239-44.

Segal, S. S., D. G. Welsh, et al. (1999). "Spread of vasodilatation and vasoconstriction along feed arteries and arterioles of hamster skeletal muscle." J Physiol **516 ( Pt 1)**: 283-91.

Si, J., Q. Wang, et al. (1999). "Essential roles of c-JUN and c-JUN N-terminal kinase (JNK) in neuregulin-increased expression of the acetylcholine receptor epsilon-subunit." J Neurosci **19**(19): 8498-508.

Simon-Chazottes, D., S. Tutois, et al. (2006). "Mutations in the gene encoding the low-density lipoprotein receptor LRP4 cause abnormal limb development in the mouse." Genomics **87**(5): 673-7.

Singleton, P. A., S. Chatchavalvanich, et al. (2009). "Akt-mediated transactivation of the S1P1 receptor in caveolin-enriched microdomains regulates endothelial barrier enhancement by oxidized phospholipids." Circ Res **104**(8): 978-86.

Smythe, G. M., J. C. Eby, et al. (2003). "A caveolin-3 mutant that causes limb girdle muscular dystrophy type 1C disrupts Src localization and activity and induces apoptosis in skeletal myotubes." J Cell Sci **116**(Pt 23): 4739-49.

Smythe, G. M. and T. A. Rando (2006). "Altered caveolin-3 expression disrupts PI(3) kinase signaling leading to death of cultured muscle cells." Exp Cell Res **312**(15): 2816-25.

Song, K. S., P. E. Scherer, et al. (1996). "Expression of caveolin-3 in skeletal, cardiac, and smooth muscle cells. Caveolin-3 is a component of the sarcolemma and co-fractionates with dystrophin and dystrophin-associated glycoproteins." J Biol Chem **271**(25): 15160-5.

Sotgia, F., J. K. Lee, et al. (2000). "Caveolin-3 directly interacts with the C-terminal tail of beta -dystroglycan. Identification of a central WW-like domain within caveolin family members." J Biol Chem **275**(48): 38048-58.

Stan, R. V. (2005). "Structure of caveolae." Biochim Biophys Acta **1746**(3): 334-48.

Stetzkowski-Marden, F., K. Gaus, et al. (2006). "Agrin elicits membrane lipid condensation at sites of acetylcholine receptor clusters in C2C12 myotubes." J Lipid Res **47**(10): 2121-33.

Strochlic, L., A. Cartaud, et al. (2004). "14-3-3 gamma associates with muscle specific kinase and regulates synaptic gene transcription at vertebrate neuromuscular synapse." Proc Natl Acad Sci U S A **101**(52): 18189-94.

Takamori, M. (2008). "Lambert-Eaton myasthenic syndrome: search for alternative autoimmune targets and possible compensatory mechanisms based on presynaptic calcium homeostasis." J Neuroimmunol **201-202**: 145-52.

Tang, Z., P. E. Scherer, et al. (1996). "Molecular cloning of caveolin-3, a novel member of the caveolin gene family expressed predominantly in muscle." J Biol Chem **271**(4): 2255-61.

Trinidad, J. C. and J. B. Cohen (2004). "Neuregulin inhibits acetylcholine receptor aggregation in myotubes." J Biol Chem **279**(30): 31622-8.

Udd, B. and R. Griggs (2001). "Distal myopathies." Curr Opin Neurol **14**(5): 561-6.

Venema, V. J., H. Ju, et al. (1997). "Interaction of neuronal nitric-oxide synthase with caveolin-3 in skeletal muscle. Identification of a novel caveolin scaffolding/inhibitory domain." J Biol Chem **272**(45): 28187-90.

Vincent, A. (2008). "Autoimmune disorders of the neuromuscular junction." Neurol India **56**(3): 305-13.

Volonte, D., A. J. Peoples, et al. (2003). "Modulation of myoblast fusion by caveolin-3 in dystrophic skeletal muscle cells: implications for Duchenne muscular dystrophy and limb-girdle muscular dystrophy-1C." Mol Biol Cell **14**(10): 4075-88.

Walter, M. C., C. Braun, et al. (2003). "Variable reduction of caveolin-3 in patients with LGMD2B/MM." J Neurol **250**(12): 1431-8.

Wanamaker, C. P., J. C. Christianson, et al. (2003). "Regulation of nicotinic acetylcholine receptor assembly." Ann N Y Acad Sci **998**: 66-80.

Wang, J., Z. Jing, et al. (2003). "Regulation of acetylcholine receptor clustering by the tumor suppressor APC." Nat Neurosci **6**(10): 1017-8.

Watty, A., G. Neubauer, et al. (2000). "The in vitro and in vivo phosphotyrosine map of activated MuSK." Proc Natl Acad Sci U S A **97**(9): 4585-90.

Weatherbee, S. D., K. V. Anderson, et al. (2006). "LDL-receptor-related protein 4 is crucial for formation of the neuromuscular junction." Development **133**(24): 4993-5000.

Weiss, N., H. Couchoux, et al. (2008). "Expression of the muscular dystrophy-associated caveolin-3(P104L) mutant in adult mouse skeletal muscle specifically alters the Ca(2+) channel function of the dihydropyridine receptor." Pflugers Arch **457**(2): 361-75.

Wessler, I. and C. J. Kirkpatrick (2008). "Acetylcholine beyond neurons: the non-neuronal cholinergic system in humans." Br J Pharmacol **154**(8): 1558-71.

Weston, C., C. Gordon, et al. (2003). "Cooperative regulation by Rac and Rho of agrin-induced acetylcholine receptor clustering in muscle cells." J Biol Chem **278**(8): 6450-5.

Weston, C., B. Yee, et al. (2000). "Agrin-induced acetylcholine receptor clustering is mediated by the small guanosine triphosphatases Rac and Cdc42." J Cell Biol **150**(1): 205-12.

Weston, C. A., G. Teressa, et al. (2007). "Agrin and laminin induce acetylcholine receptor clustering by convergent, Rho GTPase-dependent signaling pathways." J Cell Sci **120**(Pt 5): 868-75.

Whitehead, R. H., P. E. VanEeden, et al. (1993). "Establishment of conditionally immortalized epithelial cell lines from both colon and small intestine of adult H-2Kb-tsA58 transgenic mice." Proc Natl Acad Sci U S A **90**(2): 587-91.

Wiesner, A. and C. Fuhrer (2006). "Regulation of nicotinic acetylcholine receptors by tyrosine kinases in the peripheral and central nervous system: same players, different roles." Cell Mol Life Sci **63**(23): 2818-28.

Williams, T. M. and M. P. Lisanti (2004). "The Caveolin genes: from cell biology to medicine." Ann Med **36**(8): 584-95.

Witzemann, V. (2006). "Development of the neuromuscular junction." Cell Tissue Res **326**(2): 263-71.

Woodman, S. E., M. W. Cheung, et al. (2004). "Urogenital alterations in aged male caveolin-1 knockout mice." J Urol **171**(2 Pt 1): 950-7.

Woodman, S. E., F. Sotgia, et al. (2004). "Caveolinopathies: mutations in caveolin-3 cause four distinct autosomal dominant muscle diseases." Neurology **62**(4): 538-43.

Yamamoto, M., Y. Toya, et al. (1999). "Caveolin is an inhibitor of platelet-derived growth factor receptor signaling." Exp Cell Res **247**(2): 380-8.

Yarbrough, T. L., T. Lu, et al. (2002). "Localization of cardiac sodium channels in caveolin-rich membrane domains: regulation of sodium current amplitude." Circ Res **90**(4): 443-9.

Zhang, B., S. Luo, et al. (2008). "LRP4 serves as a coreceptor of agrin." Neuron **60**(2): 285-97.

Zhu, D., W. C. Xiong, et al. (2006). "Lipid rafts serve as a signaling platform for nicotinic acetylcholine receptor clustering." J Neurosci **26**(18): 4841-51.

Zuo, L., M. Ushio-Fukai, et al. (2005). "Caveolin-1 is essential for activation of Rac1 and NAD(P)H oxidase after angiotensin II type 1 receptor stimulation in vascular smooth muscle cells: role in redox signaling and vascular hypertrophy." Arterioscler Thromb Vasc Biol **25**(9): 1824-30.